UNIVERSIDAD NACIONAL AUTÓNOMA DE MÉXICO

PROGRAMA DE MAESTRÍA Y DOCTORADO EN INGENIERÍA
ENERGÍA – SISTEMAS ENERGÉTICOS

STUDY ON THE LONG LIFE CYCLE FUEL MANAGEMENT OF A FAST BREEDER STATIONARY WAVE REACTOR

TESIS
QUE PARA OPTAR POR EL GRADO DE:
DOCTOR EN INGENIERÍA

PRESENTA:
ROBERTO CARLOS LÓPEZ SOLÍS

TUTOR PRINCIPAL
DR. JUAN LUIS FRANCOIS LACOUTURE, FI-UNAM
COMITÉ TUTOR
DR. GILBERTO ESPINOSA PAREDES, UAM-I
DRA. CECILIA MARTÍN DEL CAMPO MÁRQUEZ, FI-UNAM
DR. JAIME BALTAZAR MORALES SANDOVAL, FI-UNAM
DR. RODOLFO VÁZQUEZ RODRÍGUEZ, UAM-I

MÉXICO, D. F. NOVIEMBRE 2015

JURADO ASIGNADO:

Presidente:	Dr. Gilberto Espinosa Paredes
Secretario:	Dra. Cecilia Martín del Campo Márquez
Vocal:	Dr. Juan Luis Francois Lacouture
1er. Suplente:	Dr. Jaime Baltazar Morales Sandoval
2do. Suplente:	Dr. Rodolfo Vázquez Rodríguez

Lugar o lugares donde se realizó la tesis: MÉXICO DF

TUTOR DE TESIS:

Juan Luis Francois Lacouture

FIRMA

(Segunda hoja)

Agradecimientos / Acknowledgements

Una sección en la tesis no es suficiente para alcanzar a a agradecer a todos los que me han apoyado, sin embargo haré un esfuerzo para mencionar a los principales:

A mis padres por darme la vida y guiarme a lo largo de ella, sin ustedes nada de ésto hubiera sido posible.

A mis hermanos, sin quienes no puedo imaginar mi vida.

Al doctor Juan Luis Francois Lacouture por su confianza, amistad y mentoría a través de tantos años, sin usted no estaría aquí hoy.

A los doctores Gilberto Espinosa Paredes, Jaime Morales Sandoval, Cecilia Martín del Campo y Rodolfo Vázquez; por su valiosa orientación y supervisión a lo largo del proyecto.

I would like to thank doctors Victor Sanchez, Maarten Becker, Ron Dagan and Cornelis Broeders for given me the opportunity of working along them at the Karlsruhe Institute of Technology.

A los doctores Armando Gomez Torres y Jerson Sanchez Jaramillo, a quienes considero mis hermanos mayores en la profesión; por su gran apoyo y guía.

A mis queridos amigos Ing. Ángel Senties y Lic. Lorena Cavazos por siempre estar ahí cuando los he necesitado.

A la Dra. Adriana Ipiña Hernández, por su duradera amistad, por sus consejos y sus regaños.

Al M. en I. Guillermo Bastida, por ayudarme en la elaboración de las imágenes para esta tesis.

Al Consejo Nacional de Ciencia y Tecnología (CONACYT) por el apoyo recibido durante la duración de este proyecto de investigación y durante mis estancias en el extranjero.

A Universidad Nacional Autónoma de México, por darme la oportunidad de ser parte de tan honorable institución así como por el apoyo brindado mediante el proyecto de investigación PAPIIT-IN113213.

A los coordinadores del proyecto "AZTLAN Platform" por la oportunidad que me han brindado al de ser parte de su equipo.

Contents

List of Figures

List of Tables

List of Acronyms

4S	Super-Safe Small and Simple
ANL	Argone National Laboratory
ARC	Advanced Reactor Concepts
B&B	Breed and Burn
BNL	Brookhaven National Laboratory
CANDLE	Constant Axial shape of Neutron flux, nuclide density and power shape During Life of Energy production
DU	Depleted Uranium
DUPIC	Direct Use of spent PWR fuel In CANDU
EBR	Experimental fast Breeder Reactor
EM^2	Energy Multiplier Module
FMSR	Fast Mixed Spectrum Reactor
GA	General Atomics
GIF	Generation-IV International Forum
HPM	Hyperion Power Module
KANEXT	KArlsruher Neutronic EXtendable Tool
LANL	Los Alamos National Laboratory
LEU	Low Enriched Uranium
LFR	Lead Fast Reactor
LMFBR	Liquid Metal Fast Breeder Reactor
LWR	Light Water Reactor
MC	Monte Carlo
PUREX	Plutonium-URanium EXtraction
PWR	Pressurized Water Reactor
RTR	Radkowsky Thorium Reactor
RTR	Radowsky Thorium Reactor
SBU	SeedBlanket Unit
SFR	Sodium Fast Reactor

SNP	Spent Nuclear Fuel
SSFR	Sustainable Sodium Cooled Fast Reactor
SSTAR	Secure Transportable Autonomous Reactor
ULFR	Ultra-long Life Fast Reactor
UN	United Nations
UNF	Used Nuclear Fuel
VVER	Vadá Vadá Energeticheski Reactor
WNA	World Nuclear Association

Chapter 1

INTRODUCTION

The main objective of the research project is to develop a fuel reshuffling strategy for a fast Breed and Burn (B&B) Reactor and find out if it can operate for more than 40 years without the need of refueling.

The reason of choosing a breed and burn reactor, as a subject of study, is the advantages that it has over a conventional fuel cycle, such as the removal of the need of fuel reprocessing. A brief discussion of this matter is presented in this section.

Nuclear fuel reprocessing has been considered on since the 1940's for military purposes. Mainly hydrometallurgy and electrometallurgy treatments can be used to reprocess spent nuclear fuel.

PUREX (Plutonium-URanium EXtraction, an hydrometallurgy process) is the most conventional reprocessing method, where U and Pu are separated by dissolving the fuel with nitric acid and other solvents [WNA, 2015].

Pyro-processing (an electrometallurgy process) is expected to simplify reprocessing of nuclear spent fuel once is in commercial scale, and it is currently under development [ANL, 2015] [Simpson, 2012] by the Argone and Idaho National Laboratories, among others.

Even though the mentioned reprocessing methods are indeed ways of extending uranium resources and decreasing long-life actinides volumes, both for light water reactors and fast breeders, these methods also imply taking the fuel out of the core, translating the fuel to a reprocessing plant and finally to a fuel fabrication facility. This, not only increases the cost of the reprocessed fuel but also the chance of being diverted for proliferation purposes.

A breed/burn reactor would take as main fuel the Depleted Uranium (DU) left as waste in the enrichment plants, and a small portion of enriched fuel, and produce new fissile fuel by nuclear transmutation as shown in Equations 1.1 and 1.2. This new fissile fuel will be burned *in situ* inside the same nuclear core which produced it, thus eliminating the need of fuel reprocessing and avoiding all the inconveniences and costs it implies.

$$n + {}^{238}_{92}U \longrightarrow {}^{239}_{92}U \overset{\beta^- + \bar{\nu}}{\longrightarrow} {}^{239}_{93}Np \overset{\beta^- + \bar{\nu}}{\longrightarrow} {}^{239}_{94}Pu \tag{1.1}$$

$$n + {}^{232}_{90}Th \longrightarrow {}^{233}_{90}Th \overset{\beta^- + \bar{\nu}}{\longrightarrow} {}^{233}_{91}Pa \overset{\beta^- + \bar{\nu}}{\longrightarrow} {}^{233}_{92}U \tag{1.2}$$

Where:
β^- is a beta (-) particle.
$\bar{\nu}$ is an antineutrino.

This research project has been carried out considering the following keystones goals:

- State-of-the-Art review of the Breed/Burn reactor technology.
- Adoption of a nuclear code with fuel reshuffling capabilities.
- Preliminary core model design.
- Implementation of the model in the code.
- Validation of the code for the core model.
- Fuel reshuffling tests.

The code adopted was the German deterministic code KANEXT, and the reason of choosing it, over other similar codes, was mainly due to the dispositions of the developers to collaborate closely with our workgroup, and to the fact that a Monte Carlo (MC) based code will require much more computer power than the available.

After this introduction the chapters of this thesis will be presented as follows:

- Breed/Burn Reactor Technology Review
- Breed/Burn Reactor Core Model Description
- KANEXT Code Description
- Breed/Burn Reactor Core Model Implementation
- Code Validation
- Results and Discussion
- Conclusions
- Appendixes

Chapter 2

BREED/BURN REACTOR TECHNOLOGY REVIEW

In the present chapter a literature review of the historical evolution of the breed and burn (B&B) reactor concept and the fast breeder reactors in general is presented; along with a description of the main reactors aimed to utilize this B&B concept.

2.1 Fast Breeder Reactors Evolution

Fast reactors are usually divided into three main categories [Waltar et al., 2012] depending on their purpose:

- Experimental and Test Reactors. Those with power levels typically up to 100 MWth, built to demonstrate the technology (experimental purposes or for fuels and materials testing) but often with steam plant and turbine-generators to allow operation as a small power station.
- Demonstration or Prototype Reactors. Those generally in the 250-350 MWe range in which much of the scaling up required for a commercial station has been incorporated (in terms of both overall size and individual components).
- Commercial-Sized Reactors. Those developed as lead projects to demonstrate the system's capability to operate in a utility environment.

Figure 2.1 shows the development of fast reactor projects through history. Most of the early interest in fast spectrum reactors was for developing breeding capability.

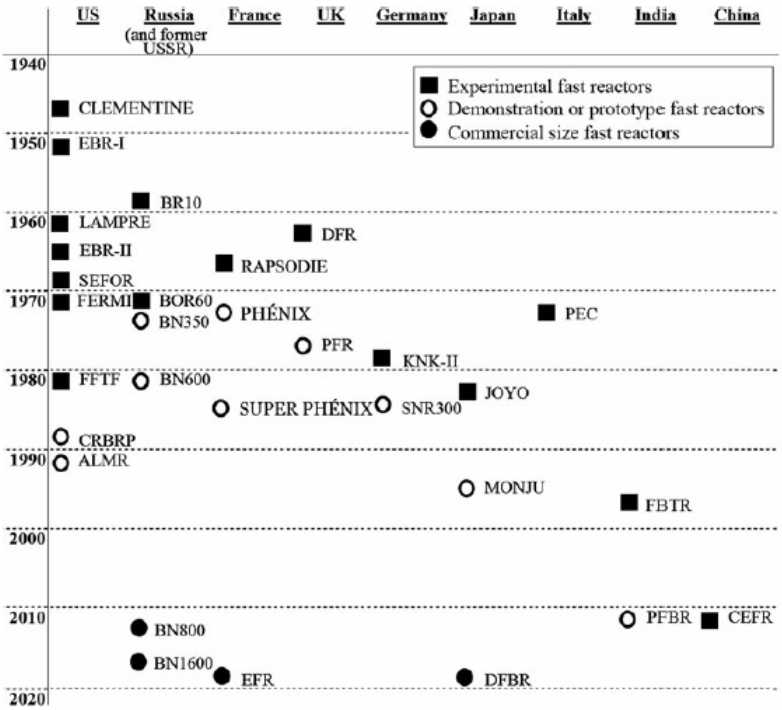

Figure 2.1: International fast reactor development through the demonstration plant phase [Waltar et al., 2012]

The first fast reactor was Clementine, built at Los Alamos National Laboratory (LANL) in 1946. The next step was the Experimental fast Breeder Reactor (EBR-I), designed by the Argonne National Laboratory (ANL). On December 20, 1951, EBR-I became the world's first nuclear plant of any type to generate electricity. The concept of the fast breeder reactor (FBR) was demonstrated and gave impetus to the prospect of a long-term reliance on nuclear fuel as a new energy source.

Approximately 30 years after EBR-I, four liquid metal (sodium) cooled fast breeder reactors (LMFBR's) in the 250–600 MWe power range began producing electricity (and desalinating water) in three European countries, and construction on a 1,200 MWe LMFBR was nearing completion. At that time, it was expected that LMFBRs in the 1,200-1,600 MWe range would soon be under construction in five countries. Hopes were high that the dream originating in the middle of the twentieth century of an economical, inexhaustible and practically independent energy source appeared likely to become a reality early in the twenty-first century for many countries having few indigenous energy resources.

By 2000 the Generation IV Forum was formed. The Generation IV International Forum (GIF) is a cooperative, international endeavour that carried out work to define and perform the research and development needed to establish the feasibility and performance capabilities of the next generation nuclear energy systems [GIF, 2015]. Three fast reactor systems had been pursued through international collaborations under the auspices of this program; the sodium-cooled fast reactor (SFR), the gas-cooled fast reactor (GFR), and the lead-cooled fast reactor (LFR) systems [GIF, 2009]. From these three systems, the SFR is the one with more experience in development.

2.2 Brief Historical Evolution of Breed/Burn Reactor Concept

In this section a brief chronology of the main works on the breed and burn core development are given.

The concept of a reactor that can generate its own fissile fuel nuclear trhough transmutation was first propossed on the second UN International Conference on Peaceful Use of Atomic Energy [Feinberg and Kunegin, 1958] by the winner of the Kurchatov Medal, Savely Moiseevich Feinberg and his college E. P. Kunegin. In their proposed concept, the nuclear reactor uses depleted uranium in the form of fertile ^{238}U as target material and a source of fissile high enriched ^{235}U on one end of a long cylinder or parallelepiped, this fissile material would have to be enough to generate critical mass.

In 1961, an article [Fuchs and Hessel, 1961] was published in the German journal *Kernenergie* by K. Fuchs and H. Hessel, this article's title translated to English is "On the material possibilities of operation of natural uranium breeder reactor without fuel treatment". In this article a fast reactor without "chemistry processing" fuel cycle is considered.

In 1979 [Fischer et al., 1979b] and then in 1980 [Loh et al., 1980], a new concept was studied, this concept called the Fast Mixed Spectrum Reactor consisted in a core with both fast and thermal zones; fertile and fissile material are placed in these zones, after a certain time new fissile fuel breed in the fertile areas is placed in the fissile zones.

In 1984 [Slesarev et al., 1984], it was studied the feasibility of the breed and burn reactor concept in a published paper named "Problems of development of fast reactors self-provision without fuel reprocessing".

Lev P. Feoktistov studied the breed and burn reactor as an intrinsically safe reactor and

published some papers which titles translated to english are "An analysis of a concept of a physically safe reactor" [Feoktistov, 1989a], "Neutron-fission wave" [Feoktistov, 1989b] and "Variant of safe reactor" [Feoktistov, 1989c] in 1989.

In 1995 an article [Seifritz, 1995] called "Non-Linear Burn-up Waves in Opaque Neutron Absorbers" was published in the german journal *Kerntechnik*. It was demonstrated that burnup waves propagate slowly though a neutron absorber medium, obeying a non-linear diferential equation.

In 1996 [Teller et al., 1996] an article called "Completely Automated Nuclear Power Reactors for Long-Term Operation" was published. In the paper new types of nuclear reactors optimized to have features such as long life are discussed. The authors are now working in TerraPower developing the Traveling Wave Reactor.

By 1998 Hugo Van Dam [Van Dam, 1998] published his study on the propagation of nuclear waves in a paper called simply "Burnup waves", where the shape and propagation of the burnup waves (regions with strong neutron absorption) were studied.

By 1999 Akhiezer and others published [Akhiezer et al., 1999] "Propagation of a Nuclear Chain Reaction in the Diffusion Approximation" and later in "Slow Nuclear Burning" [Akhiezer et al., 2001]. In the first, nuclear chain reaction in a cylindrical breeder medium was studied for both critical and sub-critical regimes. In the second the propagation of the nuclear fission wave is studied and its evolution is determined.

In the early 2000's [Sekimoto et al., 2001] development of the CANDLE (Constant Axial shape of Neutron flux, Nuclide Densities and power shape During Life of Energy production) concept was started in the Tokyo Institute of Technology. The core consist in two zones: one ignition zone with fissile material and one breeding zone with only natural or depleted uranium.

In 2003 an article [Pilipenko et al., 2003] with the title "Some aspects of Slow Nuclear Burning" was published, where the possibility of creating a Nuclear Burning Wave regime was confirmed.

In 2005 Sergii Fomin and others [Fomin et al., 2005] published his work on nuclear wave propagation. On the same year, Xue Nong Chen [Chen and Maschek, 2005] and others published their work on the nuclear wave buckling effects; and Bernard Gaveau and others [Gaveau et al., 2005] did it for their respective work on stationary waves.

On the year 2006 the company TerraPower (called Intellectual Ventures by then) started working on their concept of breed and burn reactor, called the Traveling Wave Reactor, aiming to develop it commercially.

Developments on breed and burn reactor concept have been continuously going on, but the objective of this section was to give a short historical research up to the moment when TerraPower started developing their reactor; since it was the main motivation for working in this concept.

2.3 Types of Breed and Burn Reactor Cores

In these sections some of the different breed and burn reactor concepts and similar cores aimed for long life are discussed.

2.3.1 Ultra Long Life Fast Reactor (ULFR)

The ultra-long life sodium-cooled fast reactor (ULFR) concept was developed aiming for reactor operation without refuelling over a long reactor lifetime [Kim and Taiwo, 2010a]. The average discharge burnup of typical sodium-cooled fast reactor designs is limited under the current fuel irradiation experience (10% to 20%).

Zirconium-based alloy is commonly used as metallic fuel clad in fast reactor designs due to its excellent compatibility with steel-based cladding materials, dimensional stability, high heavy metal loading and its good neutron economy. For the ULFR however, Molybdenum-based alloy is selected in order to increase the heavy metal loading in the core. Previous irradiation tests indicate that the fuel swelling of molybdenum-based metallic fuel is acceptable and its thermal properties are similar to those of zirconium-based metallic fuel [Kim and Taiwo, 2010b].

Figure 2.2 shows the layout of a ULFR, and Figure 2.3 shows the k_{eff} and the breeding ratio though core life cycle. The core consists of 342 driver assemblies, 144 internal blanket assemblies, and 174 radial blanket assemblies. The ULFR core has an annular core layout. All internal blanket assemblies are located at the core center, and are surrounded sequentially by driver assemblies and radial blankets. A sensitivity study [Kim and Taiwo, 2010b] had indicated that this annular core layout can maintain criticality longer than a core layout that has a scattered distribution of the internal blankets by propagating the burn zone. In order to achieve inward power (burnup) propagation, different uranium enrichments have been used for the driver fuels, varied along the core radial direction. The enrichments of the inner, middle, and outer core zones are 9%, 11%, and 13%, respectively. Depleted uranium fuel with ^{235}U content of 0.25% is loaded into the internal, axial and radial blanket core zones.

Several benefits have been attributed to the ULFR; these include capital and operational cost reductions, low proliferation risk, and effectively holding LWR spent fuel without disposal until technologies for a closed nuclear fuel cycle are developed and deployed.

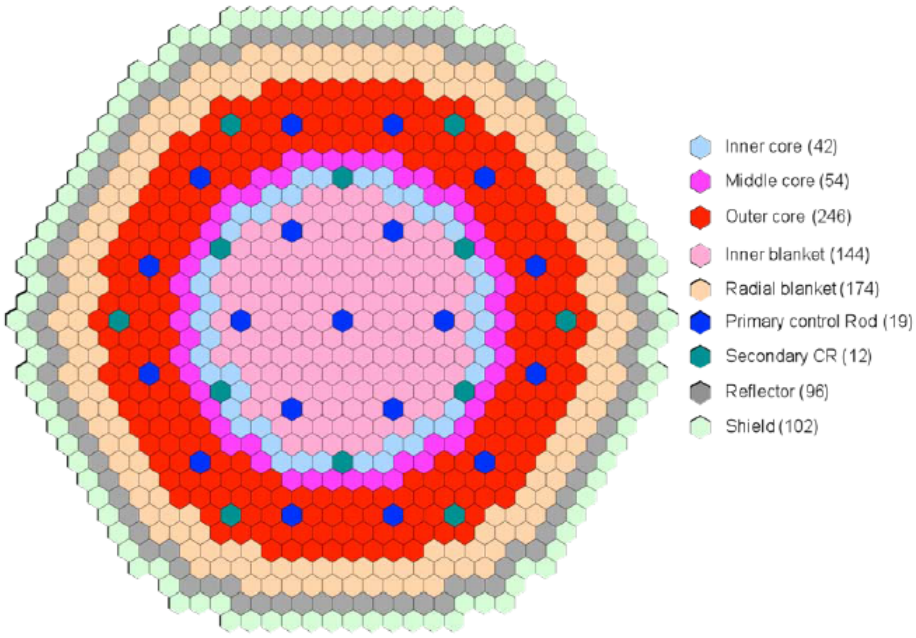

Figure 2.2: Radial layout of the ULFR [Kim and Taiwo, 2010b]

2.3.2 CANDLE Reactor

In principle, the CANDLE concept is designed to burn all the depleted uranium resulting from the creation of the initial enriched uranium fuel by increasing the core height, because the core can maintain criticality as long as the depleted uranium is available.

The CANDLE (Constant Axial shape of Neutron flux, nuclide density and power shape During Life of Energy production) reactor concept has been considered for very high uranium fuel utilization. As mentioned before the concept was proposed by researchers at the Tokyo Institute of Technology [Sekimoto et al., 2001] and its design typically has a starter zone (at core bottom) and a very tall axial depletion zone. The starter zone is used for initial power generation and for the ignition of power generation in the depletion zone. This is accomplished by the use of leaking neutrons to breed fissile material in the depleted zone.

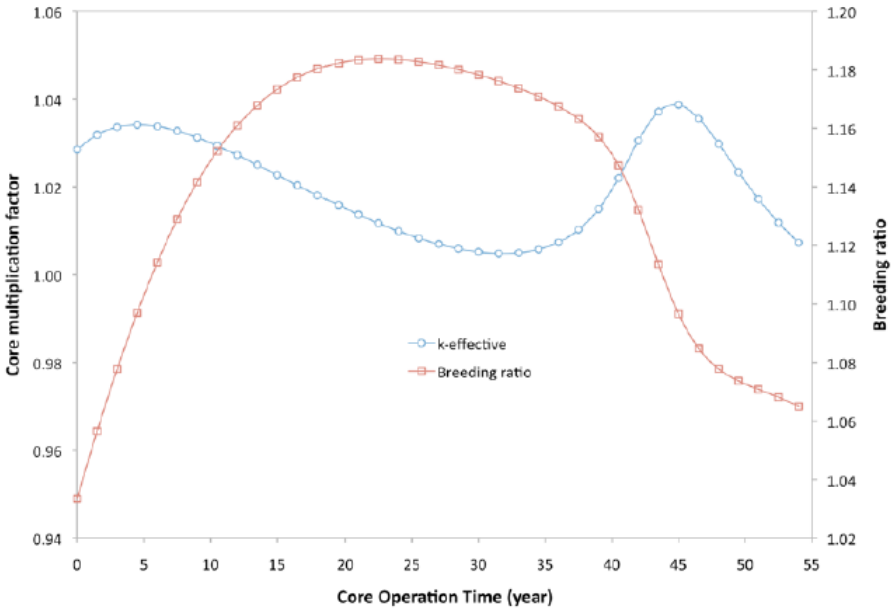

Figure 2.3: Core Multiplication Factor and Breeding Ratio of ULFR [Kim and Taiwo, 2010b]

This breeding is followed by significant power generation by the derived fissile material with continuing core operation.

As in this concept the core active burn-zone moves axially with time. However, there are various design issues to be resolved before this concept can be considered feasible for further development and deployment, including: (1) the very high fuel burnups that are possible with this design and for which no workable fuel design exists at the current time; (2) the potential difficulties with reactor control due to the very tall core; (3) the feasibility of cooling the core active zone (pressure drops), which is also associated with the long length core.

While the original CANDLE [Sekimoto et al., 2001] concept adopted a lead-bismuth cooled fast system with metallic fuel, an alternative sodium-cooled concept was later introduced [Sekimoto and Nagata, 2010]. A further study [Kim 2010b] was made where calculation of the core was done considering a sodium-cooled fast spectrum system with U-Zr binary metallic fuel. The height of the starter zone is 120 cm and it is designed to have different enriched LEU fuels axially to enhance the axial propagation of the burn-zone: 13%, 7% and 3% from the core bottom with the lengths of 80 cm, 20 cm, and 20 cm, respectively; average enrichment is 10.3%. A depletion zone of height 6.8 m, which

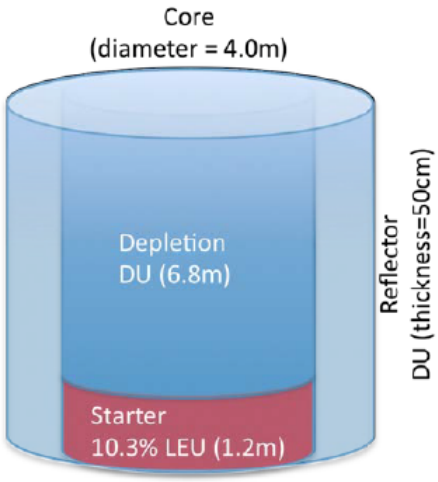

Figure 2.4: Conceptual Drawing of CANDLE Reactor [Kim and Taiwo, 2010b]

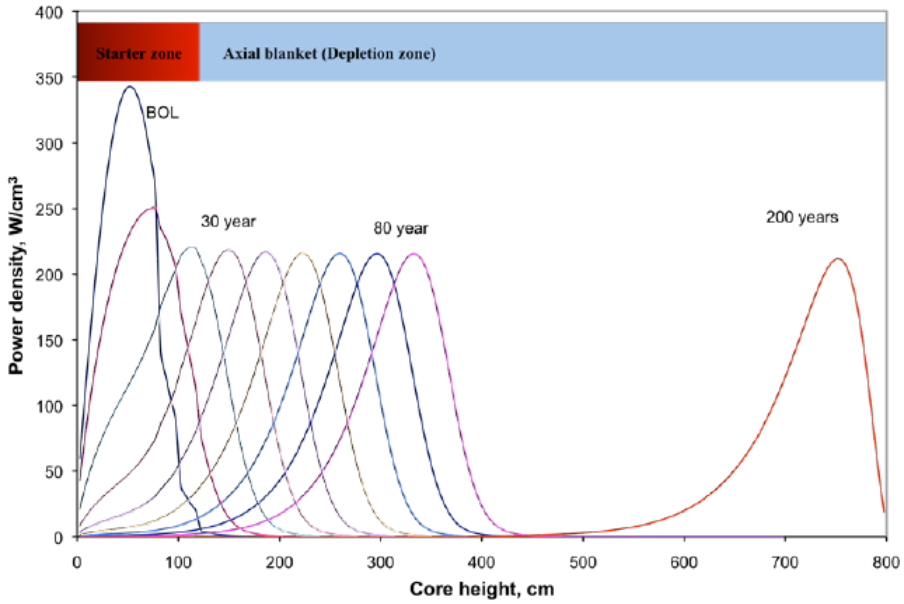

Figure 2.5: Propagation of power profile for CANDLE [Kim and Taiwo, 2010b]

contains U-Zr binary metallic fuel with depleted uranium, is located above the starter. The core has a diameter of 4.0 m and is surrounded by a 50 cm thick radial reflector made of depleted uranium. For simplicity, all fuels have the same fuel, coolant, and structure volume fractions of 37.5%, 30.0% and 20%, respectively. Figure 2.4 shows the core layout and Figure 2.5 shows the power profile though core life for the simulations made.

2.3.3 Fast Mixed Spectrum Reactor

The Fast Mixed Spectrum Reactor (FMSR) concept attempt to use traditional fuel management approaches for achieving high utilization. It was developed by the Brookhaven National Laboratory (BNL) in the 1970s. A 3000 MWt FMSR was proposed [Fischer et al., 1979a] to offer excellent non-proliferation characteristics and to achieve good utilization of uranium resources. The design is in a class of breed and burn systems in which traditional assemblies are used and fuel is charged and discharged.

In the FMSR operation, fissile (driver) and blanket fuels are supposed to be charged into the fast and thermal core zones, respectively. Then, fissile material is bred in the thermal zone during core operation. As sufficient fuel is bred and after the driver fuel assembly has reached its discharge burnup, the core is shuffled. During the shuffling process, the burned driver fuel assemblies are discharged, and the bred fuel assemblies are shuffled into the fast core zone. Then fresh depleted uranium blanket assemblies are charged into the thermal core zone and finally the core is restarted.

The FMSR core concept proposed by BNL is separated into fast and thermal core zones using Beryllium (Be) moderator. The primary purpose of the moderator claimed in bibliography [Fischer et al., 1979a] is for power flattening and reactivity management, and minimization of the fluence. Studies show that the impact of the Be moderator on the core performance characteristics is minimal.

Figure I.5 shows the conceptual drawing of the FMSR. The core has 408 fuel assemblies: 240 assemblies in the fast zone and 168 assemblies in the thermal zone. In the axial direction, the driver fuel is divided into three zones: lower axial blanket, active core and upper axial blanket. The fuel form is assumed to be U-Zr binary metallic fuel. In the BNL study, the fuel volume fraction was assumed to be 39% for gas-cooled system and 50% for sodium-cooled system, and the active core height is 160 cm and the thickness of each axial blanket is 40 cm.

In a consulted study [Kim and Taiwo, 2010b], a 34-batch fuel management scheme was adopted for the FMSR by dividing the core into 34 radial subzones: 20 subzones in the fast

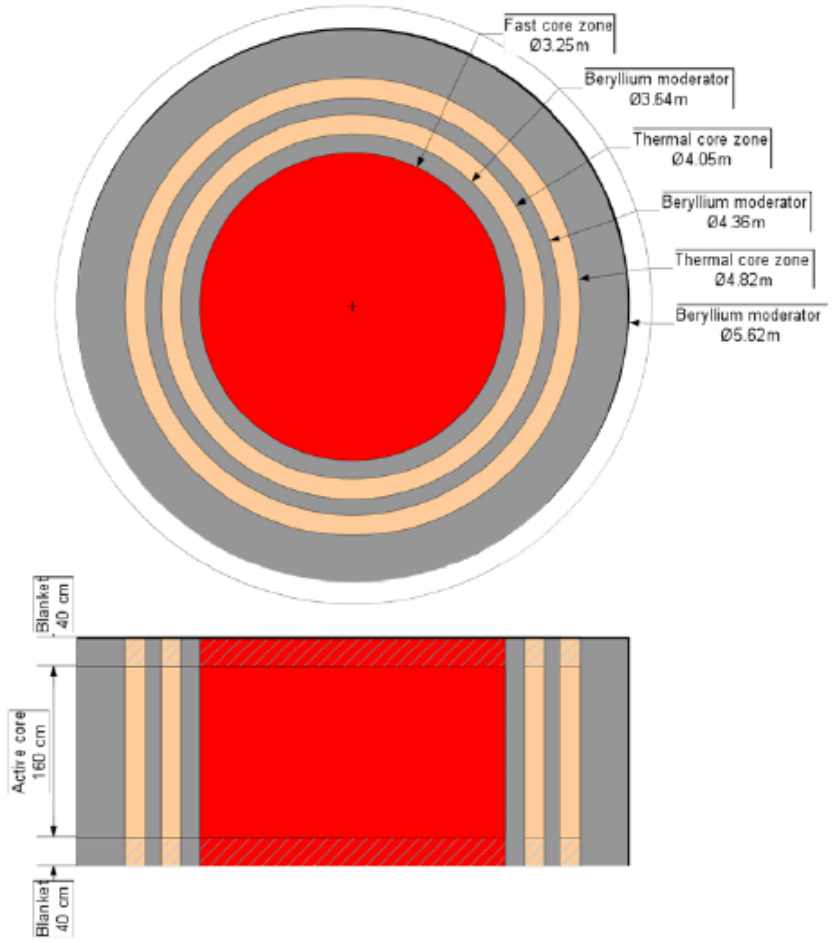

Figure 2.6: Conceptual design of FMSR [Kim and Taiwo, 2010b]

core zone and 14 subzones in the blanket zone. The core cycle length was assumed to be 1.5 years with 90% capacity factor. Each zone contains 12 fuel assemblies, and as a result, 12 fuel assemblies are replaced at the end of each cycle. Depleted uranium assemblies are loaded into the core in subsequent cycles. A fresh depleted uranium assembly is initially loaded into the outermost ring of the thermal core zone, and then it is gradually moved to the inner rings with the core reloads. The fuel resides in the thermal core zone for 14 cycles to breed sufficient plutonium. After 14 cycles, the fuel is shuffled into the fast core zone and resides an additional 20 cycles, thus the fuel resides in the core for up to 51 years, from charge to discharge. In the fast core zone, the fuel moves from the innermost ring to the outermost ring of the fast core zone.

The equilibrium cycle of the FMSR core can be maintained criticality by feeding in depleted uranium. Thus, the uranium utilization of the FMSR core approaches its discharge burnup of 27%. The BNL report on the FMSR indicated some design issues needing to be resolved in the areas of reactor physics, thermal-hydraulics, fuels and materials, before the design can be considered feasible [Fischer et al., 1979a].

Figure 2.7 shows the evolution though fuel cycles of some of the most important parameters of the studied core.

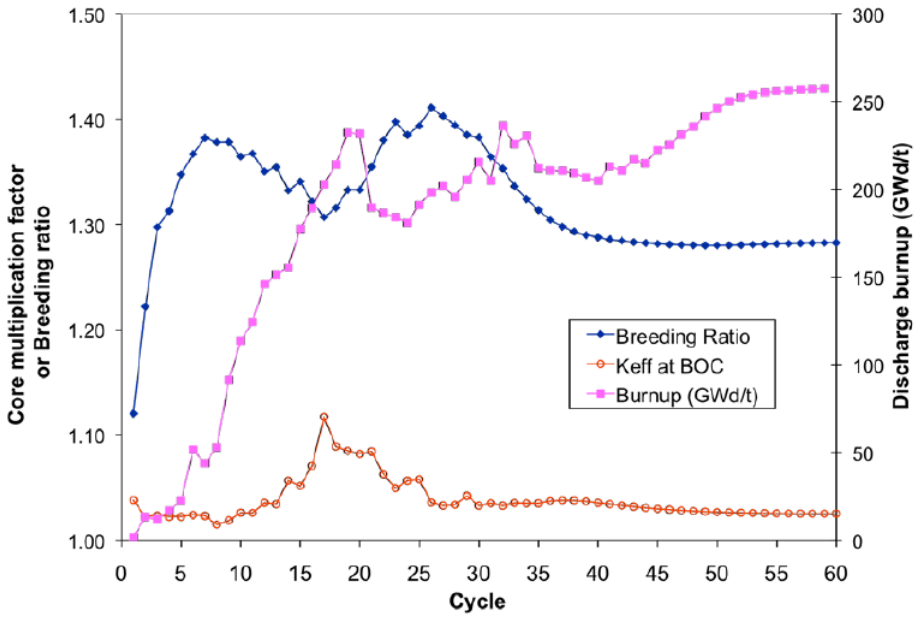

Figure 2.7: Trends of Core Physics Parameters of FMSR [Kim and Taiwo, 2010b]

2.3.4 Sustainable Sodium Cooled Fast Reactor

The primary purpose of the Sustainable Sodium Cooled Fast Reactor (SSFR) is to develop a sustainable sodium-cooled fast reactor using depleted uranium feed only, as in the FMSR design. Sustainability implies a core k_{eff} maintained at constant critical value as long as required. Since the fissile content of depleted uranium is insufficient to make the fast reactor core critical, the core requires fissile material initially. The core however becomes sustainable eventually due to the utilization of bred plutonium. For establishing a sustainable fuel cycle, the depleted uranium should be irradiated for a certain period until sufficient plutonium is bred. Unlike the FMSR, where depleted uranium is charged into the thermal core zone for breeding plutonium and then shuffled into the fast core zone when sufficient plutonium is bred, the SSFR adopts a conventional sodium-cooled fast reactor concept. It does not have a thermal zone, as the FMSR.

In a study where this core was treated [Kim and Taiwo, 2010b], core has a power rating of 3000 MWt. It consists of 408 driver assemblies. For power flattening, the first core is divided into four zones: inner, middle, outer core and depletion zones with uranium enrichments of 9.0%, 11.0%, 14.0%, and 0.25%, respectively. The active core height is 120 cm and there are upper and lower axial blankets with 40 cm thickness each. The fuel volume fraction is about 45%. The fuel assembly has 127 fuel pins and a pitch of 20 cm. Figure 2.8 sows the cross section of the core.

The mentioned study of the SSFR core adopts a 34-batch fuel management scheme with a 1.5-year cycle length. Since there are 408 fuel assemblies including the radial blanket, 12 used fuel assemblies are replaced by fresh depleted uranium fuel assemblies at the beginning of each cycle. In the same work, a sensitivity study indicated that the depleted uranium fuel should be irradiated more than a lower burnup value in order to breed sufficient plutonium; it was also found that there is also an upper burnup value as the core cannot be critical when the reactivity penalty from the accumulation of fission products becomes significant.

Figure 2.9 shows the value of the effective multiplication factor at the beginning and end of each of the 100 cycles that conforms the operation life of the core.

2.3.5 Energy Multiplier Module

Energy Multiplier Module (EM^2) is a development of General Atomics (GA) that improves fuel utilization and incorporates both depleted uranium and used nuclear fuel wastes into the fuel cycle without reprocessing [Schleicher et al., 2009]. The breed and burn reactor

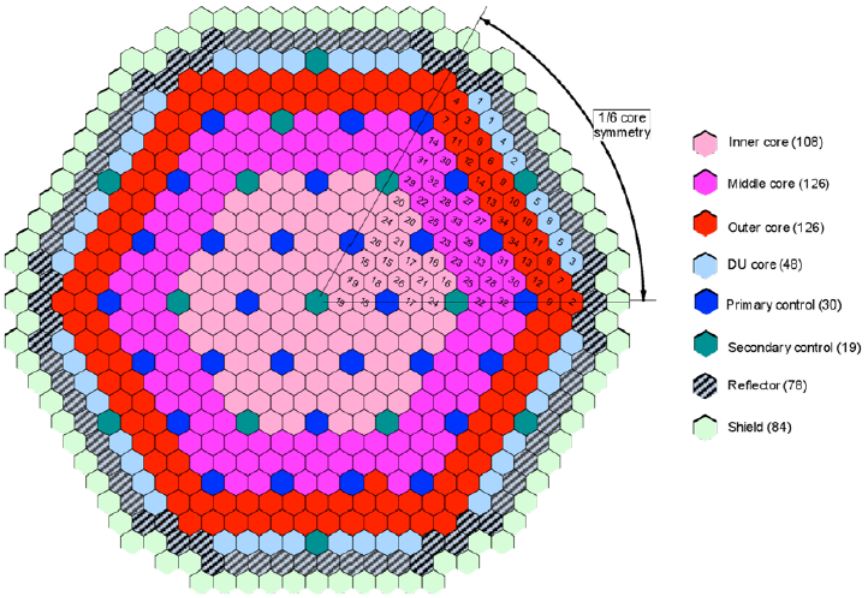

Figure 2.8: Radial Core Layout of SSFR [Kim and Taiwo, 2010b]

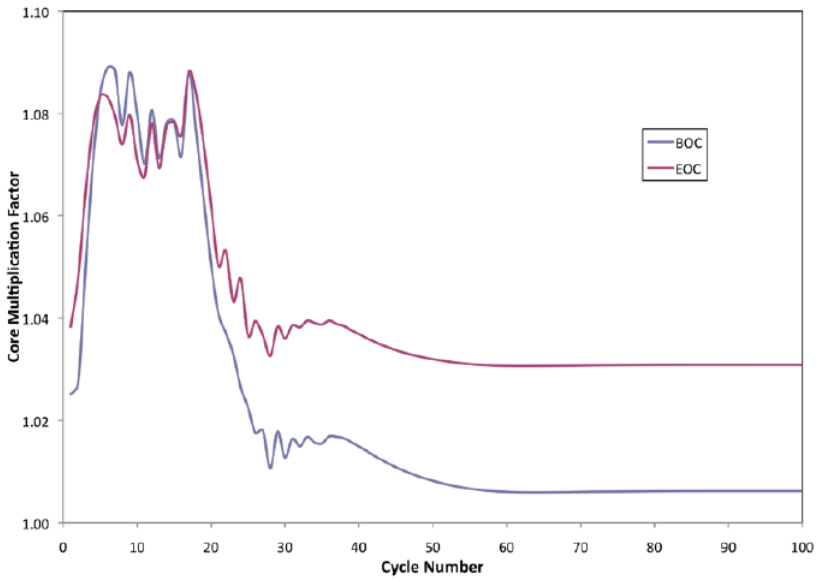

Figure 2.9: Core Multiplication Factor of SSFR [Kim and Taiwo, 2010b]

concept is used to obtain high fuel burnup (about 3 to 5 times that of operating LWRs). It is planned to have a reactor design that enables factory-built modular plants for improved economics.

The system consists of a starter section and a depleted and/or Used Nuclear Fuel (UNF) conversion section. Initially, power is generated in the starter section and excess neutrons are used for converting the fertile material into fissile fuel over the reactor life, which is targeted to be greater than 30 years. The reactor is to be coupled to a Brayton cycle with thermal efficiency of 50% according to GA [Schleicher et al., 2009].

This gas-cooled fast reactor is designed to have attractive safety characteristics, namely negative temperature coefficient over the full operating temperature range and a negligible void coefficient [Schleicher et al., 2009].

The small size of the reactor and the power conversion system allow them to be sited completely underground. This underground sitting and the lack of refuelling have been attributed to decreasing the proliferation risk of the nuclear system. [Schleicher et al., 2009].

According to GA, the non-proliferation attributes for the system are:

- Eliminates need for long-term storage of spent fuel containing significant Pu.
- Eliminates need for conventional reprocessing (isotopic separation) for the long-term future.
- Eliminates need for ^{235}U enrichment (for 2^{nd} generation EM^2 units).
- Reactor core inaccessible without special remote handling equipment.
- Low core excess reactivity cannot be easily reconfigured for material insertion/extraction.

Technology needs and research challenges identified by GA include:

- Transport and thermal-chemical behaviour of fuel and fission products over decades.
- Projecting properties of SiC composites under high neutron fluences and high temperatures.
- Efficient and effective separation of fission products from reactor discharge.
- Defining and establishing manufacturing base to realize the cost effective fabrication of modular reactors like EM^2.

It was stated that the fuel burnup achieved is identical to the total mass of the starter, the implication being that the waste at end of life is nearly the same as the waste component of initial fuelling. As a consequence, there would be no further growth of the nuclear waste inventory. GA claims that in the proposed second generation designs, and the Spent

Nuclear Fuel (SNF) storage could be essentially eliminated, and given the substantive inventories of DU and SNF, it is conceivable that these reactors could provide the entire U.S. energy supply for over 500 years without mining and enriching new uranium fuel [Schleicher et al., 2009].

Additional to the issues mentioned before, it is important to say that work is needed to qualify the performance of the material under the high temperature and irradiation fields of the EM^2 core.

GA is planning to re-use burned EM^2 fuel in subsequent cores. For spent nuclear fuel to be re-used in the EM^2, the fuel has to be processed somehow. GA does not intend to use full chemical separations avoiding with this the wet chemistry; instead a variation of the DUPIC (Direct Use of spent PWR fuel In CANDU) process is proposed where only cladding and volatile fission product removal by heating is done prior to introduction of the material into the fuel fabrication process and solid fission products are left in place. A very similar process is also being considered to modify the bred fuel at the end-of-life (which contains significant fissile material) to serve as the starter material for a subsequent generation of reactors.

2.4 Other non Breed and Burn but Long-Life Core Concepts

There is a special interest for companies to develop long life cores that does not require in site refuelling, some of them even as modular cores. In this section some of the most important concepts will be described. These are not breed and burn reactors but to mention them in the first chapter is important to understand where companies and research groups are aiming.

2.4.1 Toshiba 4S

The 4S (Super-Safe, Small and Simple) reactor is a metallic fuelled sodium cooled fast reactor which target electrical output is 10-50 MW. A remarkable feature of 4S is that its reactivity is not controlled by neutron absorber rods but by neutron reflectors to cope with a long core lifetime and a negative coolant void reactivity.

The reactor is proposed to meet the following design requirements [Ueda et al., 2005]:

- No refuelling more in than 10 years for 50 MWe system and 30 years for 10 MWe.
- Simple core burn-up control without control rod and its rod driving mechanism.
- Removal of control and adjustment components from the reactor system.
- Quality assurance and short construction period based on shop fabrication.
- Load following without operation of reactor control system.
- Minimum maintenance and inspection of reactor components.
- Negative reactivity temperature coefficients including coolant void reactivity.
- No core damage in any conceivable initial events without reactor scram.
- Safety system not dependent on the emergency power and active decay heat removal system.
- Complete containment of reactivity under any operational conditions and decommissioning.

The 4S reactor employs a reactivity control system with an annular reflector instead of the control rods and driving mechanism, which traditionally require frequent maintenance service. Reactivity is controlled only by the vertical movement of the annular reflector during plant start-up, shut-down and power generation; thus, eliminating the necessity of complicated control rod operations. The reflector is installed inside the reactor vessel and the heat generated in the reflector is cooled by sodium coolant.

The reflector is gradually lifted up to control the reactivity according to core burn-up. Regular power operation is attained at a constant speed, which is regulated in scheduled maintenance according to the reflector differential reactivity worth. Since no feedback system or control system are used due to the simplicity, reactor thermal output drifts in several percent during a maintenance interval.

Figure 2.10 shows the scheme of operation controlled by the reflector ring and also the layout of the 10 MWe reference core.

2.4.2 Hyperion Power Module

Based on their publications [Gen4 Energy 2015] the HPM (Hyperion Power Module) is one of the smallest, safest, and simplest designs.

Its main characteristics are:

1. Transportable
    - Unit will measure approximately 1.5 m wide x 2.5 m tall.

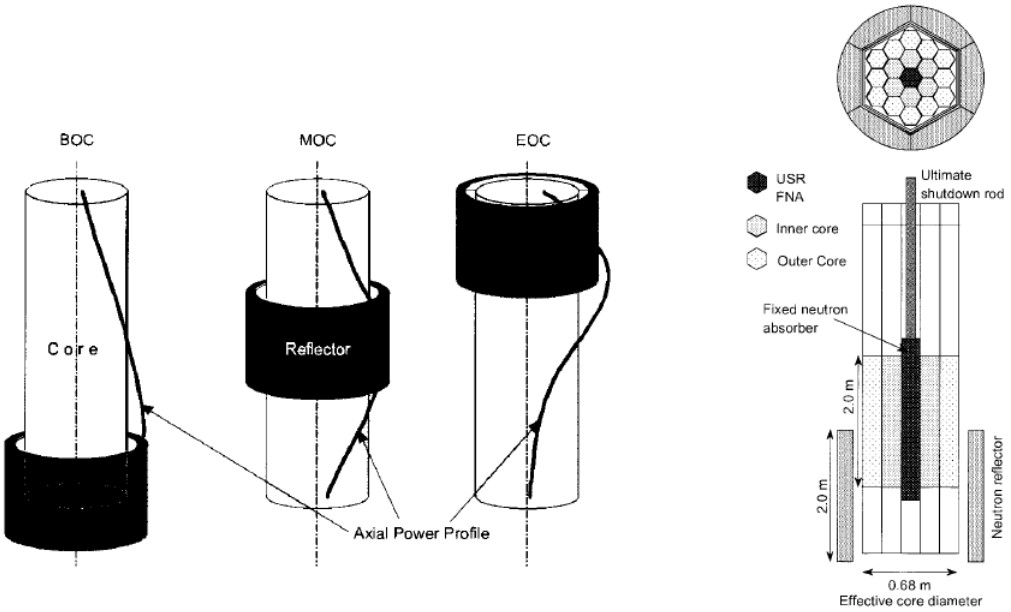

Figure 2.10: Schema of reflector controlled core burning process (left) and layout of the 10 MWe reference core (right) [Ueda et al., 2005]

- Fits into a standard fuel transport container.
- Transported via ship, rail or truck.
- Modular design for easy and safe transport.

2. Sealed Core - Safe and Secure
   - Factory sealed; no in-field refuelling, closed fuel cycle.
   - Returned to the factory for fuel and waste disposition.
3. Safety
   - System will handle any accident through a combination of inherent and engineered features.
   - Inherent negative feedback keeps the reactor stable and operating at a constant temperature.
   - Sited underground, out of sight.
   - Proliferation-resistant; never opened once installed.
4. Operational Simplicity
   - Operation limited to reactivity adjustments to maintain constant temperature output of 500 °C.
   - Produces power for 8 to 10 years, depending on use.

5. Minimal In-Core Mechanical Components
    - Operational reliability is greatly enhanced by the reduction of moving mechanical parts.
6. Isolated Power Production
    - Electric generation components requiring maintenance are completely separated from the reactor.
    - Allows existing generation facilities to be retrofitted.

As a modular reactor, HPM power plants can be "teamed" in groups of two or more to provide additional power. By teaming multiple units, a medium to large-size power plant can be constructed years faster than a plant constructed on site in the traditional manner.

Figure 2.11 shows the diagram of a 25 MWe Electric Power Plant with HPM.

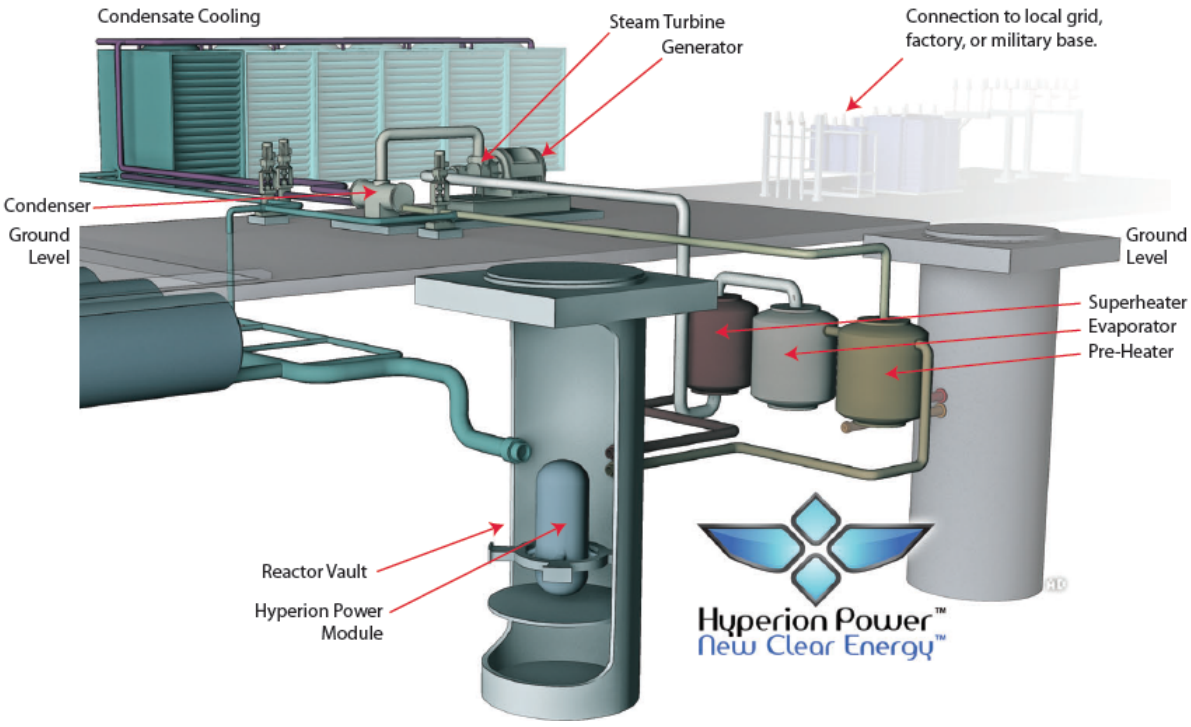

Figure 2.11: Hyperion Power Module-based 25 MWe Electric Power Plant [Gen4 Energy, 2015]

2.4.3 Advanced Reactor Concepts ARC-100

ARC-100 is a design of Advanced Reactor Concepts LCC. The ARC-100 reactor system is a 100 MWe sodium cooled “fast-neutron-spectrum” reactor using a proven metal alloy fuel design. The reactor system is comprised of a small uranium-fueled nuclear core, submerged in a tank of liquid sodium at atmospheric pressure.

Based on the developer [ARC, 2015] this reactor is characterized by five main features:

- *Small Size*: Small enough that its modularized components can be shipped and installed at the site using regular commercial equipment, such as barges, rail, trucks, and construction cranes.
- *Sodium as Coolant*: The use of sodium instead of water as the heat transfer agent in the reactor allows the reactor to operate at ambient pressure. Its containment vessel is a double walled stainless steel tank, rather than a 12-inch thick forged steel containment vessel required for traditional light water reactors.
- *Passive Safety*: Effectively "walk away" fail-safe protection of the reactor from a meltdown does not depend on extra pumps, operator intervention or any external system in the event a disaster destroys all electric power to the plant site.
- *Re-use of Nuclear Waste*: The ability of ARC-100 to recycle traditional nuclear waste and generate energy, burn or transform plutonium that could be used in further reactors and eliminate the need to bury or store large quantities of nuclear waste.
- *Twenty Year Refueling Cycle*: The proprietary reactor core of the ARC reactor is designed to operate for 20+ years without refueling.

The ARC-100 reactor’s long-life fuel "cartridge core" requires very infrequent fuel changeovers and can be replaced entirely by factory personnel. Therefore, ARC-100 customers never handle or have direct access to nuclear fuel. The reactor, control rods, and heat-exchange system are physically sealed and located in a silo below-ground, thereby simplifying the containment system and offering excellent protection against unauthorized access. After installation of the reactor vessel, the fuel cassette is inserted, fuelling the reactor for 20+ years by converting the abundant isotope of uranium (^{238}U) into fuel *in situ*, the reactor produces as much new fissile fuel as it uses. Figure 2.12 shows a diagram of the ARC-100.

2.4.4 Secure Transportable Autonomous Reactor SSTAR

The small lead-cooled fast reactor concept known as the Small Secure Transportable Autonomous Reactor (SSTAR) has been under ongoing development as part of the US ad-

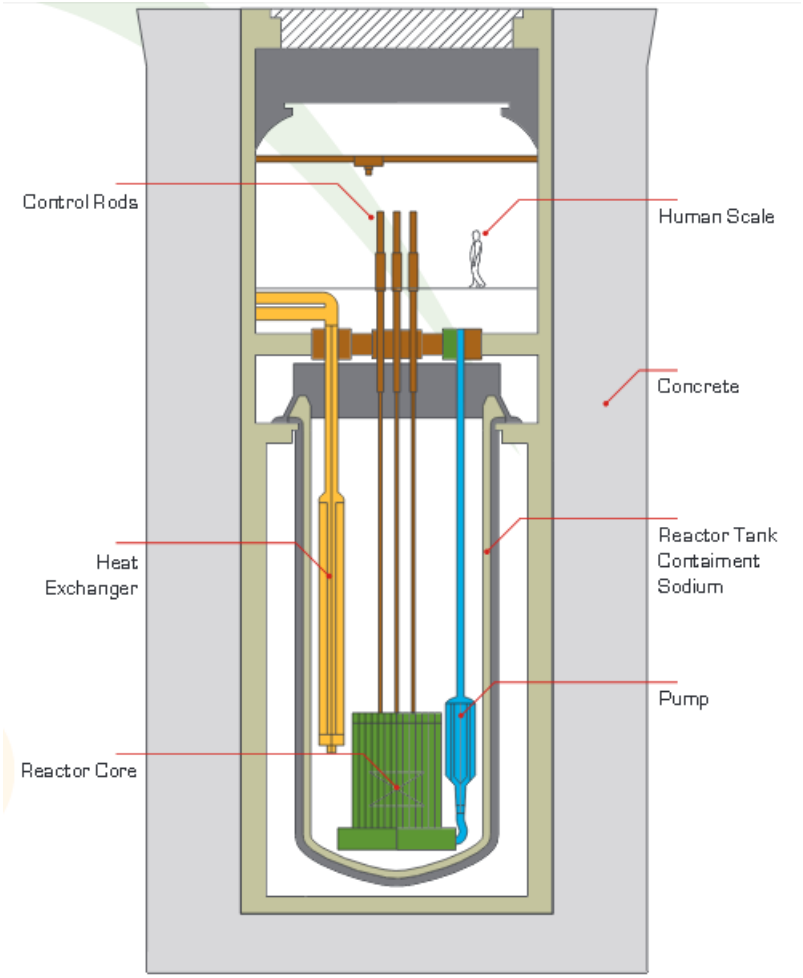

Figure 2.12: The ARC-100 reactor [ARC, 2015]

vanced nuclear energy systems programs [Smith et al., 2008].

The SSTAR initial fissile inventory is relatively large; nevertheless, the one-time initial fissile loading is substantially less than the lifetime ^{235}U consumption of a LWR for the same energy delivery.

Conversion of the core thermal power into electricity at a high plant efficiency of 44% is accomplished by utilizing a supercritical carbon dioxide Brayton cycle power converter.

Figure 2.13 shows the layout of a 20 MWe SSTAR core. The reference 20 MWe core comprises small shippable reactor (12 m x 3.2 m vessel), with a 30-year life open-lattice cassette core and large-diameter fuel pins (2.5 cm) held by spacer grids welded to control rod guide tubes. The design integrates three major features: primary cooling by natural circulation heat transport; lead (Pb) as the coolant; and transuranic nitride fuel in a pool vessel configuration.

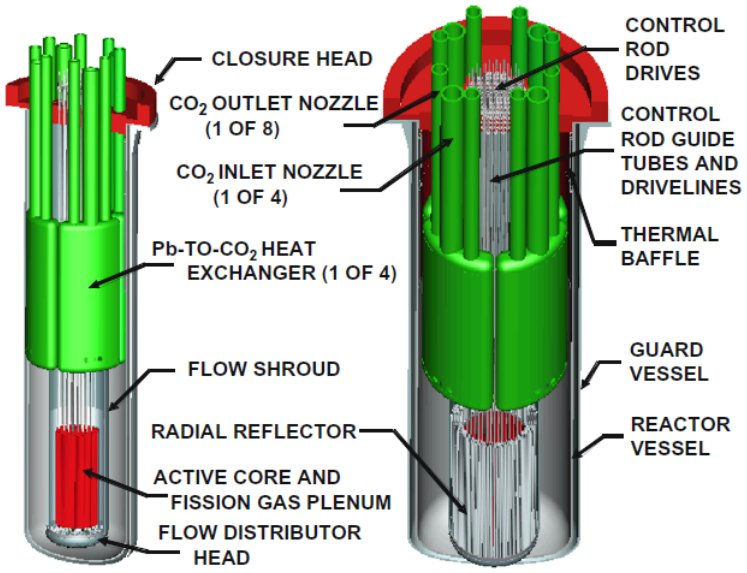

Figure 2.13: Conceptual 20 MWe (45 MWt) SSTAR reactor [Smith et al., 2008]

The main mission of the 20 MWe (45 MWt) SSTAR is to provide incremental energy generation to match the needs of developing nations and remote communities without electrical grid connections. Design features of the reference SSTAR in addition to the lead coolant, 30-year cassette core and natural circulation cooling, include autonomous load following without control rod motion, and use of a supercritical CO_2 (S-CO_2) Brayton cycle energy conversion system. The incorporation of inherent thermo-structural feedbacks

imparts walk-away passive safety, while the long-life cartridge core life imparts both energy security and strong proliferation resistance.

2.4.5 Radowsky Thorium Reactor

The original seed-blanket reactor was the Shippingport (Pennsylvania) [Kasten, 1998] reactor design for Light Water Reactors (LWRs) developed in the 1950s by the Naval Reactors Division of the US Atomic Energy Commission (USAEC) under Admiral Rickover; Radkowsky was a key member of Rickover's staff at the time. Changes in the original Shippingport design resulted in the Light Water Breeder Reactor (LWBR) utilizing ^{233}U as the fissile fuel in the "seed" regions, and thorium in the "blanket" regions. The purpose of the LWBR was to demonstrate fuel "breeding" in an LWR with fuel recycle, an objective that was attained with a "breeding ratio" of about 1.01 [Rosenthal et al., 1965].

Radkowsky Thorium Reactor (RTR) concept makes use of a seed-blanket geometry with thorium as fertile material, and uranium of less than 20% enrichment as fuel in both seed and blanket regions.

A key feature of the design is use of a heterogeneous, seed-blanket-unit (SBU) fuel assembly, with the thorium blanket part of the fuel assembly separated from the uranium-seed part. The separation allows independent fuel management of the thorium blanket and the "driving" part of the core consisting of the "seed." The intent is to have high *in situ* fissioning of the ^{233}U bred in the blanket, with the seed supplying neutrons to the blanket.

The SBU geometry provides the necessary flexibility to be compatible with existing pressurized water reactor power plants. The RTR fuel can replace a standard uranium fuel assembly in conventional PWRs or VVERs.

About 163 seed-blanket units are employed in a 1000 MWe RTR, and fuel shuffling during refuelling is used to maintain acceptable power distribution and relatively-low critical mass.

The high fuel burnups of both the blanket and seed fuels relative to that in a conventional PWR, results in a substantial decrease in the plutonium present in RTR spent fuel, and to substantial increases in the percentages of ^{238}Pu, ^{240}Pu, and ^{242}Pu in that spent fuel. The RTR reactor design features are very similar to a conventional PWRs, such that application of the general seed-blanket arrangement could be implemented rather quickly if there were no reactor safety, technical or economic concerns.

The seed fuel consisted of U/Zr-alloy rods, which was claimed to be consistent with the

fuel technology capabilities of the fuel vendor industry of the Russian Federation. The RTR blanket fuel consists of thorium with addition of slightly enriched UO_2. The uranium is added to generate power in the blanket and to "denature" the ^{233}U bred within the blanket. For reasons of fuel economy, the blanket in-core residence time is quite long (about 10 years with a burnup of 100 MWd/kg). The seed part of an SBU is replaced on an annual basis, with a three-year cycle.

A novel fuel in-core management scheme is employed. The standard multi-batch fuel management of a PWR is replaced by a more complicated scheme, based on two separate fuel flow routes (i.e., seed route and blanket route). Seed fuel is treated similarly to standard PWR assemblies, with one-third of seeds replaced annually by fresh seeds; the remaining two-thirds (partially depleted) are reshuffled/relocated. Each fresh seed is loaded into an empty blanket, forming a new fuel type. These new fuel type assemblies are reshuffled together with partially depleted blanket-seed assemblies to form a reload to configuration for the next cycle.

In summary, RTR fuel management is based on a batch-reload scheme. One-third of all seed sub-assemblies are replaced annually by fresh seeds, while the remaining two-thirds are left within corresponding blanket sub-assemblies and reshuffled as partially-depleted fuel assemblies. The in-core residence time of seed sub-assemblies is 3 years. The blanket sub-assemblies are burned for ten years, with fresh seed replacement every three years. The reload configuration is generated on the basis of 3 batches: fresh fuel, once burned fuel, and twice burned fuel. No "fresh" assemblies are loaded in peripheral positions (i.e., at reflector boundaries). Most of the peripheral positions are occupied by once-through fuel. Burnable poisons are used to compensate for local power peaking. The reactive control system of the RTR core has burnable poisons and a control rod system, without utilization of soluble-boron control during operations.

2.5 Summary of the Technology Review

Fast reactors development has been going on since the beginning of nuclear reactor technology. Their versatility of fast reactors had made them interesting options for energy generation among other applications, through the history of nuclear reactor engineering.

Breeding its own fissile fuel from fertile material, is an interesting feature that promise to extend the operative life of the current uranium resources, being this the reason of choosing this kind of core as the main subject of this research.

The brief bibliographic study on the state of the art of Breed/Burn reactors presented in this chapter gives the reader a complete picture of their evolution and where the efforts are being aimed.

Chapter 3

MODEL DESCRIPTION

This chapter describes the process of building a model of the studied BBR, starting from selected references.

It is important to note that by this point the Traveling Wave Reactor (TWR) where the breed/burn wave physically moves trhough the core, lead to several engineering challenges [Halper, 2013], as a result the project was abandoned. Therefore the "Standing Wave" reactor type was decided to be analysed.

3.1 Reference Cores

Compilation of information for a commercial project that is in development is not an easy task mainly because companies do not publish their findings to protect their proprietary data. As an example of this, Figures 3.1 and 3.2 show how TWR information is blanked in a technical study report [Kim and Taiwo, 2010b].

The core model of this research project used is the TerraPower TP-1 [Ahlfeld et al., 2011] where some of the most important design features are explained, such as geometric information, fuel cycles length, enrichment limit and core life. Figure 3.3 shows the layout of the core, and Table 3.1 shows some of the main characteristics.

Another TerraPower publication [Weaver et al., 2010] gave the fuel pin diameter and its pitch of an early model, but since assemblies had different characteristics such as number of pins by assembly and Flat-to-Flat length, these data was not considered for this model.

The active and feed fuel assemblies contain __ fuel pins arranged in a triangular pitch array. The assembly pitch at the fabrication stage is __ cm. The fuel pin diameter and cladding thickness are _ mm and ___ mm, respectively. Fuel pins are made of sealed cladding containing a lower shield, a binary metallic fuel and a gas plenum from the bottom of the pin. The fuel pin is helically wrapped with wire to maintain pin spacing so that coolant can flow freely through the pin bundle. The heights of the heated fuel pin and fission gas plenum are ___ cm and ____ cm, respectively. The overall assembly height is __ cm including the lower shield of _ cm. Sodium is used as the initial thermal bond between the fuel column and the cladding. At the fabrication state, the resulting volume fractions of fuel, structure, bond sodium and coolant sodium are ~34, ~21, ~14 and ~31 %, respectively.

A U-Zr binary metallic fuel was adopted in the TWR core concept. The initial smeared density is chosen to be _% to allow for the release of fission gas from the metallic fuel. The Zr weight fraction in the binary fuel is assumed to be _%, and ~14 % enriched uranium is used for the igniter fuel while depleted uranium is used for the feed fuel.

Figure 3.1: Censorship of TerraPower proprietary data in text [Kim and Taiwo, 2010b]

(Removed due to proprietary data)

Figure 3.13. Core Layout of Initial TWR Core Concept.

Figure 3.2: Censorship of TerraPower proprietary data in images [Kim and Taiwo, 2010b]

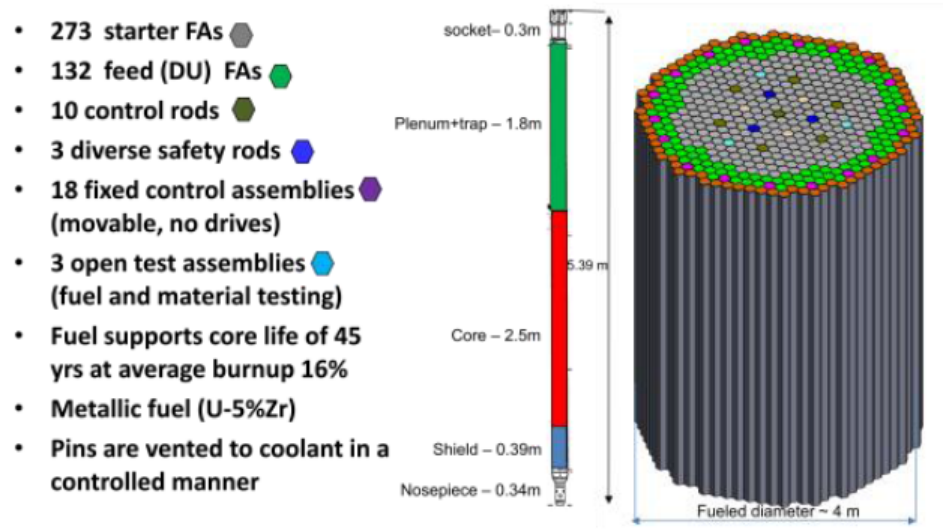

Figure 3.3: Geometry of the TP-1 core [Ahlfeld et al., 2011]

Table 3.1: Main features of TP-1 reactor

Power	1200 MWt
Core Life	40 years
Availability	90%
Pins per Assembly	169
Assembly duct Flat-to-Flat	15.99 cm
Space between ducts	6.0 mm
Enrichment Limit	20%
Fuel Cycles	18-24 months

From the same reference, it was learnt that Stainless Steel HT-9 was being considered for the design of the TWR.

As mentioned before, available technical data of TWR was limited due to proprietary issues. In order to construct a complete model it was needed to obtain data from a different core; for completing the model Superpohenix [Todreas and Kazimi, 1990][IAEA, 2007] data was taken for fuel assembly and control rod modelling.

3.2 Core Modeling

In this section the process of the core model construction is described.

3.2.1 Fuel Assembly

TWR's assembly flat-to-flat distance and number of assemblies were given on the references, no modifications were done so 15.99 cm the flat-to-flat width was established plus 0.6 cm thick channel wall. It is important to note that since every hexagonal channel is next to each other, the whole channel wall is 1.2 cm thick.

3.2.2 Fuel Pin Modeling

The first step to construct the fuel pin is to estimate its pitch. The hexagonal channel that contains the fuel assembly is divided into 169 unitary hexagonal cells, then the pin pitch is taken as the cell width as shown in Figure 3.4. The modeling process initially considered

a wire wrapping the fuel clad as in the Superphenix fuel but this was later abandoned due tof o difficulties on its implementation in the neutronic code.

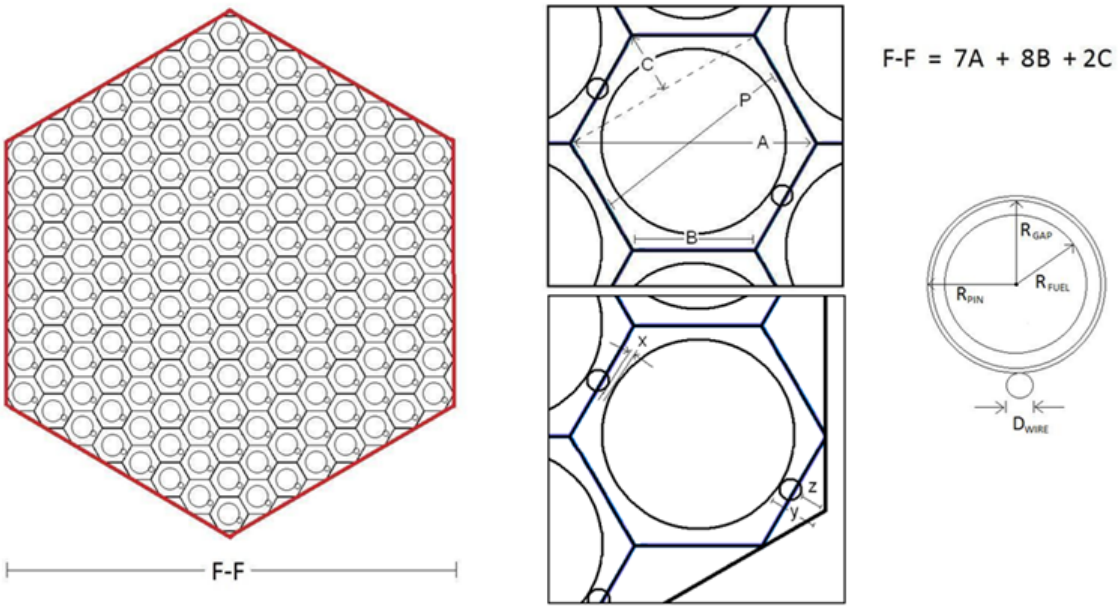

Figure 3.4: Fuel assembly (left) and pin (right) layout

the pitch was calculated with the explained method and a 12.04 mm pitch was obtained. From references it is easy to know Superphenix [Todreas and Kazimi, 1990] pitch (9.7 mm), clad thickness (0.7 mm), gap thickness (0.125 mm), fuel pellet radius (3.5 mm) and pin radius (4.325 mm). It was easy to calculate the parameters for the studied TWR fuel pin. Table 3.2 shows this data.

Table 3.2: Pin geometric data for Superphenix and TWR

	Superphenix	**TWR**
Pitch	9.7 mm	12.042 mm
Cladding thickness	0.7 mm	0.869 mm
Gap	0.125 mm	0.155 mm
Fuel pin radius	4.324 mm	5.369 mm
Fuel pellet radius	3.5 mm	4.345 mm

The Figure 3.4 shows the original model for the fuel pin included a wrapping wire and even gap. This had to be modified in order to be implemented in KANEXT, since the code

does not manage gap, instead a fuel pellet is defined and immediately next to it is the fuel cladding, then the coolant.

In order to fix this issue, the fuel pellet was swollen (increasing its radius and reducing its density) to fill also the gap. At some point it was also considered the swelling of the fuel cladding but this was later abandoned since it implied to make further correction on every zone containing steel, since by swelling it, its density should be reduced and it would have affected to al the steel present in the core. Figure 3.5 shows the original unitary cell A), and how it should be treated for KANEXT implementation B) and C); the definitive treatment was the C).

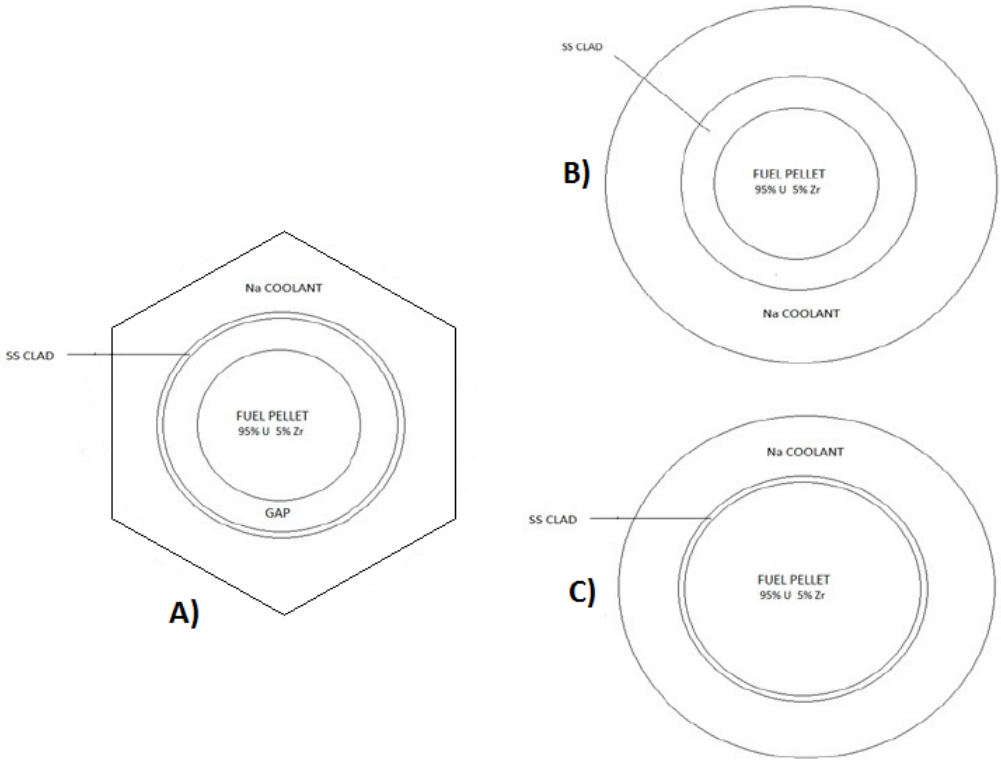

Figure 3.5: Different ways to see the unit cell

The Uranium's density is 19.1 gr/cm3 in the fuel, but when the fuel pellet is smeared to cover the gap (case C in Figure 3.5) is 17.81 gr/cm^3. We have to remember that only 95% of the fuel pellet is fuel itself, and the other 5% is Zr; this U density reduction is taken into account in the implementation process with a parameter called `FUSD`, it is explained more

deeply in the chapters "Description of the Code KANEXT" and "Model Implementation on the Code KANEXT".

Regarding the Zr contained in the fuel, the atomic density is 0.04291 at/b-cm (atoms over barn-centimetre) [Lamarsh and Baratta, 2001] and after smearing and considering its proportion on the fuel, the new density is 0.002000086 at/b-cm. The Table 3.3 shows the atomic density for each isotope of Zr.

The reason of why the fuel is calculated in mass density and Zr in atomic density will be explained in the next chapter, where the code KANEXT is described.

Table 3.3: Isotopic density of Zr in the fuel

Isotope	**Abundance**	**At. Dens. (at/b-cm)**
^{90}**Zr**	51.45 %	1.029044x10^{-3}
^{91}**Zr**	11.22 %	2.244096x10^{-4}
^{92}**Zr**	17.15 %	3.430147x10^{-4}
^{94}**Zr**	17.34 %	3.476149x10^{-4}
^{96}**Zr**	2.80 %	5.600240x10^{-5}

3.2.3 Control Rods Modeling

The control rods used for this core are identical to those of Superphenix [IAEA, 2007]. Each control rod assembly consist of 31 pins of 2.1 cm of diameter and 100 cm high (since the models used were 100 cm high). The pins consisted in B_4C with 90% enrichment in ^{10}B.

From bibliography [Wikipedia, 2015] the B_4C mass density (2.52 gr/cm^3) and the molar weight (55.255 gr/mol) are taken into account to calculate the B_4C molecule density: 2.7465x10^{22} molecules/cm^3.

Given the rods geometry previously described, it is easy to calculate that each control assembly has a volume of 10737.18 cm^3.

As it is explained in the implementation chapter, when an assembly does not contain any fissile material, as in the case of absorber assemblies, or reflector; atomic densities (averaged on the whole space and not only in the control rod volume) of every isotope present in the material must be given to the code. Table 3.4 shows isotopic inventories.

Table 3.4: B_4C inventory on control rod assembly

	Abundance	at/cm^3	Averaged (at/b-cm)
B		$1.0986x10^{23}$	
^{10}B	90.0 % %	$9.8874x10^{22}$	$4.453990x10^{-02}$
^{11}B	10.0 % %	$1.0986x10^{22}$	$4.948877x10^{-03}$
C		$1.0986x10^{23}$	
^{12}C	98.9% %	$2.7163x10^{22}$	$1.223610x10^{-02}$
^{13}C	1.10%	$3.0212x10^{20}$	$1.360941x10^{-04}$

3.2.4 Axial Reflector

The axial reflector assembly was considered to be identical in geometry as the fuel assembly, i.e. a 169-pin assembly inside a SS HT-9 channel wall of 0.6 cm thick and 15.99 cm flat-to-flat distance. The only change is that for this case, the fuel pellet is replaced with a steel pellet of the same dimensions.

The axial reflector is located above and under the active core to reduce the number of neutrons escaping in this direction.

3.2.5 Radial Reflector

Immediately outside the reactor, there are radial reflector elements. These reflective elements consist on solid hexagonal blocks of SS HT-9 with the same size as the channel that contains the assemblies, i.e. 16.59 cm flat-to-flat.

It is important to note that every place where Steel SS HT9 is present, such as SS Block, SS pellet or fuel cladding, the steel is exactly the same and its atomic density remains unchanged. In order to calculate the SS HT-9 isotopic densities [Ren et al., 2006], the isotopic composition of each element and its properties [Lamarsh and Baratta, 2001] were used. The isotopic densities of SS HT-9 are shown in Table 3.5.

Table 3.5: Isotopic density of SS HT-9

Element	%at	A	At/b-cm	Element	%at	A	At/b-cm
Fe	84.31			Ni	0.59		
		54	$3.462668x10^{-03}$			58	$2.819480x10^{-04}$
		56	$5.435648x10^{-02}$			60	$1.086059x10^{-04}$
		57	$1.255328x10^{-03}$			61	$4.721022x10^{-06}$

		58	$1.670611x10^{-04}$			62	$1.505268x10^{-05}$
Cr	12.82					64	$3.833475x10^{-06}$
		50	$3.913036x10^{-04}$	V	0.33		
		52	$7.545900x10^{-03}$			50	$5.773975x10^{-07}$
		53	$8.556445x10^{-04}$			51	$2.303816x10^{-04}$
		54	$2.129880x10^{-04}$	W	0.15		
C	0.98					180	$1.228707x10^{-07}$
		12	$6.781420x10^{-04}$			182	$2.713396x10^{-05}$
		13	$7.542530x10^{-06}$			183	$1.465234x10^{-05}$
Mn	0.70					184	$3.137300x10^{-05}$
		55	$4.925676x10^{-04}$			186	$2.911013x10^{-05}$
Mo	0.60			P	0.02		
		92	$6.218815x10^{-05}$			31	$1.646033x10^{-05}$
		94	$3.886233x10^{-05}$	Cu	0.02		
		95	$6.694594x10^{-05}$			63	$8.536200x10^{-06}$
		96	$7.023008x10^{-05}$			65	$3.808269x10^{-06}$
		97	$4.025177x10^{-05}$	Co	0.03		
		98	$1.018505x10^{-04}$			59	$1.996415x10^{-05}$
		100	$4.071492x10^{-05}$				
Si	0.60						
		28	$3.863316x10^{-04}$				
		29	$1.962595x10^{-05}$				
		29	$1.295271x10^{-05}$				

3.3 Full Core Model

In this section, the most representative core layouts, developed in this research, are shown. It is important to clarify that not all the tested layouts are shown, but only the most important, since not all of the layouts had successful results.

Through the research the whole core suffered evolution, the intention was initially to reproduce the core showed by TerraPower [Ahlfeld et al., 2011], as shown in Figure 3.6 (top left). Since the power density of the TP-1 was found very low, the next step was to modify some features of the original model in order to develop a more satisfying one. A few new layouts and number of fuelled zones were tested as seen in Figure 3.6 where every colour

represents a different enrichment.

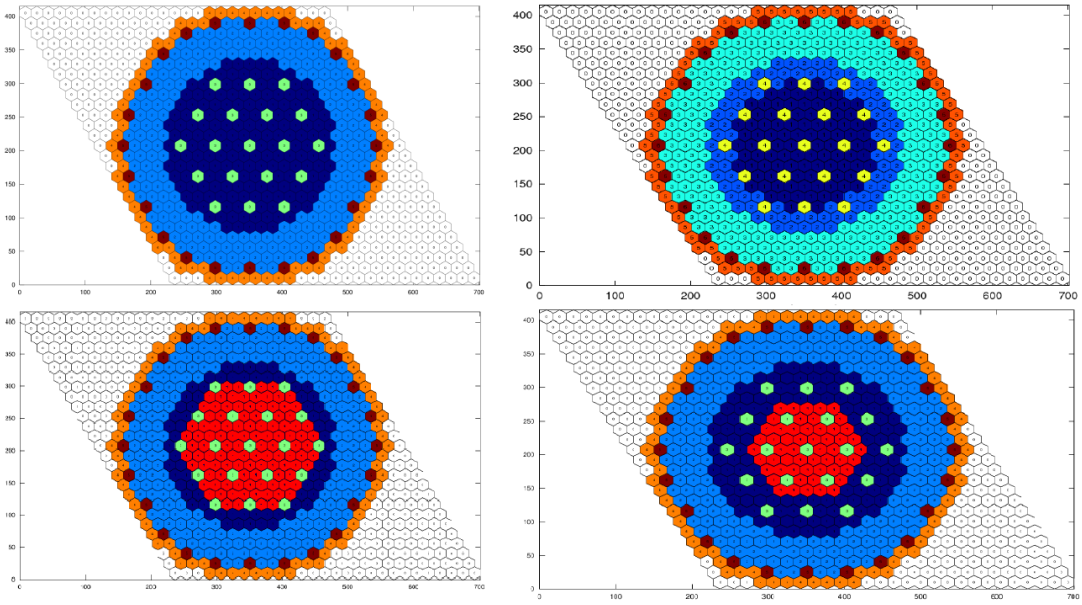

Figure 3.6: Evolution of big-sized TWR core

Further in the research, the idea of designing the TWR as a kind of small modular reactor grew, as seen Figures 3.7 and 3.8. We found out that with small reactors the possibilities of reshuffling are limited due to the small number of fuel assemblies inside the core.

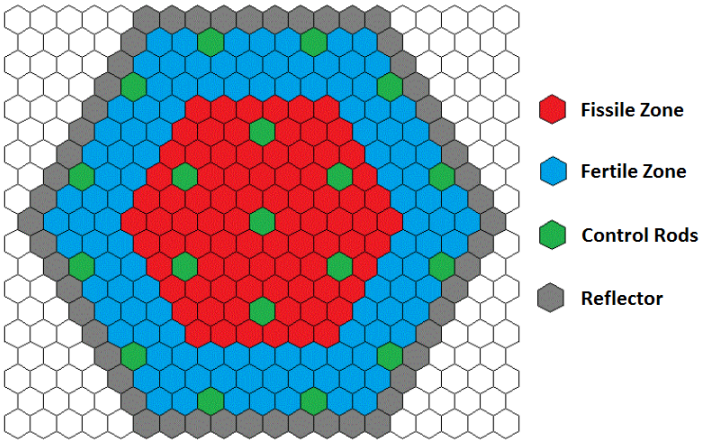

Figure 3.7: Medium-sized core

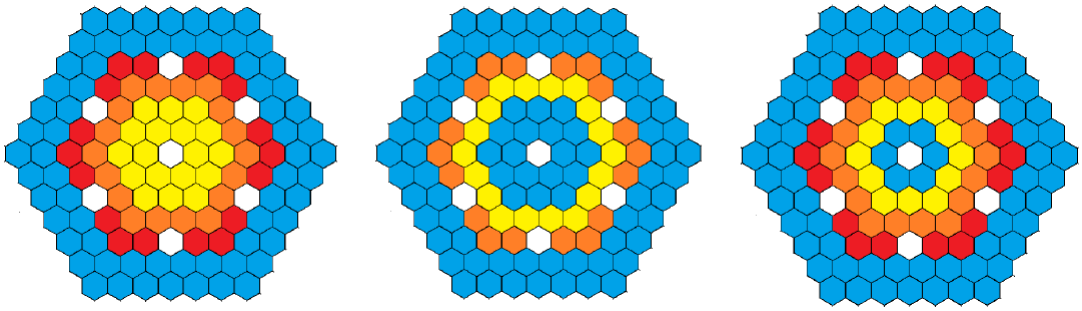

Figure 3.8: Small-sized core

Medium sized cores were develop to increase the fuel reshuffling options without increasing too much the reshuffling management. This medium-sized layouts are shown in the next chapters, since the main study cases were done with this geometry.

After abandoning the exact model of the TP-1, positive results were obtained with layouts that include two blanket zones: one internal and one external. Here the fissile zone would be placed between the two blankets. This decision was motivated by the fact that given the geometry, there would be an important population of fast neutrons in the central area, so, in order to take advantage of this, a central blanket was considered.

3.4 Reshuffling Schemes

A long life of the B&B reactor is expected to be achieved through fuel assemblies reshuffling. Fissile fuel is expected to be bred in the fertile zones and after a few cycles, this fissile fuel is burnt in the fissile areas.

Different fuel reshuffling schemes were tested. In this section only a couple of them are shown, however some cases were tested using a small sized model. It is important to note that the use of a small simplified core was possible when a better knowledge of the fuel breed/burn process was acquired, mainly in fuel management strategies and the reshuffling option in the code KANEXT.

3.4.1 Simple Reshuffling Scheme

As mentioned before, in some of the tested cores, a central blanket area was used. This is the case of the core shown in this section. The core consists in two blanket zones with depleted uranium (0.35 at% ^{235}U) and two fissile zones (17.0 at% and 20.0 at% ^{235}U). The operation power was set to 500 MWt.

The active core height is 100 cm with 100 cm axial reflector under and above the active core. Outside the core there are two rings of SS HT-9 blocks as radial reflector. Seven spaces were distributed for control rods, these spaces were filled with assemblies identical to the axial reflector, i.e. the same characteristics as the fuel assemblies but with SS HT-9 pellets.

It was observed in the simulation runs that a big reactivity step-down in the moment of the first reshuffle, since we are taking from the center an assembly that has already bred some fissile fuel and replaced it by a fertile one. In order to compensate this reactivity loss, one enriched assembly (8.0 at% ^{235}U) was placed at the peripheral zone. Once this assembly is placed in the center in the first reshuffle, the neutron multiplication factor can be sustained above 1.0.

The layout of the core is shown in Figure 3.9 (left). The fuel reshuffling scheme is also shown (right). As mentioned before, this scheme is a very simple strategy where every fuel assembly is moved one position, except for the most external one that is moved to the first position.

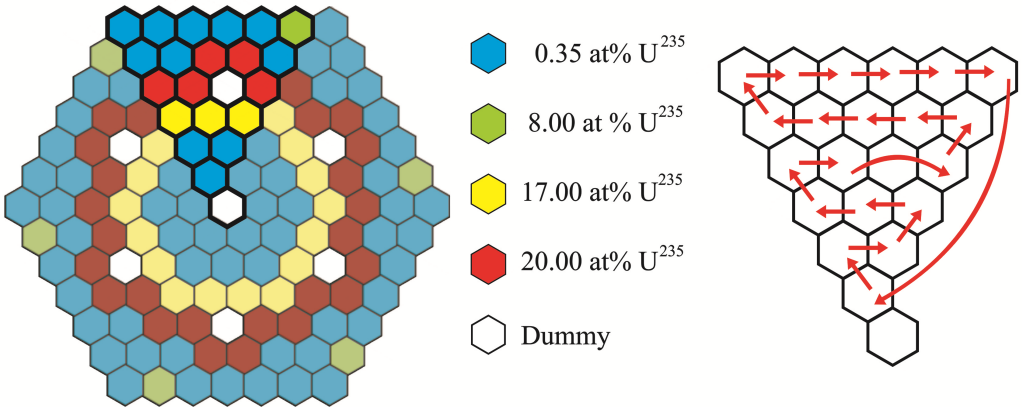

Figure 3.9: Small-sized core layout (left) and simple reshuffling scheme (right)

Table 3.6: Description of burnup steps duration of the simple reshuffling scheme

Step	Duration (days)	Years after time step	Step	Duration (days)	Years after time step	Step	Duration (days)	Years after time step
1	365	1.00	16	364	14.00	31	365	26.00
2	365	2.00	17	365	15.00	32	1	26.03
3	365	3.00	18	365	16.00	33	364	27.00
4	365	4.00	19	365	17.00	34	365	28.00
5	365	5.00	20	1	17.03	35	365	29.00
6	365	6.00	21	364	18.00	36	1	29.03
7	365	7.00	22	365	19.00	37	364	30.00
8	1	7.03	23	365	20.00	38	365	31.00
9	364	8.00	24	1	20.03	39	1	31.03
10	365	9.00	25	364	21.00	40	364	32.00
11	365	10.00	26	365	22.00	41	365	33.00
12	365	11.00	27	365	23.00	42	1	33.03
13	365	12.00	28	1	23.03	43	364	34.00
14	365	13.00	29	364	24.00	44	365	35.00
15	1	13.03	30	365	25.00			

Table 3.6 shows the burnup steps used for the simulation. For KANEXT, reshuffling is instantaneous, so in order to visualize the jumps in the neutron multiplication factor (k_{eff}), a small burnup step should be calculated after the reshuffling; in all the cases described in this thesis, a 1-day step is used. Figure 3.10 shows the evolution of k_{eff} though the core life.

As Figure 3.10 shows, operation of the core for 35 years, except for a couple peaks, the core was supercritical along this period.

3.4.2 More Elaborated Reshuffling Scheme

After testing a simple reshuffle strategy, the next step was to develop a more complex and efficient one. In this section, one of the main tests with the small-sized core model is shown.

For this case, the same geometry and power are used as the one in previoust. Fuel enrichments were modified as well as the location of the enriched assemblies. In this case, two

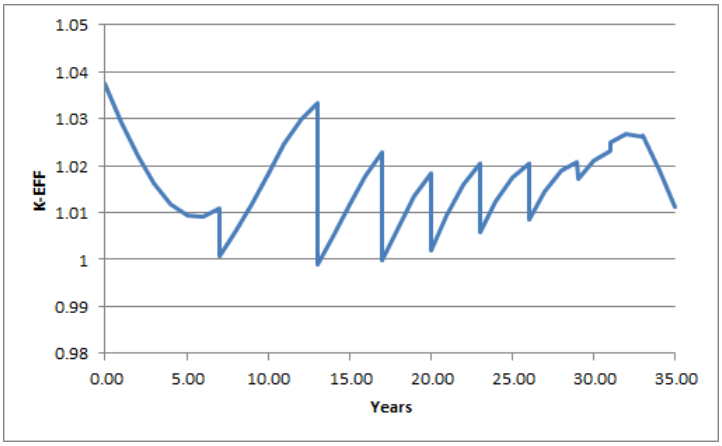

Figure 3.10: Evolution of k_{eff} with simple reshuffle scheme

enriched assemblies were located in the outskirts of the core. The space for the control rods and the two reflector rings along with the two axial reflector regions were maintained. Enrichments are shown in Figure 3.11. The used burn steps are shown in Table 3.7.

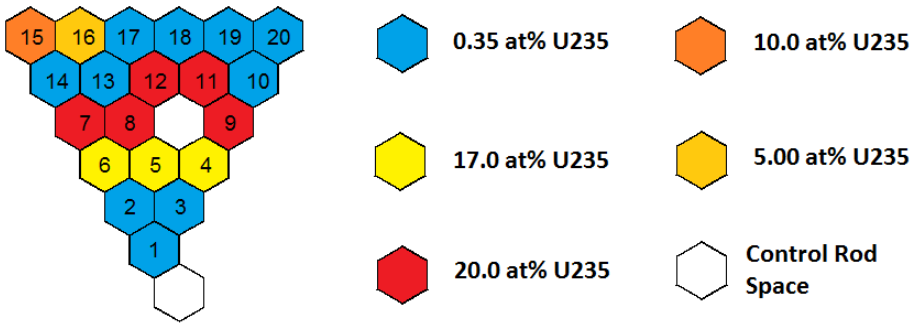

Figure 3.11: Layout of $1/6^{th}$ of the core

The fuel reshufflings are shown in Figures 3.12 to 3.20. In the left part of the figure is shown how the layout is before the reshuffle, in the middle part the reshuffle relocations are shown, and in the right part of the image is shown how the layout is left after the reshuffling.

In Figure 3.21 a plot of the k_{eff} is shown. The operation of the core was sustained super-critical for 37 years. Still, given the peaks in the first two reshuffles, it can be concluded that the enrichments in the two peripheral assemblies were too high.

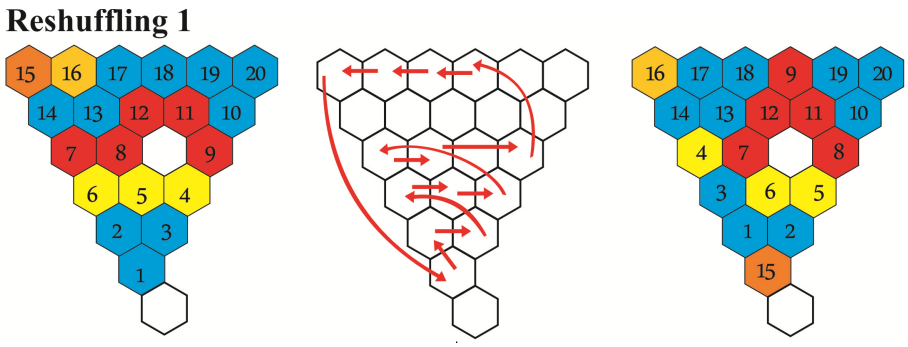

Figure 3.12: Description of the reshuffling 1.

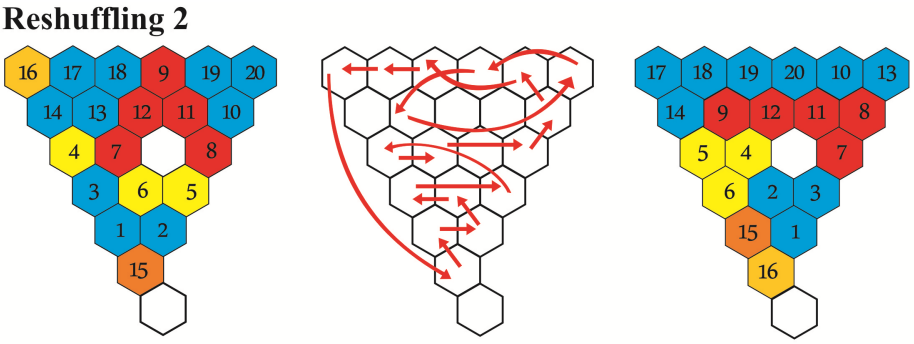

Figure 3.13: Description of the reshuffling 2.

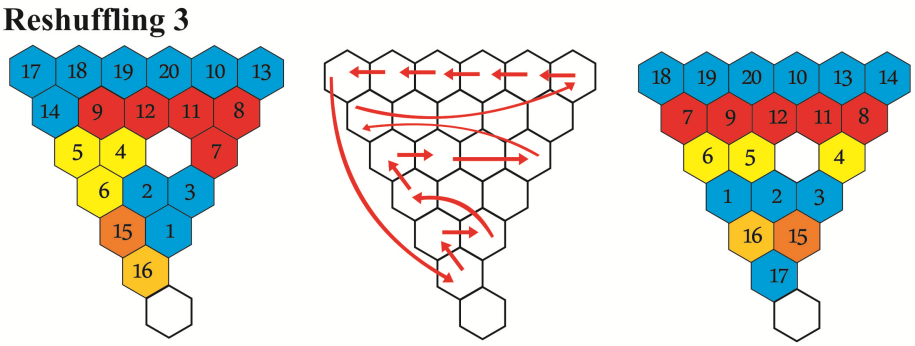

Figure 3.14: Description of the reshuffling 3.

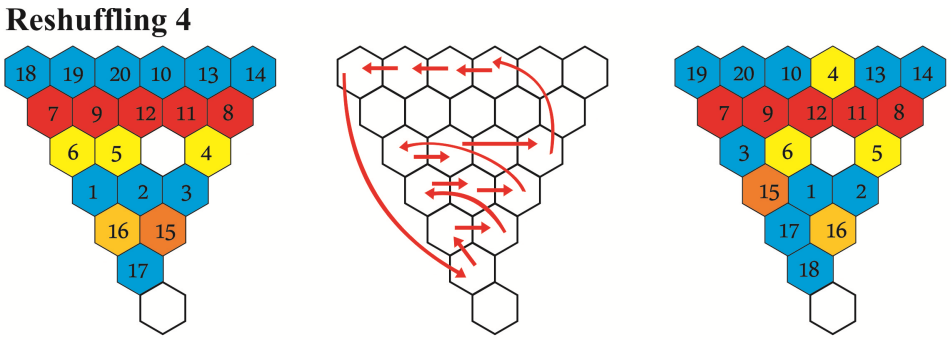

Figure 3.15: Description of the reshuffling 4.

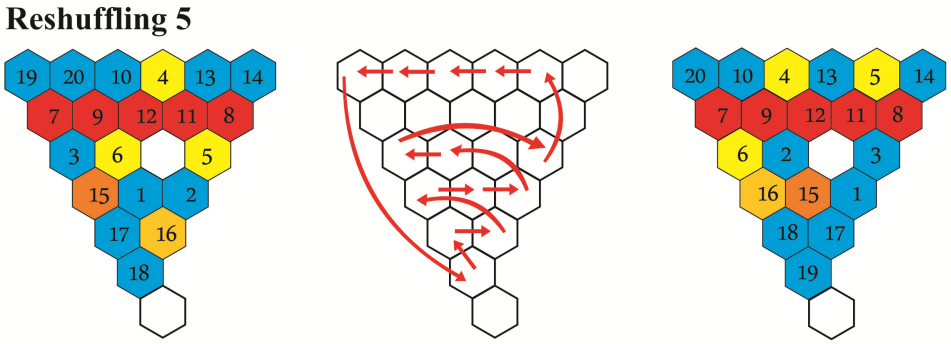

Figure 3.16: Description of the reshuffling 5.

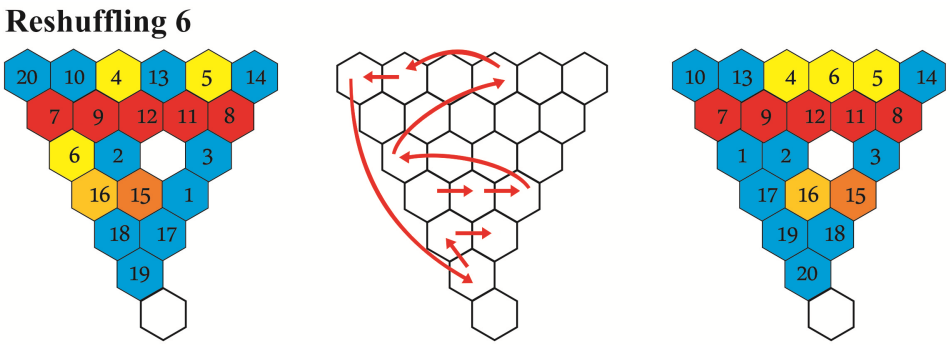

Figure 3.17: Description of the reshuffling 6.

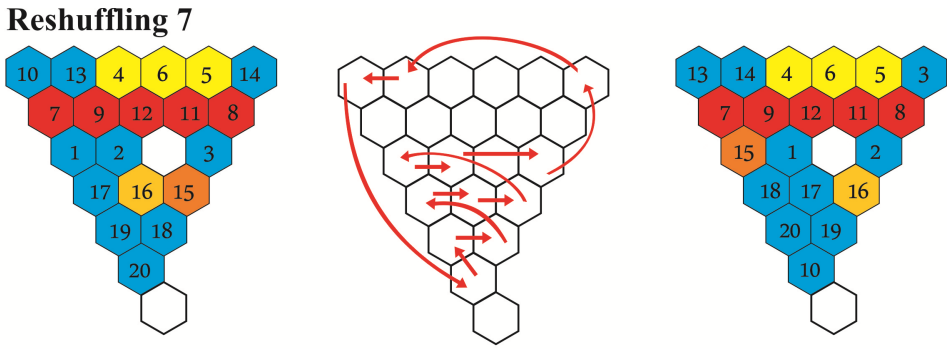

Figure 3.18: Description of the reshuffling 7.

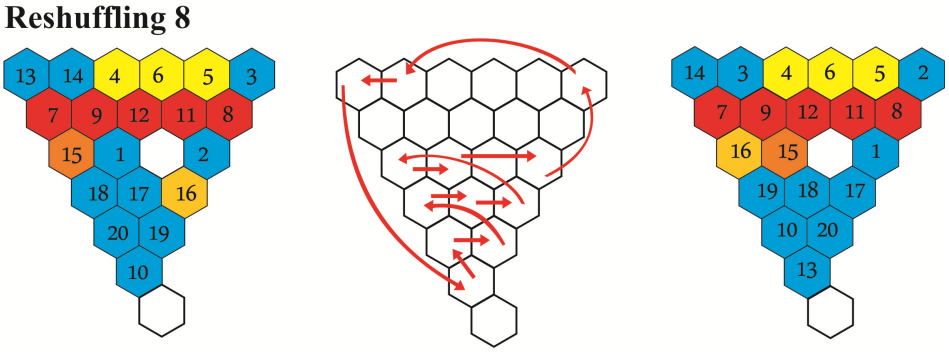

Figure 3.19: Description of the reshuffling 8.

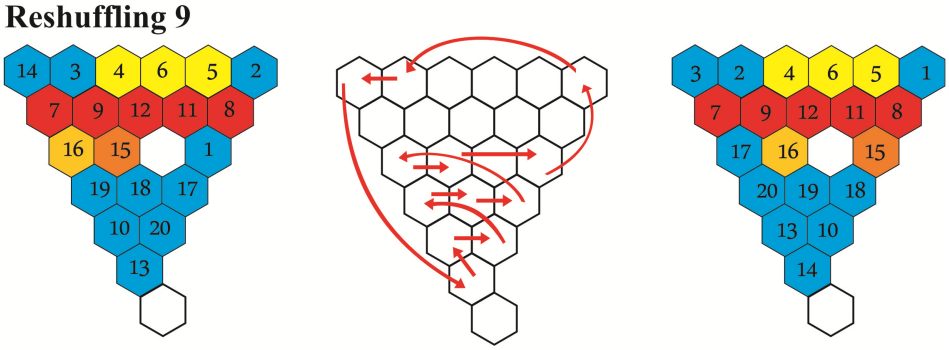

Figure 3.20: Description of the reshuffling 9.

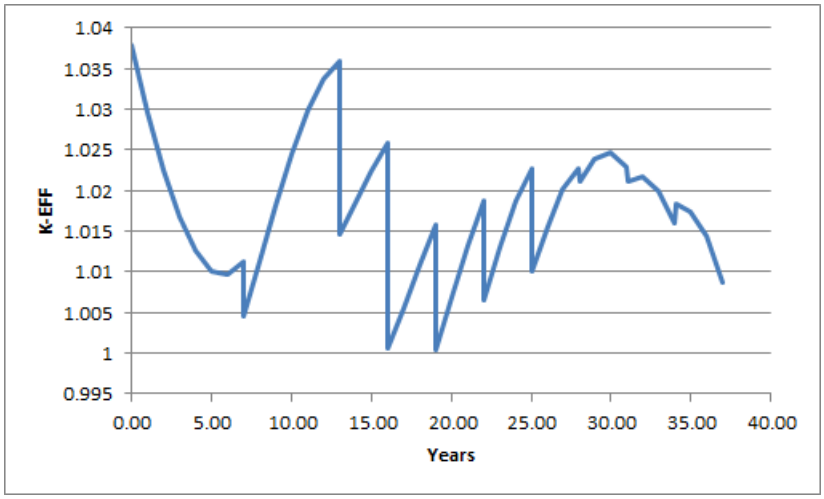

Figure 3.21: Evolution of k_{eff} with simple reshuffle scheme

At this point the work was done with reactivity excess, as can be seen in Figures 3.10 and 3.21. It was later found that a better performance can be obtained reducing this initial reactivity excess, as it will be shown in the further chapter where the more definitive models and reshuffling schemes are described.

Table 3.7: Description of burnup steps duration of the more elaborated reshuffling scheme

Step	Duration (days)	Years after time step	Step	Duration (days)	Years after time step	Step	Duration (days)	Years after time step
1	365.0	1.000	17	365.0	15.000	33	365.0	27.000
2	365.0	2.000	18	365.0	16.000	34	365.0	28.000
3	365.0	3.000	19	1.0	16.003	35	1.0	28.003
4	365.0	4.000	20	364.0	17.000	36	364.0	29.000
5	365.0	5.000	21	365.0	18.000	37	365.0	30.000
6	365.0	6.000	22	365.0	19.000	38	365.0	31.000
7	365.0	7.000	23	1.0	19.003	39	1.0	31.003
8	1.0	7.003	24	364.0	20.000	40	364.0	32.000
9	364.0	8.000	25	365.0	21.000	41	365.0	33.000
10	365.0	9.000	26	365.0	22.000	42	365.0	34.000
11	365.0	10.000	27	1.0	22.003	43	1.0	34.003
12	365.0	11.000	28	364.0	23.000	44	364.0	35.000
13	365.0	12.000	29	365.0	24.000	45	365.0	36.000

14	365.0	13.000	30	365.0	25.000	46	365.0	37.000
15	1.0	13.003	31	1.0	25.003			
16	364.0	14.000	32	364.0	26.000			

Chapter 4

DESCRIPTION OF THE CODE KANEXT

In this chapter a detailed description of the KANEXT code is given, but first a brief overview of this code and a review of its evolution is presented.

4.1 Generalities of the Code KANEXT

The KArlsruhe Neutronic EXtendable Tool KANEXT is the follow-up version of the KArlsruhe PROgram System KAPROS developed in the Karlsruhe Research Center (now Karlsruhe Institute for Technology) since the early seventies to facilitate nuclear reactor simulations [Woll, 2005].

The KANEXT code system consists mainly of one kernel and several modules:

- The *kernel* routines contain the main program and a set of interface routines to control the flow of data between the modules, and within each of them.
- *Modules* are calculation programs designed to perform specific tasks. A module have the ability to call other modules to form what is called a 'procedure'.
- *Modules* and *procedures* are available for performing various tasks. In KANEXT, the user can create own modules for a specific task [Becker et al., 2011].

KANEXT is designed for 32 and 64 bit computer architectures. It is coded mainly in Fortran, except for a few C-routines in the kernel. It has been tested using the open-source

compilers gcc (for the C code) and g95 (for the Fortran code).

Figure 4.1 shows the flow diagram of the procedure "VABUSH" (VAriant-BUrnup-reSHuffle) which is the one used in our research.

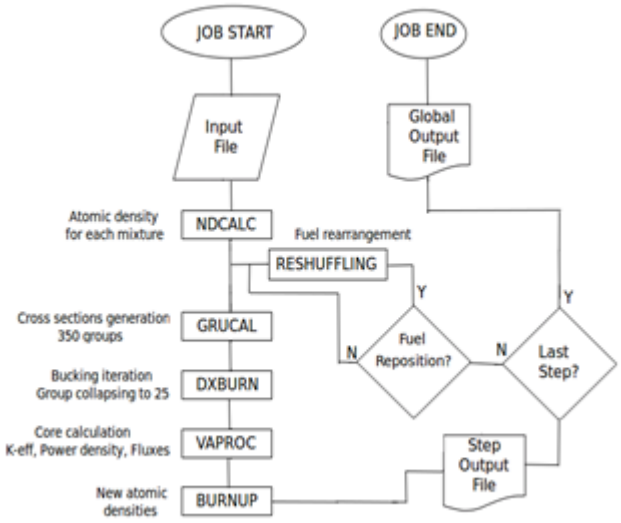

Figure 4.1: The flow diagram for the VABUSH procedure

The main modules used in the "VABUSH" procedure are described below:

- The NDCALC module calculates the mixture compositions and geometry data for every reactor zone. A number of data blocks are provided for cross section calculation and evaluation purposes. The module was initially developed for parametric investigations of tight lattice light water reactors. For this reason, the main input specifications are based on moderator-to-fuel ratio and on pin-cell and fuel specification data. During further R&D projects, a number of extensions were implemented, especially for other coolants like sodium, lead, lead/bismuth, helium, CO_2 and polyethylene.
- The module GRUCAL calculates the isotopic and mixture dependent macroscopic cross sections based on microscopic cross sections library. Resonance self-shielding is by default done by the Bondarenko method by means of the narrow resonance approximation, which is appropriate for fast reactor applications. The self-shielded group constants from fine-flux calculations can be delivered by the so-called secondary input option, which then will substitute the narrow resonance cross sections. After a burnup calculation a new self-shielding treatment is carried out for the new

cycle in GRUCAL, including new number densities and their impact on the self-shielding. Heterogeneity corrections, like Dancoff approximation for infinite lattices of Wigner-Seitz cells or smeared cells, can be defined. Microscopic cross section libraries exist from several formatted evaluations like JEFF3.1, 3.1.1 or ENDF/B 7.0.

- The module DXBURN is a module for energy group collapsing, both for few-group reactor simulations and for the determination of one-group data for burn-up calculations. The bucking iteration method applied in KANEXT stems directly from the fast reactor development in the 70's in Germany and has given good results since.
- VAPROC generates the binary input files for the VARIANT code [Palmiotti et al., 1995]. The cross section file with COMPXS format is created by calling the module GCMPXS. The geometry file GEODST and, if needed, the fixed source file FIXSRC; are written according to the VAPROC input definition. The main purpose of this module is to organize burnup and fuel management calculations, using the coupled code VARIANT for systems with hexagonal fuel assemblies and the burnup capability of KANEXT.
- The module BURNUP was developed from the code ORIGEN. The local (made in KIT) improvements of the code KORIGEN are fully adopted. In addition, ordering of library data is improved. Compatibility with KORIGEN is obtained with available auxiliary modules. Improvements of KORIGEN [Fischer and Wiese, 1983] on the original ORIGEN concern:
  - The use of reactor-physical effective cross sections for important nuclides.
  - Nuclide-specific fission energy release.
  - Neutron emission.
  - Check of the nuclear data used.
  - Input construction and verification.
  - Representation and evaluation of results.
- The module RESHUFFLING is used for material elements repositioning after a time step, whenever the call of this module is omitted the code keeps the original positions.

4.2 Deterministic Solver Parameters

KANEXT is a deterministic code, i.e. it solves the nuclear core neutron balance equations by applying numerical methods. In this section some of the main important aspects for solving this equations are presented.

4.2.1 Solution Method of the Transport Phenomena

The KANEXT code has the ability of treating the core equations with diffusion problem or transport approximation.

The solver choice is made by assigning a number at the KANEXT card called `'FLEX'` that consist in two digit `MN` where `M` is the order of the flux P_N expansion and `N` is the order of the leakage P_N expansion, the possible values are:
`M=1` P_1 Flux Expansion
`M=3` P_3 Flux Expansion
`M=5` P_5 Flux Expansion
`N=1` P_1 Leakage Expansion
`N=3` P_3 Leakage Expansion
`N=5` P_5 Leakage Expansion
Note that:
When `MN = 11`, it becomes a diffusion problem P_1.
When no `FLEX` card is added, a default value `MN = 33` is used for the code.
Whenever `MN` is negative, a simplified spherical harmonics approximation SP_N is used.

4.2.2 Energy Group Collapsing

As mentioned previously in this chapter, module NDCALC generates the cross sections for a big number of energy groups and later are collapsed to a smaller number of groups by DXBURN.

In the case of the work presented in this thesis, JEFF 3.1 cross section library is used and 350-group cross section (XS) data is generated by NDCALC. The energy spectrum breakdown is shown in Table 4.1

The group collapsing by DXBURN would depend on the user's needs. In the next chapter is described how group collapsing is declared by the user.

Table 4.1: 350-group segmentation for XS generation

	MeV		MeV		MeV		MeV		MeV
1	$1.96x10^{1}$	71	$5.58x10^{-1}$	141	$1.27x10^{-2}$	211	$3.67x10^{-4}$	281	$1.04x10^{-5}$
2	$1.73x10^{1}$	72	$5.28x10^{-1}$	142	$1.20x10^{-2}$	212	$3.49x10^{-4}$	282	$9.88x10^{-6}$
3	$1.69x10^{1}$	73	$5.00x10^{-1}$	143	$1.14x10^{-2}$	213	$3.32x10^{-4}$	283	$9.39x10^{-6}$
4	$1.65x10^{1}$	74	$4.75x10^{-1}$	144	$1.08x10^{-2}$	214	$3.16x10^{-4}$	284	$8.93x10^{-6}$

5	$1.57x10^{1}$	75	$4.52x10^{-1}$	145	$1.02x10^{-2}$	215	$3.00x10^{-4}$	285	$8.50x10^{-6}$
6	$1.49x10^{1}$	76	$4.30x10^{-1}$	146	$9.64x10^{-3}$	216	$2.86x10^{-4}$	286	$8.08x10^{-6}$
7	$1.46x10^{1}$	77	$4.09x10^{-1}$	147	$9.12x10^{-3}$	217	$2.72x10^{-4}$	287	$7.88x10^{-6}$
8	$1.42x10^{1}$	78	$3.89x10^{-1}$	148	$8.67x10^{-3}$	218	$2.58x10^{-4}$	288	$7.68x10^{-6}$
9	$1.38x10^{1}$	79	$3.70x10^{-1}$	149	$8.25x10^{-3}$	219	$2.46x10^{-4}$	289	$7.49x10^{-6}$
10	$1.35x10^{1}$	80	$3.52x10^{-1}$	150	$7.85x10^{-3}$	220	$2.34x10^{-4}$	290	$7.31x10^{-6}$
11	$1.28x10^{1}$	81	$3.34x10^{-1}$	151	$7.47x10^{-3}$	221	$2.22x10^{-4}$	291	$7.13x10^{-6}$
12	$1.25x10^{1}$	82	$3.18x10^{-1}$	152	$7.10x10^{-3}$	222	$2.11x10^{-4}$	292	$6.95x10^{-6}$
13	$1.22x10^{1}$	83	$3.03x10^{-1}$	153	$6.75x10^{-3}$	223	$2.01x10^{-4}$	293	$6.78x10^{-6}$
14	$1.16x10^{1}$	84	$2.88x10^{-1}$	154	$6.43x10^{-3}$	224	$1.91x10^{-4}$	294	$6.61x10^{-6}$
15	$1.11x10^{1}$	85	$2.74x10^{-1}$	155	$6.11x10^{-3}$	225	$1.82x10^{-4}$	295	$6.45x10^{-6}$
16	$1.05x10^{1}$	86	$2.60x10^{-1}$	156	$5.81x10^{-3}$	226	$1.73x10^{-4}$	296	$6.29x10^{-6}$
17	$1.00x10^{1}$	87	$2.47x10^{-1}$	157	$5.53x10^{-3}$	227	$1.64x10^{-4}$	297	$6.13x10^{-6}$
18	$9.46x10^{0}$	88	$2.35x10^{-1}$	158	$5.26x10^{-3}$	228	$1.56x10^{-4}$	298	$5.98x10^{-6}$
19	$8.95x10^{0}$	89	$2.24x10^{-1}$	159	$5.00x10^{-3}$	229	$1.49x10^{-4}$	299	$5.83x10^{-6}$
20	$8.46x10^{0}$	90	$2.13x10^{-1}$	160	$4.76x10^{-3}$	230	$1.41x10^{-4}$	300	$5.68x10^{-6}$
21	$8.01x10^{0}$	91	$2.02x10^{-1}$	161	$4.52x10^{-3}$	231	$1.34x10^{-4}$	301	$5.54x10^{-6}$
22	$7.57x10^{0}$	92	$1.92x10^{-1}$	162	$4.30x10^{-3}$	232	$1.27x10^{-4}$	302	$5.41x10^{-6}$
23	$7.17x10^{0}$	93	$1.83x10^{-1}$	163	$4.09x10^{-3}$	233	$1.21x10^{-4}$	303	$5.27x10^{-6}$
24	$6.78x10^{0}$	94	$1.73x10^{-1}$	164	$3.89x10^{-3}$	234	$1.15x10^{-4}$	304	$5.14x10^{-6}$
25	$6.41x10^{0}$	95	$1.64x10^{-1}$	165	$3.70x10^{-3}$	235	$1.09x10^{-4}$	305	$4.89x10^{-6}$
26	$6.07x10^{0}$	96	$1.55x10^{-1}$	166	$3.52x10^{-3}$	236	$1.03x10^{-4}$	306	$4.65x10^{-6}$
27	$5.74x10^{0}$	97	$1.47x10^{-1}$	167	$3.35x10^{-3}$	237	$9.80x10^{-5}$	307	$4.42x10^{-6}$
28	$5.43x10^{0}$	98	$1.39x10^{-1}$	168	$3.18x10^{-3}$	238	$9.30x10^{-5}$	308	$4.21x10^{-6}$
29	$5.13x10^{0}$	99	$1.31x10^{-1}$	169	$3.03x10^{-3}$	239	$8.83x10^{-5}$	309	$4.00x10^{-6}$
30	$4.86x10^{0}$	100	$1.24x10^{-1}$	170	$2.88x10^{-3}$	240	$8.38x10^{-5}$	310	$3.30x10^{-6}$
31	$4.59x10^{0}$	101	$1.17x10^{-1}$	171	$2.74x10^{-3}$	241	$7.95x10^{-5}$	311	$2.60x10^{-6}$
32	$4.35x10^{0}$	102	$1.11x10^{-1}$	172	$2.60x10^{-3}$	242	$7.55x10^{-5}$	312	$2.10x10^{-6}$
33	$4.11x10^{0}$	103	$1.05x10^{-1}$	173	$2.48x10^{-3}$	243	$7.18x10^{-5}$	313	$1.50x10^{-6}$
34	$3.89x10^{0}$	104	$9.93x10^{-2}$	174	$2.35x10^{-3}$	244	$6.83x10^{-5}$	314	$1.30x10^{-6}$
35	$3.68x10^{0}$	105	$9.40x10^{-2}$	175	$2.24x10^{-3}$	245	$6.49x10^{-5}$	315	$1.15x10^{-6}$
36	$3.50x10^{0}$	106	$8.89x10^{-2}$	176	$2.13x10^{-3}$	246	$6.18x10^{-5}$	316	$1.12x10^{-6}$
37	$3.33x10^{0}$	107	$8.41x10^{-2}$	177	$2.03x10^{-3}$	247	$5.87x10^{-5}$	317	$1.10x10^{-6}$
38	$3.17x10^{0}$	108	$7.95x10^{-2}$	178	$1.93x10^{-3}$	248	$5.59x10^{-5}$	318	$1.07x10^{-6}$
39	$3.01x10^{0}$	109	$7.53x10^{-2}$	179	$1.83x10^{-3}$	249	$5.31x10^{-5}$	319	$1.05x10^{-6}$

40	$2.86x10^{0}$	110	$7.12x10^{-2}$	180	$1.74x10^{-3}$	250	$5.05x10^{-5}$	320	$1.02x10^{-6}$
41	$2.73x10^{0}$	111	$6.73x10^{-2}$	181	$1.66x10^{-3}$	251	$4.81x10^{-5}$	321	$9.96x10^{-7}$
42	$2.59x10^{0}$	112	$6.37x10^{-2}$	182	$1.58x10^{-3}$	252	$4.57x10^{-5}$	322	$9.72x10^{-7}$
43	$2.47x10^{0}$	113	$6.03x10^{-2}$	183	$1.50x10^{-3}$	253	$4.35x10^{-5}$	323	$9.50x10^{-7}$
44	$2.35x10^{0}$	114	$5.70x10^{-2}$	184	$1.43x10^{-3}$	254	$4.13x10^{-5}$	324	$9.10x10^{-7}$
45	$2.23x10^{0}$	115	$5.39x10^{-2}$	185	$1.36x10^{-3}$	255	$3.93x10^{-5}$	325	$8.50x10^{-7}$
46	$2.12x10^{0}$	116	$5.10x10^{-2}$	186	$1.29x10^{-3}$	256	$3.74x10^{-5}$	326	$7.80x10^{-7}$
47	$2.02x10^{0}$	117	$4.83x10^{-2}$	187	$1.23x10^{-3}$	257	$3.56x10^{-5}$	327	$6.25x10^{-7}$
48	$1.92x10^{0}$	118	$4.56x10^{-2}$	188	$1.17x10^{-3}$	258	$3.38x10^{-5}$	328	$5.00x10^{-7}$
49	$1.83x10^{0}$	119	$4.32x10^{-2}$	189	$1.11x10^{-3}$	259	$3.22x10^{-5}$	329	$4.00x10^{-7}$
50	$1.74x10^{0}$	120	$4.09x10^{-2}$	190	$1.05x10^{-3}$	260	$3.06x10^{-5}$	330	$3.50x10^{-7}$
51	$1.65x10^{0}$	121	$3.86x10^{-2}$	191	$1.00x10^{-3}$	261	$2.91x10^{-5}$	331	$3.20x10^{-7}$
52	$1.57x10^{0}$	122	$3.66x10^{-2}$	192	$9.54x10^{-4}$	262	$2.77x10^{-5}$	332	$3.00x10^{-7}$
53	$1.50x10^{0}$	123	$3.46x10^{-2}$	193	$9.07x10^{-4}$	263	$2.63x10^{-5}$	333	$2.80x10^{-7}$
54	$1.42x10^{0}$	124	$3.27x10^{-2}$	194	$8.62x10^{-4}$	264	$2.51x10^{-5}$	334	$2.50x10^{-7}$
55	$1.35x10^{0}$	125	$3.09x10^{-2}$	195	$8.20x10^{-4}$	265	$2.38x10^{-5}$	335	$2.20x10^{-7}$
56	$1.28x10^{0}$	126	$2.93x10^{-2}$	196	$7.80x10^{-4}$	266	$2.27x10^{-5}$	336	$1.80x10^{-7}$
57	$1.21x10^{0}$	127	$2.77x10^{-2}$	197	$7.42x10^{-4}$	267	$2.16x10^{-5}$	337	$1.40x10^{-7}$
58	$1.15x10^{0}$	128	$2.62x10^{-2}$	198	$7.06x10^{-4}$	268	$2.05x10^{-5}$	338	$1.00x10^{-7}$
59	$1.08x10^{0}$	129	$2.48x10^{-2}$	199	$6.71x10^{-4}$	269	$1.95x10^{-5}$	339	$8.00x10^{-8}$
60	$1.03x10^{0}$	130	$2.34x10^{-2}$	200	$6.38x10^{-4}$	270	$1.86x10^{-5}$	340	$6.70x10^{-8}$
61	$9.70x10^{-1}$	131	$2.22x10^{-2}$	201	$6.07x10^{-4}$	271	$1.77x10^{-5}$	341	$5.80x10^{-8}$
62	$9.17x10^{-1}$	132	$2.10x10^{-2}$	202	$5.77x10^{-4}$	272	$1.68x10^{-5}$	342	$5.00x10^{-8}$
63	$8.68x10^{-1}$	133	$1.98x10^{-2}$	203	$5.49x10^{-4}$	273	$1.60x10^{-5}$	343	$4.20x10^{-8}$
64	$8.21x10^{-1}$	134	$1.88x10^{-2}$	204	$5.22x10^{-4}$	274	$1.51x10^{-5}$	344	$3.50x10^{-8}$
65	$7.77x10^{-1}$	135	$1.78x10^{-2}$	205	$4.96x10^{-4}$	275	$1.44x10^{-5}$	345	$3.00x10^{-8}$
66	$7.35x10^{-1}$	136	$1.68x10^{-2}$	206	$4.72x10^{-4}$	276	$1.36x10^{-5}$	346	$2.50x10^{-8}$
67	$6.96x10^{-1}$	137	$1.59x10^{-2}$	207	$4.49x10^{-4}$	277	$1.29x10^{-5}$	347	$2.00x10^{-8}$
68	$6.59x10^{-1}$	138	$1.50x10^{-2}$	208	$4.27x10^{-4}$	278	$1.22x10^{-5}$	348	$1.50x10^{-8}$
69	$6.23x10^{-1}$	139	$1.42x10^{-2}$	209	$4.06x10^{-4}$	279	$1.16x10^{-5}$	349	$1.00x10^{-8}$
70	$5.90x10^{-1}$	140	$1.35x10^{-2}$	210	$3.86x10^{-4}$	280	$1.10x10^{-5}$	350	$5.00x10^{-9}$

4.3 Geometric Parameters in KANEXT

In this section, the main parameters used for the geometric definitions are explained. First, how the fuel assemblies are modeled, and then how they are arranged to form a whole reactor core.

4.3.1 Fuel Assembly Geometry Description

Figure 4.2 shows the fuel assembly (left) and the regular unit cell (right). For fuel assembly definition the geometry of the fuel unit cell is very important. In the figure, the white hexagons represent the unit cells, i.e. hexagons that contains a fuel element. For the areas on the fuel assemblies that does not belong to the regular unit cells (in red and blue in Figure 4.2) a special treatment is followed and later in this section it will be discussed.

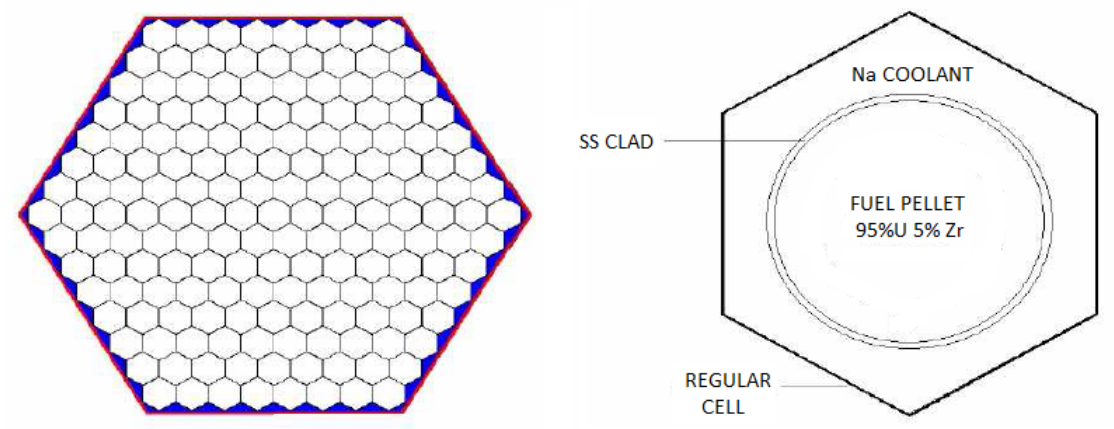

Figure 4.2: Fuel assembly (left) and re regular unit cell (right)

As any other deterministic code, KANEXT works homogenizing the content of a given region into an averaged mixture, even though the users enter geometrical data of a fuel assembly into the input of the code.

Before start defining the fuel assemblies, three vectors must be declared so the code can use them for the assemblies definition. These three vectors are called `'PVEC'` that contains the transuranic, `'UVEC'` that contains the uranium isotopes and `'SVEC'` that contains all the isotopes in the structural material, in the cases shown in this thesis SS HT-9.

'PVEC' and 'UVEC' have the following format:

```
'PVEC' (or 'UVEC')
X
'ISO_1' Mass_dens Mass_num_1.  ID_1
'ISO_2' Mass_dens Mass_num_2.  ID_2
...
```

Where:

- `X` is the number of isotopes contained in the vector.
- `'ISO_N'` is the identifier of the isotope N.
- `Mass_dens` is the density in gr/cm^3 of the mixture composed by the vector, in proportions that are used in the assemblies definition.
- `Mass_num_N` is the mass number of isotope N, it must be followed by a dot `'.'`.
- `ID_N` is an identifier number, 1 for fissile isotopes and 0 for non-fissile.

The `'SVEC'` vector is filled in the same form except that no `ID_N` is added in the list.

Even though the `'PVEC'`, `'UVEC'` and `'SVEC'` are defined before, the first step to define an assembly is to use the card `'MINP'` to tell the code how many mixtures will be declared in the input.

After `'MINP'` is used and the number of mixtures is declared, each mixture is defined separately.

It would be important to note that even when the core can have hundreds of mixtures after radial and axial nodalization, in this section of material definition only the basic mixtures (from which the others derive) are defined.

It is recommended that the reader can review the second reshuffling case shown in the previous chapter. There are 20 fuel assemblies for each 1/6th of the core plus seven control rods and two kind of reflectors, nevertheless, there are only 8 different mixtures: 4 fissile (5.0 at%, 10.0 at%, 17.0 at% and 20.0 at%), 1 fertile (0.35 at%), 1 control rod, 1 axial reflector and 1 radial reflector. For repeating mixtures, a special card named `'REMI'` is used. In the next chapter this function is explained with more detail.

The main parameters used for modeling an assembly in KANEXT are:

`FUTEMP`	Fuel Temperature in K.
`CATEMP`	Cladding Temperature in K.
`COTEMP`	Coolant Temperature in K.
`VMVF`	Coolant/Pin volume fraction.
`FIST`	Plutonium fraction in fuel (in our case we do not use Pu so FIST=0)

VMOD	Coolant fraction in region not belonging to a regular cell. In Figure 4.2 these regions are shown in blue, and this fraction is the sum of those blue areas divided over the area inside the channel.
VSTRUC	Structural material fraction not belonging to a regular cell. In 4.2 it is shown that the only structural materials not belonging to a regular cell is the wall itself and is marked in red. This value is the result of the division of the area of these walls over the area inside the channel.
RF	Inner clad radius in cm.
DC	Clad thickness in cm.
FUSD	Ratio of actual to theoretical (which is given by the user before) fuel density.
COSD	Ratio of actual to theoretical (which is given by the user before) coolant density.

After these parameters, four isotopic vectors must be declared:

- Transuranic vector: proportions for the fuel of every isotope contained in 'PVEC'.
- Uranium vector: proportions for the fuel of every isotope contained in 'UVEC'.
- Cladding material vector: proportions for the cladding of every isotope contained in 'SVEC'.
- Structural material vector: proportions for the channel walls of every isotope contained in 'SVEC'.

Even though both cladding and structural material are the same material in our cases of study, in general this does not need to be true. In a more general case 'SVEC' can contain all the isotopes in both structural material and cladding as long as it is correctly defined in their proper vectors.

The number of pins per assemblies and height of the assembly must be given at the end of each assembly definition.

4.3.2 Radial Nodalization

As mentioned previously, once all the mixtures are defined with 'MINP' and then 'REMI', the next step is to construct the full core with them.

In order to construct the core, a matrix *NxN* must be given in the input. Going back again to the second reshuffle scheme showed up in previous chapter, the Figure 4.3 shows how the mixtures are arranged in a matrix so they can form the core.

On the matrix, each position (m,n) represents one assembly, depending on the symmetry it is possible to repeat patterns.In the case of the tests described in this work, given the $1/6^{th}$

5	5	5	5	5	5	5	5	5	0	0	0	0	0	0	0	0
5	5	5	5	5	5	5	5	5	5	0	0	0	0	0	0	0
5	5	35	40	39	38	37	36	35	5	5	0	0	0	0	0	0
5	5	36	34	30	31	32	33	34	40	5	5	0	0	0	0	0
5	5	37	33	27	29	4	28	27	30	39	5	5	0	0	0	0
5	5	38	32	28	26	24	25	26	29	31	38	5	5	0	0	0
5	5	39	31	4	25	22	23	22	24	4	32	37	5	5	0	0
5	5	40	30	29	24	23	21	21	23	25	28	33	36	5	5	0
5	5	35	34	27	26	22	21	4	21	22	26	27	34	35	5	5
0	5	5	36	33	28	25	23	21	21	23	24	29	30	40	5	5
0	0	5	5	37	32	4	24	22	23	22	25	4	31	39	5	5
0	0	0	5	5	38	31	29	26	25	24	26	28	32	38	5	5
0	0	0	0	5	5	39	30	27	28	4	29	27	33	37	5	5
0	0	0	0	0	5	5	40	34	33	32	31	30	34	36	5	5
0	0	0	0	0	0	5	5	35	36	37	38	39	40	35	5	5
0	0	0	0	0	0	0	5	5	5	5	5	5	5	5	5	5
0	0	0	0	0	0	0	0	5	5	5	5	5	5	5	5	5

Figure 4.3: Example of core matrix construction

symmetry, only $1/6^{th}$ of the assemblies were defined as mixtures to be then reproduced on the other $5/6^{th}$ of the core.

At the beginning of the cycle, the core is divided in various zones, these zones can contains more than one assembly with identical fuel. Nevertheless, for a correct representation of the phenomena in the core all assemblies must be represented as a different mixture since, due to factors such as the neutronic flux in the position of a particular assembly, they will evolve differently though time.

4.3.3 Axial Nodalization

KANEXT allows the user to divide the core height into various axial layers as thick as desired.

The complete form of the core's matrix is a *NxNxM* matrix, since every axial layer must be *NxN* and can have as many *M* layers as the user needs. The way to instruct the code about how to complete the core is by adding in the input:

- The N, N , M values.
- The total number of mixtures in the core.
- The borders (in cm) of each axial layer (for example 0.0 20.0 40.0 60.0 ... for a core composed of 20.0 cm thick layers).

- The matrix for each axial layer, similar to Figure 4.3.

As in the case of the radial nodalization, it is also better to divide the core into different axial layers.

4.4 Material Parameters in KANEXT

So far, the generalities of modeling a core in KANEXT code have been described. Nevertheless, a few differences on how modeling fueled and non-fueled mixtures exists, here they will be explained as a complement of what was seen previously in this chapter.

4.4.1 Fission Products Tracking

The user has to give a list of the isotopes that KANEXT will track, these lists are given after the card `'BUTP'`, and its format is the following:

```
'BUTB'
N
'ISO_1'
'ISO_2'
'ISO_3'
...
'ISO_N'
```

Where:

- `N` is the number of fission products to track.
- `'ISO_I'` is the identifier of the i-th isotope on the list.

4.4.2 Fuel Elements

How to declare the materials contained in a fuel assembly, along with its geometry was explained previously in this chapter. In some cases, it is needed to add extra material in the fuel or coolant, this can be due, for example, by the addition of boron on the sodium coolant, or as in the particular case of the work presented here, by the addition of Zr in the fuel.

For these cases, two new vectors can be added in the assembly definition: 'ADDF' to add materials in the fuel, and 'ADDM' to add it in the moderator. The word moderator is a legacy of previous version of KAPROS (pecursor of KANEXT) which was used in an early stage for LWR where coolant acts also moderator, in the case o of Fast Reactors it reffers to coolant.

Their format differs a little from the others vectors, since they work with atomic densities instead of proportions:

```
'ADDF' X
'ISO_1' Temp_1.  At_dens_1
'ISO_2' Temp_2.  At_dens_2
'ISO_3' Temp_3.  At_dens_3
...
```

Where:

- X is the number of isotopes included in the vector.
- 'ISO_N' is the identifier of the isotope N.
- Temp_N is the temperature of the material in which new isotopes are added.
- 'At_dens_N is the atomic density of the added isotope in the region where it is added (not in the whole assembly or unit cell, but in the moderator or fuel).

4.4.3 Non-fuel Elements

When a mixture is defined without fuel, a special treatment must be done. The factor VMVF is set to the value 1.0e09; any other factor does not make any difference except for VSTRUC, VMOD (since it is possible to add structural material or moderator/coolant) and COSD (since density of the coolant can be altered when present.

By setting VMVF = 1.0e09 the space containing the material is emptied, it is possible to fill it with structural material VSTRUC=1, coolant VMOD=1, add these materials without filling the whole assembly channel (VSTRUC or VMOD <1) or a combination of them.

If the space contains coolant it is possible to add aditional isotopes by using the card 'ADDM' as indicated previously.

Chapter 5

VALIDATION OF THE CODE KANEXT

Even though KANEXT has been validated with experimental data and code-to-code comparisons [Van Criekingen et al., 2009], it is important to do a proper validation work related to the type of reactor treated in this thesis.

In the present section an effort to compare KANEXT with a more well-known reactor physics code is presented. The selected reference code was the Monte Carlo based SERPENT, due to its rapid increase in popularity, and its versatility in the applications [SERPENT, 2015].

5.1 Description of the Nuclear Code SERPENT

In this section, the SERPENT nuclear code will be presented and described. As KANEXT was already described in a previous chapter it is not be described again here.

In a nutshell, SERPENT is a three-dimensional continuous-energy Monte Carlo reactor physics code with burnup capability that has been developed at VTT Technical Research Centre of Finland since 2004

The Serpent code is written in standard ANSI-C language. The code is mainly developed in the Linux operating system, but it has also been compiled and tested in MAC OS X and some UNIX machines [Leppänen, 2013].

5.1.1 Applications of SERPENT

According to the developers [SERPENT 2015] SEPRNET main capabilities are listed below:

- Spatial homogenization and group constant generation for deterministic reactor calculations.
- Fuel cycle studies involving detailed assembly-level burnup calculations.
- Validation of deterministic lattice transport codes.
- Full-core modeling of research reactors, SMR's, and other closely coupled systems.
- Coupled multi-physics applications.
- Educational purposes and demonstration of reactor physics phenomena.

As mentioned, it can be used for generating energy group constants to be used in deterministic codes. This is because when the project was started in 2004, it was intended for spatial homogenization. Currently group constant generation capability covers:

- Homogenized few-group reaction cross sections.
- Scattering and scattering production cross sections and matrices up to Legendre order 7.
- Diffusion coefficients.
- Assembly discontinuity factors (ADF's), surface and corner fluxes and currents for square and hexagonal fuel lattices.
- Group-wise peaking factors for pin-power reconstruction.
- Poison cross sections for ^{135}Xe and ^{149}Sm and their precursors.

5.1.2 Calculation Methodology of SERPENT

SERPENT uses the continuous-energy Monte Carlo criticality source method for simulating neutron transport in a self-sustaining system. Cross sections are read from ACE format data libraries and reconstructed on a single unionized energy grid to speed up the calculation. Interaction physics is based on classical collision kinematics and ENDF reaction laws.

Interaction data is available for 432 nuclides at 6 temperatures between 300 and 1800 K. Thermal bound-atom scattering data is included for light and heavy water and graphite. Since the data format is shared with MCNP, any continuous-energy ACE format data library generated for MCNP can be used with Serpent as well.

The burnup capability in Serpent is entirely based on built-in calculation routines, without any external coupling.

Serpent has two fundamentally different options for solving the Bateman depletion equations. The first method is the Transmutation Trajectory Analysis (TTA) method [Cetnar, 2006], based on the analytical solution of linearized depletion chains. The second option is the Chebyshev Rational Approximation Method (CRAM), an advanced matrix exponential solution developed for Serpent at VTT [Pusa and Leppänen, 2013]. The two methods have shown to yield consistent results when used with SERPENT [Leppänen and Pusa, 2009] and in separate methodological studies [Isotalo and Aarnio, 2011].

Fission products and actinide daughter nuclides are selected for the calculation without additional user effort, and burnable materials can be sub-divided into depletion zones automatically.

5.1.3 Geometry Definition in SERPENT

Similar to other Monte Carlo codes, such as MCNP and Keno-VI, Serpent uses a universe-based Combinatorial Solid Geometry (CSG) model, which allows the description of practically any two or three-dimensional fuel or reactor configuration.

The geometry consists of material cells, defined by elementary quadratic and derived macrobody surface types.

The code also provides some additional geometry features specifically for fuel design. These features include simplified definition of cylindrical fuel pins and spherical fuel particles, square and hexagonal lattices for LWR and fast reactor geometries, and circular cluster arrays for CANDU fuels. The random dispersion of microscopic fuel particles in high-temperature gas-cooled reactor fuels and pebble distributions in pebble-bed type HTGR cores can be modeled using geometry types specifically designed for the task.

The explicit HTGR geometry model in Serpent reads the coordinates of fuel particles or pebbles from a separate input file, and generates the geometry as it is defined, without any approximations. The model works on several levels (particles inside a pebble and pebbles inside the core) and it has been tested in realistic double-heterogeneous reactor configurations consisting of over 60 million randomly positioned units [Suikkanen and Kyrki-Rajamäki, 2010].

5.1.4 Output Information of SERPENT

All numerical outputs are written in MATLAB m-format files to simplify the post-processing of the results. The code also has a geometry plotter feature and a reaction rate plotter, which is convenient for visualizing the neutronics and tally results.

Output for burnup calculation consists of isotopic compositions, activities, spontaneous fission rates and decay heat data. The results are given as both material-wise and total values. Group constants and all the other output parameters are calculated and printed for each burnup step. The irradiation history is defined in units of time or burnup.

5.1.5 Parallelization Capability of SERPENT

Depending on the version of SERPENT, different parallelization approaches are used.

SERPENT 1 uses the Message Passing Interface (MPI) for parallel calculation. Parallelization of the transport routine is implemented by dividing the neutron histories between the parallel tasks and combining the results after the simulation has been completed. This approach is simple and efficient, but it lacks error tolerance and dynamic load sharing. The overall calculation time is dependent on the slowest task, which is why the method is best applied in a symmetric parallel environment.

Parallelization in SERPENT 2 is based on a hybrid OpenMP/MPI approach. The main advantage of thread-based OpenMP is that all CPU cores within the computational node are accessing the same memory space, which makes it possible to use all available cores in the calculation without running into problems with excessive memory usage.

In addition to the neutronics simulation, parallelization in the burnup calculation mode divides also the preprocessing and depletion routines between several CPU's.

For fuel depletion analysis, by default, SERPENT solves the Bateman's depletion equation according to the Chebyshev Rational Approximation Method (CRAM), which is based on the predictor midpoint step technique [Chersola et al., 2014]. SERPENT also uses a methodology to better represent the changes due to material composition variation. This code uses a predictor–corrector method with linear interpolation based on Euler's method [Pusa and Leppänen, 2010].

5.1.6 Validation of SERPENT

Each SERPENT update is validated by comparison to MCNP by running a standard set of assembly calculation problems.

Effective multiplication factors and homogenized few-group reaction cross sections are within the statistical accuracy from the reference results, when the same ACE libraries are used in the calculations.

Validation against MCNP has been carried out with equally good results for calculations involving individual nuclides, by comparing the flux spectra produced by the two codes. Differences with other Monte Carlo codes (Keno-VI) are small, but statistically significant discrepancies can be observed in some cases.

Differences with deterministic lattice codes are generally larger, mainly due to the fundamental differences between the calculation methods.

5.2 Description of the Studied Core

The core consists of 120 active fuel assemblies (FA) of 100 cm height. In Figure 5.1, it can be seen that the core consists of three radial regions, each of them with different ^{235}U enrichment. In addition, two outer rings represent steel reflectors which are hexagonal blocks of the same size as a fuel assembly channell including the walls, and within the fueleld zone there are also 7 steel dummy assemblies where the control rods would be positioned.

The compositions for all these regions are described in Table 5.1. The power of the core was set to 1095 MWth, resulting in a power density of 784.53 MW/m^3 of fuel.

Table 5.1: Description of core elements and fuel regions

Fuel Assemblies	120	Color	Material	Enrichment
Dummy assemblies	7	Orange	Fuel	10%/at.
Fuel composition	95%U/5%Zr	Red	Fuel	15%/at.
Active height	100 cm	Yellow	Fuel	3.5%/at.
Axial reflectot	100 cm	Dark gray	SS Block	N/A
Radial reflector	2 rings	Light gray	SS Block	N/A

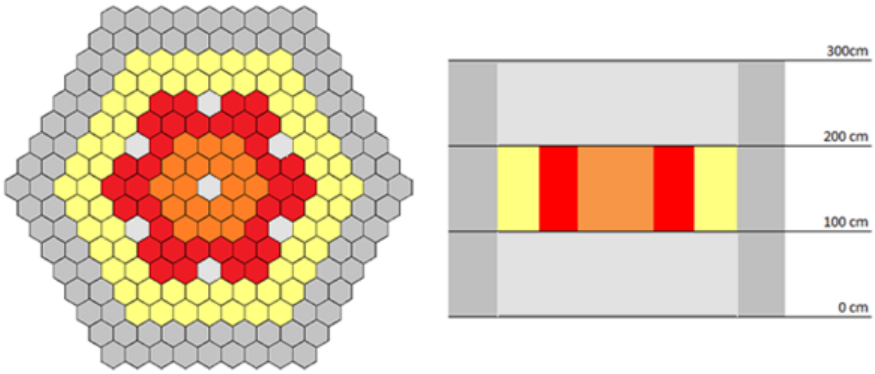

Figure 5.1: Radial and axial nodalisation of the SFR core

Each fuel assembly consists of 169 steel cladded fuel pins; the steel used is of HT-9 type. In Figure 5.2 a layout and geometric characteristics of each fuel assembly is presented.

The 7 dummy assemblies are identical to the reflector assemblies. In further studies, real dummies with the exact geometrical characteristics of the fuel assemblies but with a steel pellet will be considered and later on real control rods would be placed.

Under and above the active zone of the core, there is a 100 cm height axial reflector (shown in light grey in Figure 5.1). As in the case of the dummies, the reflector consists of steel blocks, and also in further studies they will be replaced with assemblies with steel pellets.

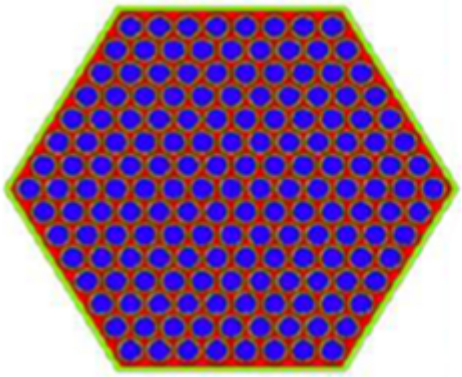

	mm
Channel width	165.4
Wall width	5.00
Pin pitch	12.5
R(pin)	5.58
R(pellet)	4.49
Gap	0.18
Cladding	0.89

Figure 5.2: Fuel assembly layout and geometric characteristics

5.3 Core Modeling Considerations

For the VARIANT solver of KANEXT, the core is discretized in the following manner: one radial zone per fuel assembly type and one radial zone per reflector element; and axially the core is subdivided in one axial node for the active part and one node for the upper and lower reflector.

This may be over simplistic but it was a manner to have a similar model for KANEXT and SERPENT, since, as it will be described later, in SERPENT one material was defined by fuel region and more refinement would have taken high costs in computing power and time.

Assuming that all fuel assembly types are axially uniform, i.e. the same enrichment, KANEXT will generate a complete set of homogenized and condensed cross sections for each material. The material data of each fuel assembly type (three FA types and one axial reflector and another one for the radial reflector) used for KANEXT is the same one used also for SERPENT.

For SERPENT, as a MC-based code, no nodal but regional definition is made. One fuel assembly type was defined and used by each fuel and reflector region. The same original fuel inventory and assembly geometry as KANEXT was defined for SERPENT, as well as the SS definition and the Zr added to the fuel. The goal was to make two identical models for both codes.

It is important to note that even when it is easy to increase the number of axial and radial nodes in KANEXT, by defining them as different fuel mixtures that will evolve independently; in SERPENT, even when it is possible, this would require very high computational power.

Axial discretization sensitivity tests were done with KANEXT, in which we conclude that for this core, axial node reduction has not important effect on the effective neutron multiplication factor (k_{eff}) and fuel inventories, which are the parameters tracked in this work.

No special radial or axial boundary conditions were used either for the KANEXT or SERPENT simulations, i.e. no reflective boundaries or other considerations were taken after the external boundary of the steel reflectors, beyond reflectors there is only vacuum.

5.4 Depletion Simulations

As this is a neutronic analysis, no termohydraulical consideration were made, other than material temperature for the cross sections. These temperatures are described for each material in Table 5.2 and are used in KANEXT and SERPENT with the JEFF-3.1 cross section library.

Table 5.2: Materials temperature

Material	**Temp. (K)**
Fuel	1200
SS HT-9	600
Coolant (Na)	600
Zr (in fuel)	1200

Tables 5.3, 5.4 and 5.5 describe the isotopes used in the fuel, the steel and the tracked fission products, respectively.

As the simulation started with fresh fuel, originally fuel consisted only of ^{235}U, ^{238}U and Zr; without any trace of plutonium or other isotope.

Elements with no isotope number means that they are included by default with their natural proportions.

Table 5.3: Isotopes present in fuel

^{234}U	^{240}Pu	^{243}Am	^{245}Cm
^{235}U	^{241}Pu	^{237}Np	^{90}Zr
^{236}U	^{242}Pu	^{239}Np	^{91}Zr
^{238}U	^{241}Am	^{242}Cm	^{92}Zr
^{238}Pu	^{242}Am	^{243}Cm	^{94}Zr
^{239}Pu	^{42m}Am	^{244}Cm	^{96}Zr

Regarding the solution methods, transport option P_3 and diffusion (P_1) were selected in the KANEXT solver. For SERPENT, two cases of 230 cycles with 20,000 and 30,000 neutron histories each were run, with the first 30 cycles skipped; therefore, a total 4,000,000 and 6,000,000 neutron histories, respectively, were simulated and the statistical uncertainty in the k_{eff} prediction was about 40 pcm.

Table 5.4: Isotopes in Stainless Steel HT-9

^{54}Fe	^{54}Cr	^{182}W	^{96}Mo	^{30}Si
^{56}Fe	^{58}Ni	^{183}W	^{97}Mo	V
^{57}Fe	^{60}Ni	^{184}W	^{98}Mo	C
^{58}Fe	^{61}Ni	^{186}W	^{100}Mo	^{31}P
^{50}Cr	^{62}Ni	^{92}Mo	^{55}Mn	^{63}Cu
^{52}Cr	^{64}Ni	^{94}Mo	^{28}Si	^{65}Cu
^{53}Cr	^{180}W	^{95}Mo	^{29}Si	^{59}Cu

Table 5.5: Isotopes tracked as fission products

^{83}Kr	^{99}Tc	^{103}Rh	^{115}In	^{133}Cs	^{144}Nd	^{48m}Pm	^{155}Eu	^{164}Dy
^{91}Zr	^{101}Ru	^{105}Rh	^{127}I	^{134}Cs	^{145}Nd	^{147}Sm	^{154}Gd	^{176}Lu
^{93}Zr	^{102}Ru	^{105}Pd	^{129}I	^{135}Cs	^{146}Nd	^{149}Sm	^{155}Gd	^{148}Sm
^{96}Zr	^{103}Ru	^{106}Pd	^{131}Xe	^{139}La	^{147}Nd	^{150}Sm	^{156}Gd	^{107}Pd
^{95}Mo	^{104}Ru	^{108}Pd	^{132}Xe	^{141}Ce	^{148}Nd	^{151}Sm	^{157}Gd	^{95}Nb
^{97}Mo	^{106}Ru	^{109}Ag	^{133}Xe	^{141}Pr	^{150}Nd	^{152}Sm	^{158}Gd	
^{98}Mo	^{101}Rb	^{111}Cd	^{134}Xe	^{143}Pr	^{147}Pm	^{153}Eu	^{160}Gd	
^{100}Mo	^{103}Rb	^{113}Cd	^{135}Xe	^{143}Nd	^{148}Pm	^{154}Eu	^{159}Tb	

It is important to note that even when it was said in a previous chapter that in SERPENT there are only two options for the Bateman's equations, there is a third which is a variation of one of those. So the three solution methods are:

1. Transmutation Trajectory Analysis (TTA), based on the analytical solution of linearized transmutation chains.
2. Advanced matrix exponential solution based on the Chebyshev Rational Approximation Method (CRAM).
3. The variation TTA method (TTA-Mod), in which cyclic transmutation chains are handled by inducing small variations in the coefficients instead of solving the extended TTA equations.

Regarding computer time, similar cases (transport P_3 and diffusion P_1 in KANEXT, and CRAM with 20,000 neutrons in SERPENT) were run in a desktop with an AMD ATHLON II X2 250 3.0 GHZ processor with 4 GB in RAM. Job running time was 56m 40s for the transport solution and 30m 20s for the diffusion solution in the case of KANEXT and 2 days 13h 56m 20s for SERPENT

5.5 Results and Discussion

The effective neutron multiplication factor (k_{eff}) for all cases is presented in Figure 5.3. As it can be seen in this figure, SERPENT results does not change significantly depending on the solution method of the Bateman's equations; therefore, the CRAM option with 30,000 neutron histories will be used for comparing with KANEXT. As for KANEXT, both solution options, transport and diffusion, will be used in order to compare the effect of method complexity.

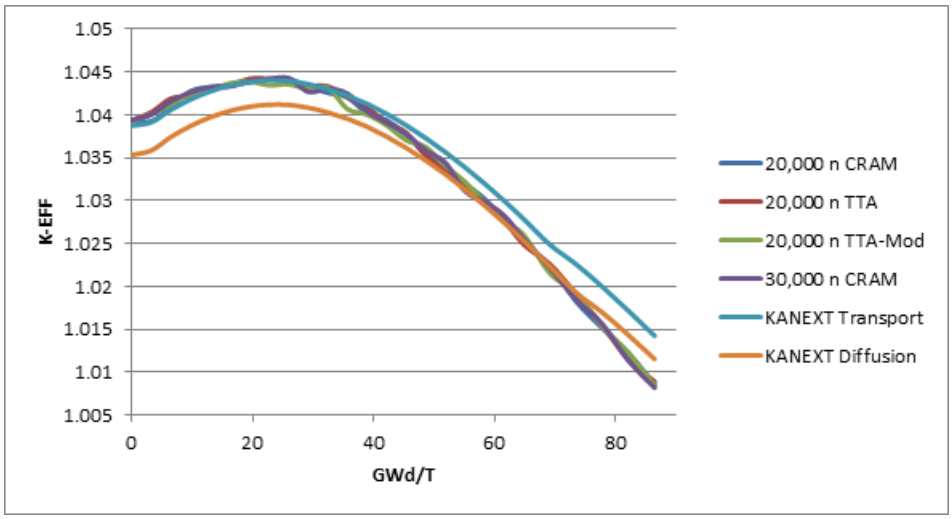

Figure 5.3: k_{eff} comparison between KANEXT and SERPENT

Regarding the comparison KENEXT vs SERPENT, KANEXT transport (P_3) and diffusion (P_1) values are a couple hundreds of pcm from SERPENT values. Differences of a few hundreds of pcm have been found in previous studies between KANEXT and MCNP [Ponomarev et al., 2010] for fresh core calculations. The average of the k_{eff} absolute differences with SERPENT are 165.81 pcm and 219.58 pcm for transport and diffusion, respectively (see Table 5.6). Even when these differences are not non-negligible, especially at the end of life for transport and at the beginning for diffusion, the tendency in the k_{eff} curve is very similar between codes and, as mentioned, in the case of transport the difference is very low along the burnup until the final part of the cycle where small errors are accumulated.

This gives the certainty that, as it will be shown later, both codes are depleting the fuel at the same rate. For the diffusion solution, the average difference is still higher, which

could be expected for a simplified solution method. It can be seen that the form of the curves is similar in all the cases, which can be found in the small standard deviation of both comparisons (see Table 5.6).

Table 5.6: k_{eff} differences between KANEXT and SERPENT

Days	Burnup (Gwd/T)	SERPENT	Transport KANEXT	Difussion KANEXT	dk_{eff} (pcm) |Serp-Transp.|	dk_{eff} (pcm) |Serp-Diff.|
0	0	1.03938	1.03873	1.03533	65	405
75	3.243	1.04004	1.03914	1.03586	90	418
150	6.485	1.04159	1.04061	1.03744	98	415
225	9.728	1.04263	1.04178	1.0387	85	393
300	12.971	1.04321	1.04273	1.03972	48	349
375	16.214	1.0433	1.04339	1.04045	9	285
450	19.456	1.0439	1.04383	1.04095	7	295
525	22.699	1.04416	1.04401	1.04118	15	298
600	25.942	1.04428	1.04393	1.04115	35	313
675	29.185	1.04268	1.04358	1.04083	90	185
750	32.427	1.04301	1.043	1.04027	1	274
825	35.67	1.04247	1.04223	1.03954	24	293
900	38.913	1.04041	1.04128	1.03862	87	179
975	42.156	1.03909	1.04012	1.03747	103	162
1050	45.398	1.03776	1.03877	1.03615	101	161
1125	48.641	1.03586	1.03728	1.03468	142	118
1200	51.884	1.03441	1.03565	1.03306	124	135
1275	55.127	1.03111	1.03387	1.03129	276	18
1350	58.369	1.02987	1.03198	1.02942	211	45
1425	61.612	1.02826	1.02997	1.02742	171	84
1500	64.855	1.02553	1.02784	1.0253	231	23
1600	69.178	1.02216	1.02487	1.02234	271	18
1700	73.502	1.0185	1.02259	1.01929	409	79
1800	77.826	1.01565	1.01998	1.01698	433	133
1900	82.149	1.01138	1.01718	1.01435	580	297
2000	86.473	1.00821	1.01426	1.01155	605	334
				Average	**165.81 pcm**	**219.58 pcm**

The observed differences can be due to the approximation used in KANEXT (transport or diffusion); the energy collapsing (25 groups in this study), and in particular how res-

onances treatment are managed by KANEXT (explained in a previous chapter: module GRUCAL), which is different to the continuous spectrum of SERPENT and other MC codes. Additionaly, the effect of neutron leakages (which are very important in a small fast reactor) can be added to the differences (this is related with the manner that the reflector is scattering back neutrons to the core and the way codes are simulating it), and, indeed, the solution method itself: deterministic vs stochastic.

Absolute k_{eff} differences (SERPENT minus KANEXT) through the core life are shown in Figure 5.4; for easier interpretation, the average difference is shown as a constant line.

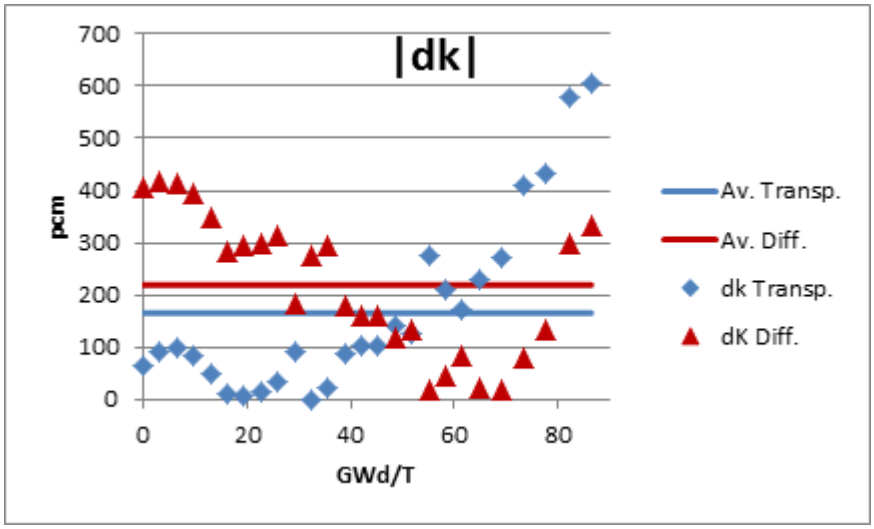

Figure 5.4: Absolute values of k_{eff} differences (SERPENT minus KANEXT).

Comparisons of some isotopes were done for each region. Main fissile (^{235}U, ^{239}Pu and ^{241}Pu) and fertile (^{238}U and ^{240}Pu) isotopes were tracked during the core life, along with selected minor actinides (^{241}Am and ^{243}Am) and fission products (^{135}Xe and ^{149}Sm). Figures 5.5, 5.6 and 5.7 give a quick overview of the inventories for regions 1, 2 and 3, respectively, while Table 5.7 and 5.8 present quantitative information about the atomic density relative differences between SERPENT and KANEXT for the selected isotopes; the average and the standard deviation of the relative differences (obtained over all the burnup steps) are shown.

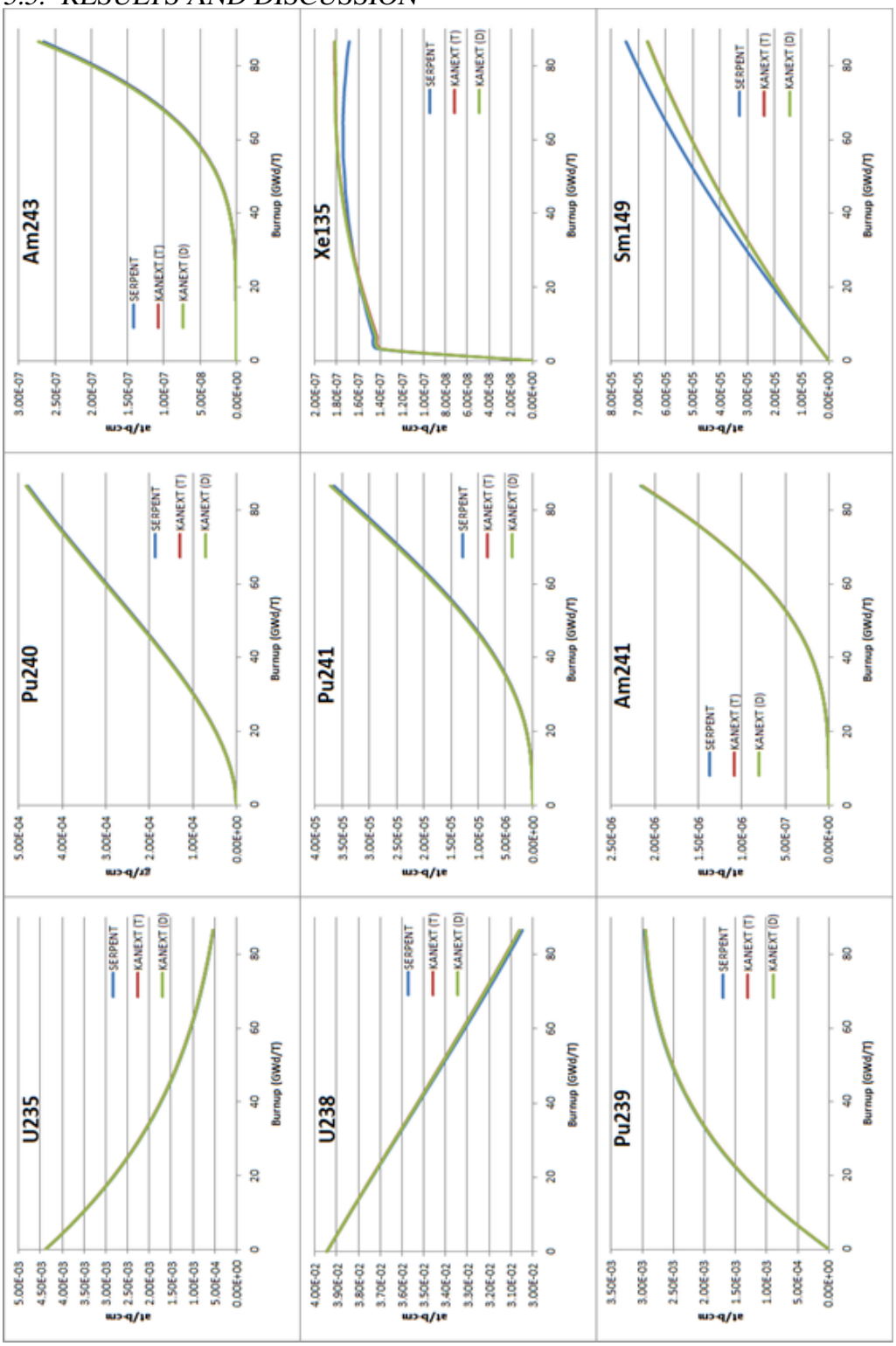

Figure 5.5: Comparison of some isotopes in region 1.

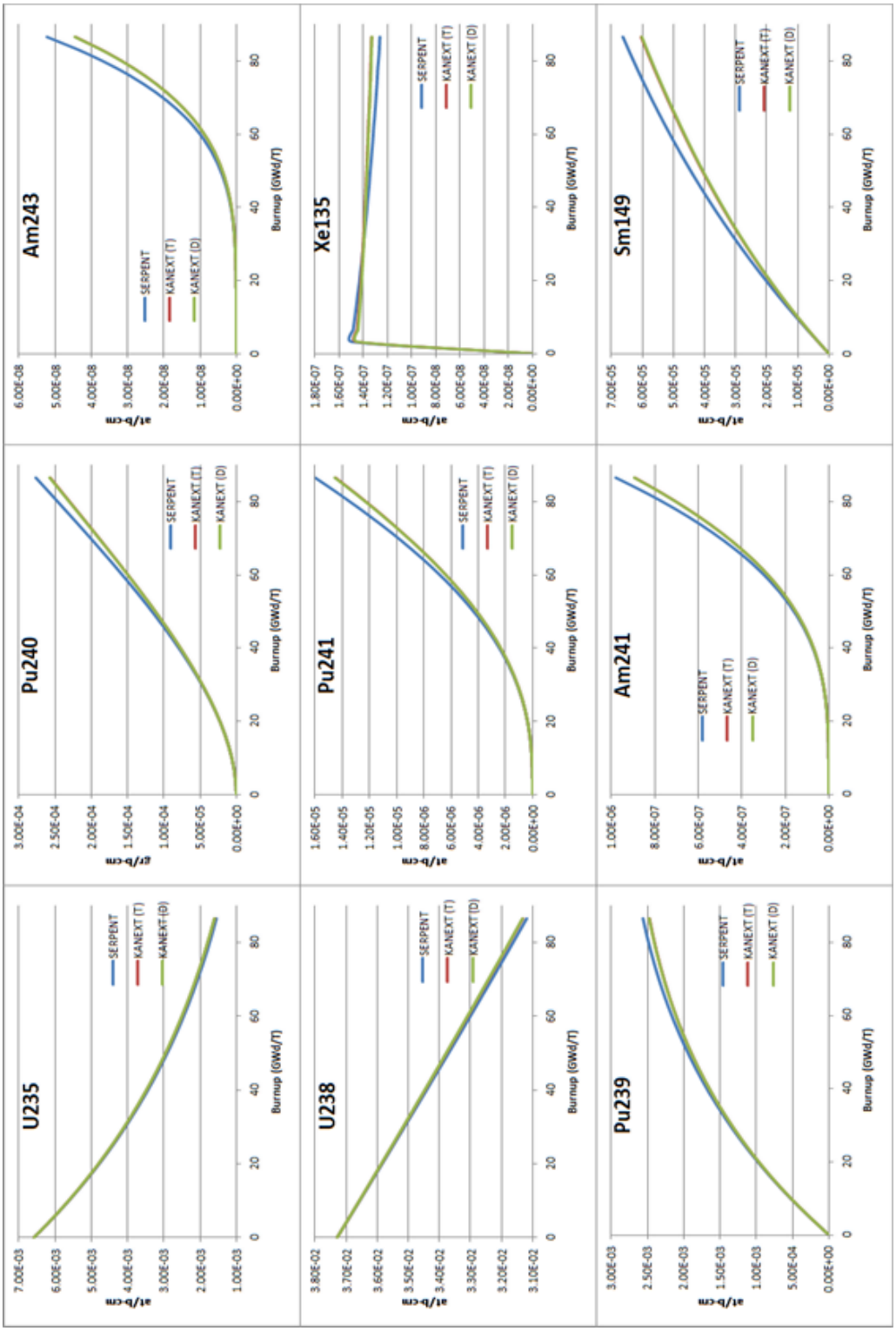

Figure 5.6: Comparison of some isotopes in region 2.

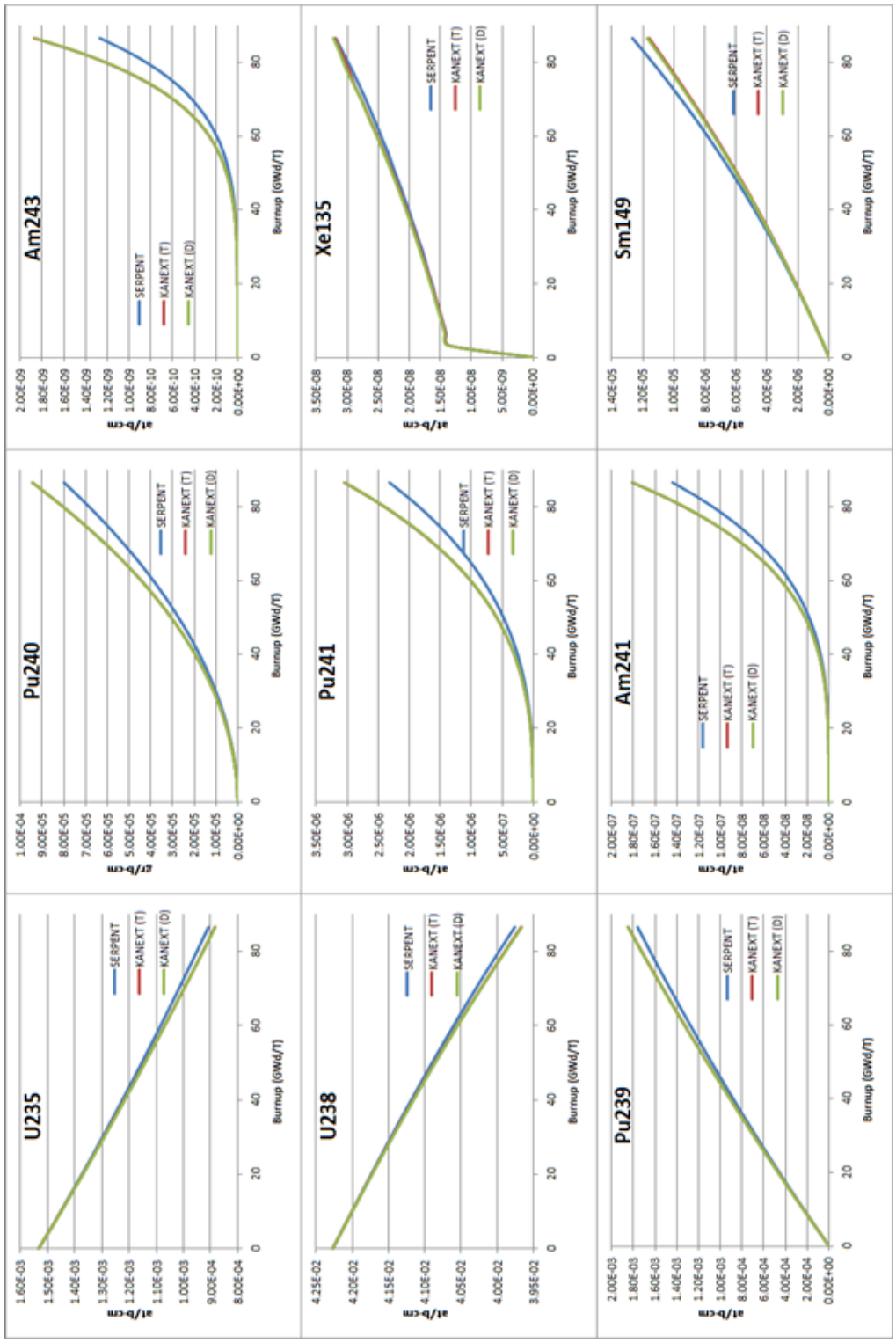

Figure 5.7: Comparison of some isotopes in region 3.

Table 5.7: Relative differences* SERPENT and KANEXT (transport) for the selected isotopes

	Region 1		Region 2		Region 3	
Isotope	Average	Std. Dev	Average	Std. Dev	Average	Std. Dev
^{235}U	-0.8	0.42	-1.25	0.96	0.88	0.78
^{238}U	-0.2	0.14	-0.17	0.12	0.08	0.07
^{239}Pu	0.62	0.16	2.08	0.83	-3.15	1.11
^{240}Pu	-1.3	0.45	2.85	2.85	-11.62	3.76
^{241}Pu	-2.6	1.46	3.46	4.4	-22.56	4.55
^{240}Am	-1.53	2.62	2.94	4.85	-19.97	2.9
^{243}Am	-2.45	2.93	6.85	7.58	-30.29	9.27
^{135}Xe	-1.73	2.76	-1.42	2.4	-1.34	0.83
^{149}Sm	8.42	2.62	7.17	2.16	4.48	2.56

*100% x [N_i(Serpent)-N_i(Kanext)]/N_i(Serpent)
N_i: atomic density of isotope i

Table 5.8: Relative differences* SERPENT and KANEXT (difussion) for the selected isotopes

	Region 1		Region 2		Region 3	
Isotope	Average	Std. Dev	Average	Std. Dev	Average	Std. Dev
^{235}U	-0.51	0.33	-1.38	1.01	0.96	0.82
^{238}U	-0.16	0.12	-0.19	0.13	0.09	0.07
^{239}Pu	0.41	0.08	2.09	0.73	-3.48	0.98
^{240}Pu	-1.87	0.80	2.88	2.68	-11.87	3.53
^{241}Pu	-3.47	1.88	3.54	4.17	-22.3	4.40
^{240}Am	-2.54	3.03	3.09	4.65	-19.69	2.79
^{243}Am	-4.08	3.5	7.13	7.24	-30.03	8.82
^{135}Xe	-1.96	2.47	-1.13	2.51	-2.06	0.69
^{149}Sm	8.00	2.76	7.57	2.09	3.36	2.64

*100% x [N_i(Serpent)-N_i(Kanext)]/N_i(Serpent)
N_i: atomic density of isotope i

The comparison of the isotopes inventory was successful for most of the isotopes, except for ^{149}Sm where some discrepancies were observed in regions 1 and 2, and for ^{240}Pu, ^{241}Pu, ^{241}Am and ^{243}Am in region 3 (see numbers in bold font in Tables 5.7 and 5.8). Despite these cases, in general, results from both codes showed the same tendencies and

comparable values for the three zones, in particular for the main isotopes (in terms of higher atomic density) ^{235}U, ^{238}U and ^{239}Pu, which show that both codes are depleting the fuel at the same rate. Discrepancies observed towards the end of the core life, for some isotopes, can be due to accumulation of differences due to the solving methods of the Bateman's equations of both codes. Other factor that can affect the evolution of the analyzed isotopes inventory is the number of isotopes tracked by KANEXT, in this case 69 fission products and 19 fuel isotopes. In the case of SERPENT, burnup calculations involve over 250 actinide and fission product nuclides.

Regarding region 3, this is the most external fueled zone, into which neutrons will be scattered back from the steel reflector, thus neutron spectrum will be more thermalized than in the central zones of the core.

By looking at the total cross sections of the heavy isotopes analyzed in this work (see Figure 5.8), it can be noticed that ^{240}Pu has a big resonance at 1 eV, and ^{243}Am has also a quite big resonance very close to that of ^{240}Pu; ^{241}Pu and ^{243}Am resonances are also present in that energy spectrum (between 1 and 5 eV) with important values.

All these resonances could be a factor to explain the discrepances, it is very possible that in KANEXT the resonance treatment in the group collapsing is not accurate enough in this region of resonances, and has more impact in region 3, where the neutron spectrum is softer than the other two regions. Probably a 33-group energy structure like that used in ERANOS [Ponomarev et al., 2010] for sodium cooled fast reactors could improve the results.

Concerning the Sm-149 discrepancy, by looking to the total cross section versus energy of this isotope and that of Xe-135 (see Figure 5.9, it can be seen that Sm-149 has an important zone of resonances in the epithermal region (while Xe-135 does not), that can be affecting the results if cross sections are not computed properly during the generation process (from basic libraries: ENDF or JEFF), or during the resonance treatment process in module GRUCAL. This effect is more important in region 1 and 2 where the neutron spectrum is harder than in region 3. This is not the case of Xe-135 where there are not resonances, the cross section behavior is quite smooth along all the energy range, and the comparisons (KANEXT/SERPENT) are good for the three regions.

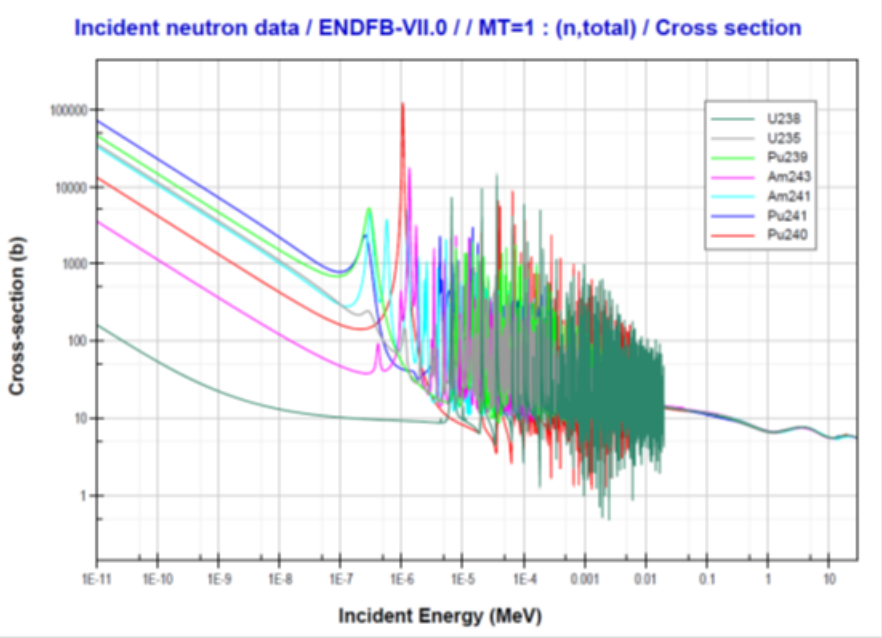

Figure 5.8: Total cross section of selected fuel isotopes.

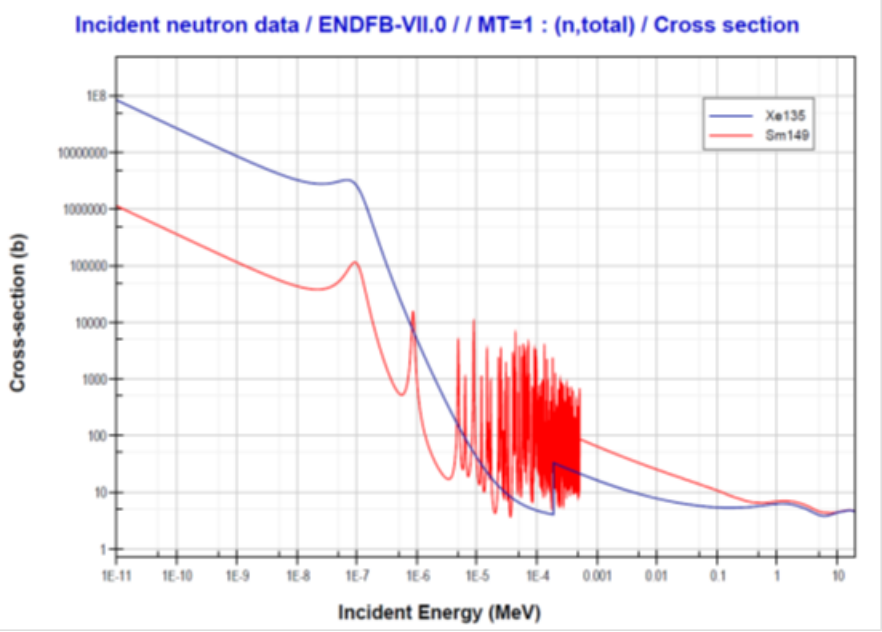

Figure 5.9: Total cross section of selected fission products.

5.6 Conclusions

The objective of this section of the project research, and a very important one, was to tests KANEXT code by comparing its results against a well-known MC code, in this case SERPENT. Results obtained by KANEXT are comparable with the ones obtained with SERPENT.

One of the main motivation of using a deterministic code is the computing time reduction, which was observed in this work, where a great amount of time (about 98.5%) was saved on running the codes on the same computer; which motivates to keep using KANEXT as a main tool in fast reactor core simulations.

Regarding SERPENT fuel depletion calculations, it was found, that results does not change significantly depending on the solution method of the Bateman's equations: CRAM, TTV or TTV-modified. Furthermore, a population of 20,000 neutrons per cycle is enough to give practically the same results of a population of 30,000 neutrons.

As observed in the results section, the comparison KANEXT-SERPENT of the effective neutron multiplication factor was satisfactory, but in less extent for the diffusion solution compared with the results for transport P_3 solution of KANEXT, having differences between codes in the order of a couple hundreds pcm in average. Regarding this, it is possible to conclude that both codes show the same tendency in k_{eff} versus burnup. It is to be taken into account that, in addition to differences in the transport method solution (deterministic vs MC), there are additional factors related to decay and fission yield data, methods used for solving the Bateman equations, number of nuclide concentrations tracked for each burnable material, depletion algorithms, etc., and those factors provoke the atomic density differences found between KANEXT and SERPENT, mainly for ^{149}Sm, ^{240}Pu, ^{241}Pu, ^{241}Am and ^{243}Am.

Since in our work team, KANEXT is intended for sodium cooled fast breeder core design and fuel management analyses [Lopez and Francois, 2015], the observed issues regarding some fuel inventories differences must be carefully studied in a different work, out of the scope of this thesis research. Further work on different energy group structure in KANEXT (e.g. 33 groups) and other strategies, as a higher number of actinides and fission products tracked during burnup calculations, will be carried out.

In summary, it is possible conclude that so far, the results obtained for k_{eff} and isotope inventories give enough confidence to keep using KANEXT for the purpose of fuel management analysis of SFRs in the future and results obtained for this thesis are good enough, considering that the code is still in continuous development and this carries on frequent

improvements.

Chapter 6

MODEL IMPLEMENTATION ON THE CODE KANEXT

In this chapter the parameters for assemblies modeling will be calculated and the core matrix will also be constructed; all of these parameters apply on the three main study cases presented in this thesis, except when explicitly said.

The intention is to keep the structure of the code description chapter, so that the reader can easily locate the wanted parameter.

6.1 Deterministic Solver Parameters

A previous read of the chapter "Description of the code KANEXT" section "Geometric Parameters in KANEXT" is recommended to familiarize on what is presented in this section.

6.1.1 Solution Method of the Transport Phenomena

As indicated before, three orders of Legendre expansion can be used for the transport equation problem, these are P_1, P_3 and P_5, additional to these, their simplified polynomial expansion can also be used: SP_1, SP_3 and SP_5.

A card named 'FLEX' defines the code option to be used. In all the cases shown in this thesis, the option P_3 will be used ('FLEX' 33).

Other options like P_1 and SP_3 were also used in the trial and error tests stage, since their simplifications imply time savings in the calculations. To illustrate this, Table 6.1 shows the calculation time of a sensitivity test made to know the difference in time when calculations were made with three different 'FLEX' options, and with different numbers of radial reflector rings. The core used here was an early version, its geometry is not shown here.

Table 6.1: Sensitivity tests on solution method

Rings	**'FLEX'**	**Method**	**Iterations**	k_{eff}	**Time**
2	33	P_3	145	1.27119	4h 24m 2s
2	-33	SP_3	134	1.27143	13m 21s
2	11	P_1	25	1.26940	6m 14s
1	33	P_3	100	1.27119	2h 40m 48s
1	-33	SP_3	39	1.27143	12m 44s
1	11	P_1	26	1.26940	5m 31s

It was shown that for short-timed obtained or not very strict results, the selection of diffusion P_1 or the simplified SP_3 can be very useful.

6.1.2 Energy Group Collapsing

It was mentioned in a the previous chapter that cross section generation by the module NDCALC is made with 350 groups, and later collapsed to the number of groups defined by the user.

The way of choosing the collapsing grouping is by the use of the card 'GRC2' which has a format as the following:
'GRC2' N G1 G2 G3 ... G_N

Where:
- N is the number of groups wanted.
- G_i is the i-th group energy break from the 350-group break list given in Table 4.1.

In the cases presented in this thesis, energy collapsing card was as follows:
'GRC2' 25 8 17 26 35 45 55 60 64 73 83 93 102 111 120 129 138 147 157

```
166 175 184 211 242 310 350
```

Which leads to the energy grouping shown in Table 6.2.

Table 6.2: Sensitivity tests on solution method

#	MeV	#	MeV	#	MeV
1	$1.41910\text{x}10^{1}$	11	$1.83000\text{x}10^{-1}$	21	$1.42510\text{x}10^{-3}$
2	$1.00000\text{x}10^{1}$	12	$1.11000\text{x}10^{-1}$	22	$3.67262\text{x}10^{-4}$
3	$6.06550\text{x}10^{0}$	13	$6.73400\text{x}10^{-2}$	23	$7.55014\text{x}10^{-5}$
4	$3.67900\text{x}10^{0}$	14	$4.08500\text{x}10^{-2}$	24	$3.30000\text{x}10^{-6}$
5	$2.23100\text{x}10^{0}$	15	$2.47800\text{x}10^{-2}$	25	$5.00000\text{x}10^{-9}$
6	$1.35300\text{x}10^{0}$	16	$1.50300\text{x}10^{-2}$		
7	$1.02510\text{x}10^{0}$	17	$9.11800\text{x}10^{-3}$		
8	$8.21000\text{x}10^{-1}$	18	$5.53000\text{x}10^{-3}$		
9	$5.00000\text{x}10^{-1}$	19	$3.51910\text{x}10^{-3}$		
10	$3.02500\text{x}10^{-1}$	20	$2.23945\text{x}10^{-3}$		

In the used energy groups, there has been a preference on the fast spectrum, as it can be seen, almost half of the energy breaks are above 0.1 MeV.

6.2 Geometric Parameters in KANEXT

As mentioned in the previous chapter, before the definition of the assemblies, three material vectors need to be written, these vectors `'PVEC'`, `'UVEC'` and `'SVEC'` are presented here:

```
'PVEC'
15
'PU238' 19.816 238 0
'PU239' 19.816 239 1
'PU240' 19.816 240 0
'PU241' 19.816 241 1
'PU242' 19.816 242 0
'AM241' 19.816 241 0
'AM242' 19.816 242 0
'AM42M' 19.816 242 1
'AM243' 19.816 243 0
```

```
'NP237' 19.816 237 0
'NP239' 19.816 239 0
'CM242' 19.816 242 0
'CM243' 19.816 243 0
'CM244' 19.816 244 0
'CM245' 19.816 245 0

'UVEC'
4
'U 234' 18.15 234 0
'U 235' 18.15 235 1
'U 236' 18.15 236 0
'U 238' 18.15 238 0

'SVEC'
35
'FE 54 ' 7.718111672 55.18520091
'FE 56 ' 7.718111672 55.18520091
'FE 57 ' 7.718111672 55.18520091
'FE 58 ' 7.718111672 55.18520091
'CR 50 ' 7.718111672 55.18520091
'CR 52 ' 7.718111672 55.18520091
'CR 53 ' 7.718111672 55.18520091
'CR 54 ' 7.718111672 55.18520091
'NI 58 ' 7.718111672 55.18520091
'NI 60 ' 7.718111672 55.18520091
'NI 61 ' 7.718111672 55.18520091
'NI 62 ' 7.718111672 55.18520091
'NI 64 ' 7.718111672 55.18520091
'W 180 ' 7.718111672 55.18520091
'W 182 ' 7.718111672 55.18520091
'W 183 ' 7.718111672 55.18520091
'W 184 ' 7.718111672 55.18520091
'W 186 ' 7.718111672 55.18520091
'MO 92 ' 7.718111672 55.18520091
'MO 94 ' 7.718111672 55.18520091
'MO 95 ' 7.718111672 55.18520091
'MO 96 ' 7.718111672 55.18520091
```

```
'MO 97 ' 7.718111672 55.18520091
'MO 98 ' 7.718111672 55.18520091
'MO 100' 7.718111672 55.18520091
'MN 55 ' 7.718111672 55.18520091
'SI 28 ' 7.718111672 55.18520091
'SI 29 ' 7.718111672 55.18520091
'SI 30 ' 7.718111672 55.18520091
'V     ' 7.718111672 55.18520091
'C     ' 7.718111672 55.18520091
'P  31 ' 7.718111672 55.18520091
'CU 63 ' 7.718111672 55.18520091
'CU 65 ' 7.718111672 55.18520091
'CO 59 ' 7.718111672 55.18520091
```

Note that the uranium density is not 19.1 gr/cm^3 but 18.15 gr/cm^3, because it was already considered the absence of gap and the expansion of the fuel pellet, as mentioned in a previous chapter.

It is important to note that density and molar weight in `'SVEC'` were calculated with the atomic fractions of each element in the SS HT-9, multiplying it by their respective density and molar mass.

6.2.1 Fuel Assembly Geometry Description

Once these vectors were included, the next step is to define the mixtures for each assembly type.

In the core, there are five types of fuel with different enrichment: four enriched and one depleted. These fuel assemblies are defined exactly the same way, except with the `'UVEC'` with values dependent on the enrichment.

The values for the factors are:

```
FUTEMP 1500.
CATEMP 900.
COTEMP 800.
VMVF   0.373865414
FIST   0.0
VMOD   0.0415885947
```

```
VSTRUC 0.1245743345
RF     0.4500
DC     0.0869
FUSD   0.95
COSD   1.0
```

Note that FUSD is set to 0.95 because the fuel is 5% volume fraction of Zr.

The fuel, cladding and coolant temperatures were taken from a previous work on SFR [Ponomarev et al., 2010].

Then PVEC, UVEC, SVEC and SVEC2 should be given. As mentioned before these vectors will be identical in all fuels except for the UVEC, which depend on the enrichment; here the term U235_FR to refer the proportion of ^{235}U contained in the fuel, and (1-U235_FR) to refer the fraction of ^{238}U, as it can be seen the presence of ^{234}U is not considered.

```
*$ PVEC
0.0 1.0 0.0 0.0 0.0
0.0 0.0 0.0 0.0
0.0 0.0
0.0 0.0 0.0 0.0

*$ UVEC 0.0 U235_FR 0.0 (1-U235_FR)

*$ SVEC
0.04872752 0.76491778 0.01766529 0.00235093
0.00550652 0.10618775 0.01204084 0.00299722
0.00396764 0.00152833 0.00006644 0.00021183 0.00005395
0.00000173 0.00038184 0.00020619 0.00044149 0.00040964
0.00087513 0.00054688 0.00094208 0.00098829 0.00056643
0.00143326 0.00057295
0.00693153
0.00543655 0.00027618 0.00018227
0.00325011
0.00964912
0.00023163
0.00012012 0.00005359
0.00028094
```

```
*$ SVEC 2
0.04872752 0.76491778 0.01766529 0.00235093
0.00550652 0.10618775 0.01204084 0.00299722
0.00396764 0.00152833 0.00006644 0.00021183 0.00005395
0.00000173 0.00038184 0.00020619 0.00044149 0.00040964
0.00087513 0.00054688 0.00094208 0.00098829 0.00056643
0.00143326 0.00057295
0.00693153
0.00543655 0.00027618 0.00018227
0.00325011
0.00964912
0.00023163
0.00012012 0.00005359
0.00028094
```

At this point, the zirconium is still not added, this has to be done by the addition of an extra vector, this is done in the next section.

In a previous chapter, the function `'REMI'` was mentioned, which allows the user to define mixtures based on mixtures previously defined.

To understand the function `'REMI'` an example would be helpful. Lets imagine that six mixtures have been defined: 1, 2, 3, 4, 5, 6. Mixtures 1, 2 and 3 are fuel and they have to be reproduced in order to fill a core, it is needed 20 of mixture 1, 25 of mixture 2 and 30 of mixture 3. Instead of defining again other mixtures with the same characteristics as 1, 2 and 3, the function 'REMI' is a time saving tool, it works as described here:

```
'REMI'
4
14 6
20 1
25 2
30 3
```

Where:

- The first line is the number of reproductions that will take place (it can also be seen as the number of lines that will follow).
- In the second line, Mixture 6 is reproduced 14 times (from mixture 7 to 20). This is not a requirement but is a good practice to leave the first 20 mixture for material

definition and not include them in the core matrix, since the project can change and the need of defining extra materials can appear later. If the core matrix would have started with the next mixture (7 in this case) it would take more time to correct (every mixture should be changed in the mixture matrix) if a seventh material definition is required.

- In the lines three, four and five the fuels 1, 2 and 3 are being reproduced 20, 25 and 30 times respectively. The result is that mixtures 21 to 40 are equal to mixture 1, mixtures 41 to 65 are equal to mixture 2 and mixtures 66 to 95 are equal to mixture 3.

In this case, the mixtures 4, 5 and 6 can be structural material or other mixtures that will not be depleted so there is no need to reproduce them, but in the case we want, we would be able to do it exactly as described.

6.2.2 Radial Nodalization

Figure 6.1 shows the cross section of the core used, it is seen that the core is divided into five fuel regions. As explained before, even when more than one fuel assemblies are identical at the beginning of cycle, they must be tracked independently in order to have more trustful results.

For the cases presented, every fueled assembly represents a node. The only simplification done is that considering the $1/6^{th}$ geometry symmetry, only $1/6^{th}$ of the total number of assemblies were modeled in KANEXT, Figure 6.1 shows this.

6.2.3 Axial Nodalization

As mentioned before, keeping track of different zones inside one fuel assembly aids to the correct simulation of the core.

The active height of the core is 99.9 cm, this height was chosen to fit an odd number and take advantage of the geometry. Every fuel assembly is divided into nine sections of 11.1 cm thick. Because of the geometry, only five of them will be modeled and tracked, Figure V.2 shows this graphically.

To calculate the total of tracked fuel assembly sections, it is needed to multiply the number of modeled assemblies (210/6 = 35) times the number of the tracked axial segments for each assembly (5), the total is 175 fuel mixtures.

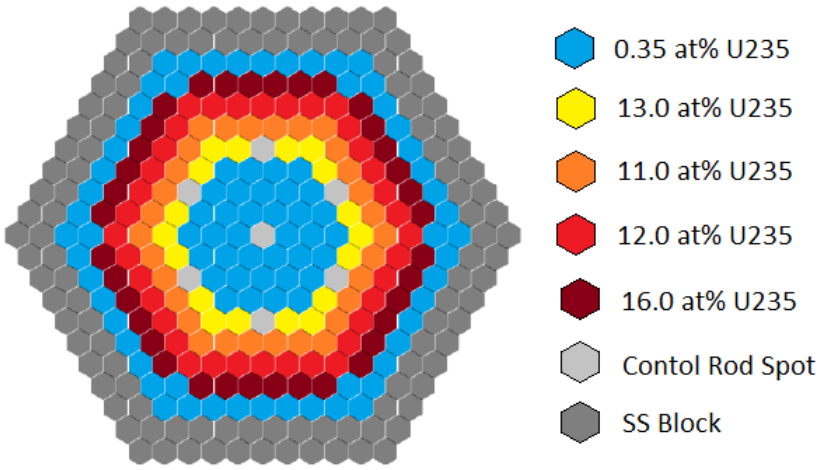

Figure 6.1: Radial layout of the core used for tests.

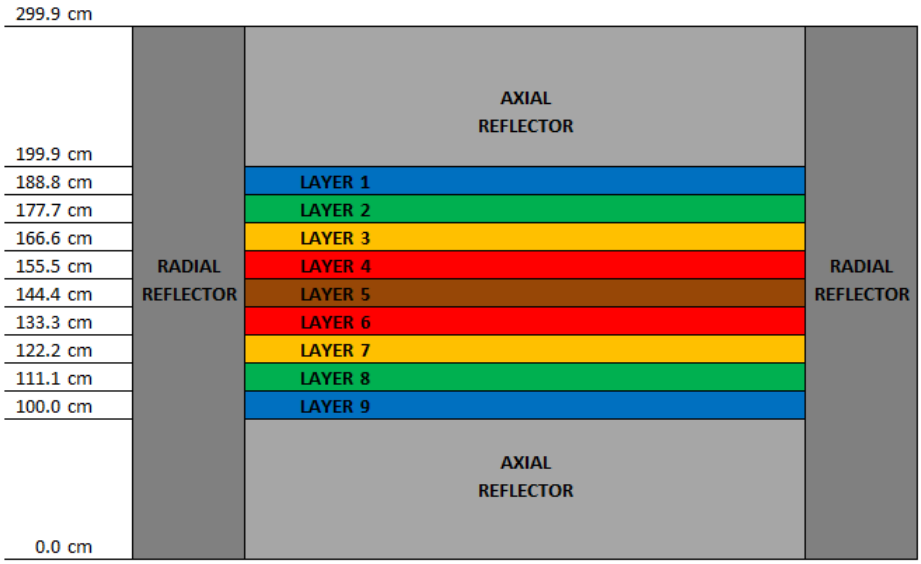

Figure 6.2: Axial layout of the core used for tests.

It is important to meditate a while here. This simplification on the axial nodalization is valid here due to only the neutronic effect of the sodium is considered and because of that the temperature of the sodium was kept constant through the core. This would not be the case if thermo dynamical effects are also considered in the core, since it would be increasing temperature as it passes though the core, so that in the upper part of the core conditions are not equal to those at the bottom, making necessary to model every axial section separately.

The part where the axial layers length are given:
`0. 100. 111.1 122.2 133.3 144.4 155.5 166.6 177.7 188.8 199.9 299.9`
Where:
- `0. 100.` Represents the bottom axial reflector layer.
- `100. 111.1 122.2 ... 188.8 199.9` Represents the active core's axial layers.
- `199.9 299.9` Represents the upper axial reflector layer.

The core matrixes are constructed as follows:

```
*$ AXIAL LAYER REFLECTOR
  5  5  5  5  5  5  5  5  5  5  5  0  0  0  0  0  0  0  0  0  0
  5  5  5  5  5  5  5  5  5  5  5  5  0  0  0  0  0  0  0  0  0
  5  5  4  4  4  4  4  4  4  4  4  5  5  0  0  0  0  0  0  0  0
  5  5  4  4  4  4  4  4  4  4  4  4  5  5  0  0  0  0  0  0  0
  5  5  4  4  4  4  4  4  4  4  4  4  4  5  5  0  0  0  0  0  0
  5  5  4  4  4  4  4  4  4  4  4  4  4  4  5  5  0  0  0  0  0
  5  5  4  4  4  4  4  4  4  4  4  4  4  4  4  5  5  0  0  0  0
  5  5  4  4  4  4  4  4  4  4  4  4  4  4  4  4  5  5  0  0  0
  5  5  4  4  4  4  4  4  4  4  4  4  4  4  4  4  4  5  5  0  0
  5  5  4  4  4  4  4  4  4  4  4  4  4  4  4  4  4  4  5  5  0
  5  5  4  4  4  4  4  4  4  4  4  4  4  4  4  4  4  4  4  5  5
  0  5  5  4  4  4  4  4  4  4  4  4  4  4  4  4  4  4  4  5  5
  0  0  5  5  4  4  4  4  4  4  4  4  4  4  4  4  4  4  4  5  5
  0  0  0  5  5  4  4  4  4  4  4  4  4  4  4  4  4  4  4  5  5
  0  0  0  0  5  5  4  4  4  4  4  4  4  4  4  4  4  4  4  5  5
  0  0  0  0  0  5  5  4  4  4  4  4  4  4  4  4  4  4  4  5  5
  0  0  0  0  0  0  5  5  4  4  4  4  4  4  4  4  4  4  4  5  5
  0  0  0  0  0  0  0  5  5  4  4  4  4  4  4  4  4  4  4  5  5
  0  0  0  0  0  0  0  0  5  5  4  4  4  4  4  4  4  4  4  5  5
  0  0  0  0  0  0  0  0  0  5  5  5  5  5  5  5  5  5  5  5  5
  0  0  0  0  0  0  0  0  0  0  5  5  5  5  5  5  5  5  5  5  5
*$ AXIAL LAYER 1
   5   5   5   5   5   5   5   5   5   5   5   0   0   0   0   0   0   0   0   0   0
   5   5   5   5   5   5   5   5   5   5   5   5   0   0   0   0   0   0   0   0   0
   5   5  48  55  54  53  52  51  50  49  48   5   5   0   0   0   0   0   0   0   0
   5   5  49  47  41  42  43  44  45  46  47  55   5   5   0   0   0   0   0   0   0
   5   5  50  46  35  40  39  38  37  36  35  41  54   5   5   0   0   0   0   0   0
   5   5  51  45  36  34  30  31  32  33  34  40  42  53   5   5   0   0   0   0   0
   5   5  52  44  37  33  27  29   4  28  27  30  39  43  52   5   5   0   0   0   0
   5   5  53  43  38  32  28  26  24  25  26  29  31  38  44  51   5   5   0   0   0
   5   5  54  42  39  31   4  25  22  23  22  24   4  32  37  45  50   5   5   0   0
   5   5  55  41  40  30  29  24  23  21  21  23  25  28  33  36  46  49   5   5   0
```

```
   5   5  48  47  35  34  27  26  22  21   7  21  22  26  27  34  35  47  48   5   5
   0   5   5  49  46  36  33  28  25  23  21  21  23  24  29  30  40  41  55   5   5
   0   0   5   5  50  45  37  32   4  24  22  23  22  25   4  31  39  42  54   5   5
   0   0   0   5   5  51  44  38  31  29  26  25  24  26  28  32  38  43  53   5   5
   0   0   0   0   5   5  52  43  39  30  27  28   4  29  27  33  37  44  52   5   5
   0   0   0   0   0   5   5  53  42  40  34  33  32  31  30  34  36  45  51   5   5
   0   0   0   0   0   0   5   5  54  41  35  36  37  38  39  40  35  46  50   5   5
   0   0   0   0   0   0   0   5   5  55  47  46  45  44  43  42  41  47  49   5   5
   0   0   0   0   0   0   0   0   5   5  48  49  50  51  52  53  54  55  48   5   5
   0   0   0   0   0   0   0   0   0   5   5   5   5   5   5   5   5   5   5   5   5
   0   0   0   0   0   0   0   0   0   0   5   5   5   5   5   5   5   5   5   5   5
*$ AXIAL LAYER 2
   5   5   5   5   5   5   5   5   5   5   5   0   0   0   0   0   0   0   0   0   0
   5   5   5   5   5   5   5   5   5   5   5   5   0   0   0   0   0   0   0   0   0
   5   5  83  90  89  88  87  86  85  84  83   5   5   0   0   0   0   0   0   0   0
   5   5  84  82  76  77  78  79  80  81  82  90   5   5   0   0   0   0   0   0   0
   5   5  85  81  70  75  74  73  72  71  70  76  89   5   5   0   0   0   0   0   0
   5   5  86  80  71  69  65  66  67  68  69  75  77  88   5   5   0   0   0   0   0
   5   5  87  79  72  68  62  64   4  63  62  65  74  78  87   5   5   0   0   0   0
   5   5  88  78  73  67  63  61  59  60  61  64  66  73  79  86   5   5   0   0   0
   5   5  89  77  74  66   4  60  57  58  57  59   4  67  72  80  85   5   5   0   0
   5   5  90  76  75  65  64  59  58  56  56  58  60  63  68  71  81  84   5   5   0
   5   5  83  82  70  69  62  61  57  56   7  56  57  61  62  69  70  82  83   5   5
   0   5   5  84  81  71  68  63  60  58  56  56  58  59  64  65  75  76  90   5   5
   0   0   5   5  85  80  72  67   4  59  57  58  57  60   4  66  74  77  89   5   5
   0   0   0   5   5  86  79  73  66  64  61  60  59  61  63  67  73  78  88   5   5
   0   0   0   0   5   5  87  78  74  65  62  63   4  64  62  68  72  79  87   5   5
   0   0   0   0   0   5   5  88  77  75  69  68  67  66  65  69  71  80  86   5   5
   0   0   0   0   0   0   5   5  89  76  70  71  72  73  74  75  70  81  85   5   5
   0   0   0   0   0   0   0   5   5  90  82  81  80  79  78  77  76  82  84   5   5
   0   0   0   0   0   0   0   0   5   5  83  84  85  86  87  88  89  90  83   5   5
   0   0   0   0   0   0   0   0   0   5   5   5   5   5   5   5   5   5   5   5   5
   0   0   0   0   0   0   0   0   0   0   5   5   5   5   5   5   5   5   5   5   5
*$ AXIAL LAYER 3
   5   5   5   5   5   5   5   5   5   5   5   0   0   0   0   0   0   0   0   0   0
   5   5   5   5   5   5   5   5   5   5   5   5   0   0   0   0   0   0   0   0   0
   5   5 118 125 124 123 122 121 120 119 118   5   5   0   0   0   0   0   0   0   0
   5   5 119 117 111 112 113 114 115 116 117 125   5   5   0   0   0   0   0   0   0
   5   5 120 116 105 110 109 108 107 106 105 111 124   5   5   0   0   0   0   0   0
   5   5 121 115 106 104 100 101 102 103 104 110 112 123   5   5   0   0   0   0   0
   5   5 122 114 107 103  97  99   4  98  97 100 109 113 122   5   5   0   0   0   0
   5   5 123 113 108 102  98  96  94  95  96  99 101 108 114 121   5   5   0   0   0
   5   5 124 112 109 101   4  95  92  93  92  94   4 102 107 115 120   5   5   0   0
   5   5 125 111 110 100  99  94  93  91  91  93  95  98 103 106 116 119   5   5   0
   5   5 118 117 105 104  97  96  92  91   7  91  92  96  97 104 105 117 118   5   5
   0   5   5 119 116 106 103  98  95  93  91  91  93  94  99 100 110 111 125   5   5
   0   0   5   5 120 115 107 102   4  94  92  93  92  95   4 101 109 112 124   5   5
   0   0   0   5   5 121 114 108 101  99  96  95  94  96  98 102 108 113 123   5   5
   0   0   0   0   5   5 122 113 109 100  97  98   4  99  97 103 107 114 122   5   5
   0   0   0   0   0   5   5 123 112 110 104 103 102 101 100 104 106 115 121   5   5
   0   0   0   0   0   0   5   5 124 111 105 106 107 108 109 110 105 116 120   5   5
   0   0   0   0   0   0   0   5   5 125 117 116 115 114 113 112 111 117 119   5   5
   0   0   0   0   0   0   0   0   5   5 118 119 120 121 122 123 124 125 118   5   5
   0   0   0   0   0   0   0   0   0   5   5   5   5   5   5   5   5   5   5   5   5
   0   0   0   0   0   0   0   0   0   0   5   5   5   5   5   5   5   5   5   5   5
*$ AXIAL LAYER 4
   5   5   5   5   5   5   5   5   5   5   5   0   0   0   0   0   0   0   0   0   0
   5   5   5   5   5   5   5   5   5   5   5   5   0   0   0   0   0   0   0   0   0
```

```
   5   5 153 160 159 158 157 156 155 154 153   5   5   0   0   0   0   0   0   0   0
   5   5 154 152 146 147 148 149 150 151 152 160   5   5   0   0   0   0   0   0   0
   5   5 155 151 140 145 144 143 142 141 140 146 159   5   5   0   0   0   0   0   0
   5   5 156 150 141 139 135 136 137 138 139 145 147 158   5   5   0   0   0   0   0
   5   5 157 149 142 138 132 134   4 133 132 135 144 148 157   5   5   0   0   0   0
   5   5 158 148 143 137 133 131 129 130 131 134 136 143 149 156   5   5   0   0   0
   5   5 159 147 144 136   4 130 127 128 127 129   4 137 142 150 155   5   5   0   0
   5   5 160 146 145 135 134 129 128 126 126 128 130 133 138 141 151 154   5   5   0
   5   5 153 152 140 139 132 131 127 126   7 126 127 131 132 139 140 152 153   5   5
   0   5   5 154 151 141 138 133 130 128 126 126 128 129 134 135 145 146 160   5   5
   0   0   5   5 155 150 142 137   4 129 127 128 127 130   4 136 144 147 159   5   5
   0   0   0   5   5 156 149 143 136 134 131 130 129 131 133 137 143 148 158   5   5
   0   0   0   0   5   5 157 148 144 135 132 133   4 134 132 138 142 149 157   5   5
   0   0   0   0   0   5   5 158 147 145 139 138 137 136 135 139 141 150 156   5   5
   0   0   0   0   0   0   5   5 159 146 140 141 142 143 144 145 140 151 155   5   5
   0   0   0   0   0   0   0   5   5 160 152 151 150 149 148 147 146 152 154   5   5
   0   0   0   0   0   0   0   0   5   5 153 154 155 156 157 158 159 160 153   5   5
   0   0   0   0   0   0   0   0   0   5   5   5   5   5   5   5   5   5   5   5   5
   0   0   0   0   0   0   0   0   0   0   5   5   5   5   5   5   5   5   5   5   5
*$ AXIAL LAYER 5
   5   5   5   5   5   5   5   5   5   5   5   0   0   0   0   0   0   0   0   0   0
   5   5   5   5   5   5   5   5   5   5   5   5   0   0   0   0   0   0   0   0   0
   5   5 188 195 194 193 192 191 190 189 188   5   5   0   0   0   0   0   0   0   0
   5   5 189 187 181 182 183 184 185 186 187 195   5   5   0   0   0   0   0   0   0
   5   5 190 186 175 180 179 178 177 176 175 181 194   5   5   0   0   0   0   0   0
   5   5 191 185 176 174 170 171 172 173 174 180 182 193   5   5   0   0   0   0   0
   5   5 192 184 177 173 167 169   4 168 167 170 179 183 192   5   5   0   0   0   0
   5   5 193 183 178 172 168 166 164 165 166 169 171 178 184 191   5   5   0   0   0
   5   5 194 182 179 171   4 165 162 163 162 164   4 172 177 185 190   5   5   0   0
   5   5 195 181 180 170 169 164 163 161 161 163 165 168 173 176 186 189   5   5   0
   5   5 188 187 175 174 167 166 162 161   7 161 162 166 167 174 175 187 188   5   5
   0   5   5 189 186 176 173 168 165 163 161 161 163 164 169 170 180 181 195   5   5
   0   0   5   5 190 185 177 172   4 164 162 163 162 165   4 171 179 182 194   5   5
   0   0   0   5   5 191 184 178 171 169 166 165 164 166 168 172 178 183 193   5   5
   0   0   0   0   5   5 192 183 179 170 167 168   4 169 167 173 177 184 192   5   5
   0   0   0   0   0   5   5 193 182 180 174 173 172 171 170 174 176 185 191   5   5
   0   0   0   0   0   0   5   5 194 181 175 176 177 178 179 180 175 186 190   5   5
   0   0   0   0   0   0   0   5   5 195 187 186 185 184 183 182 181 187 189   5   5
   0   0   0   0   0   0   0   0   5   5 188 189 190 191 192 193 194 195 188   5   5
   0   0   0   0   0   0   0   0   0   5   5   5   5   5   5   5   5   5   5   5   5
   0   0   0   0   0   0   0   0   0   0   5   5   5   5   5   5   5   5   5   5   5
```

The missing layers are identical to the ones previously described, so that:
AXIAL LAYER 6 is identical to AXIAL LAYER 4
AXIAL LAYER 7 is identical to AXIAL LAYER 3
AXIAL LAYER 8 is identical to AXIAL LAYER 2
AXIAL LAYER 9 is identical to AXIAL LAYER 1
AXIAL LAYER REFLECTOR is identical to AXIAL LAYER REFLECTOR

6.3 Material Parameters in KANEXT

In this section, the rest of the parameters not given in the previous section will be exposed.

6.3.1 Fission Products Tracking

As mentioned in the previous chapter, a list of the fission products to be tracked has to be given to the code. The following list is included in all the presented cases:

```
'BUTB'
69
                        'KR 83    ' 'ZR 91    ' 'ZR 93    ' 'ZR 96    '
'NB 95    ' 'MO 95    ' 'MO 97    ' 'MO 98    ' 'MO100    ' 'TC 99    '
'RU101    ' 'RU102    ' 'RU103    ' 'RU104    ' 'RU106    ' 'RB101    '
'RB103    ' 'RH103    ' 'RH105    ' 'PD105    ' 'PD106    ' 'PD108    '
'AG109    ' 'CD111    ' 'CD113    ' 'IN115    ' 'I 127    ' 'I 129    '
'XE131    ' 'XE132    ' 'XE133    ' 'XE134    ' 'XE135    ' 'CS133    '
'CS134    ' 'CS135    ' 'LA139    ' 'CE141    ' 'PR141    ' 'PR143    '
'ND143    ' 'ND144    ' 'ND145    ' 'ND146    ' 'ND147    ' 'ND148    '
'ND150    ' 'PM147    ' 'PM148    ' 'PM48M    ' 'SM147    ' 'SM149    '
'SM150    ' 'SM151    ' 'SM152    ' 'EU153    ' 'EU154    ' 'EU155    '
'GD154    ' 'GD155    ' 'GD156    ' 'GD157    ' 'GD158    ' 'GD160    '
'TB159    ' 'DY164    ' 'LU176    ' 'SM148    ' 'PD107    '
```

6.3.2 Fuel Elements

It was mentioned previously that when is wanted to add material in the fuel that is not included in the previously defined `'UVEC'` or `'PVEC'`, it is needed to add an additional material vector `'ADDF'`.

```
'ADDF' 74
'ZR 90 ' 1200.  1.029044E-03
'ZR 91 ' 1200.  2.244096E-04
'ZR 92 ' 1200.  3.476149E-04
'ZR 94 ' 1200.  3.476149E-04
'ZR 96 ' 1200.  5.600240E-05
```

Note that 74 is written after 'ADDF', this is because the vector of fission products has to be added in the fuel in order to be tracked, in this example it is omitted but the idea must be clear.

6.3.3 Non-fuel Elements

It was mentioned earlier that non-fueled mixtures are defined different as the ones with fuel, here we are going to describe each of the mixtures used.

Radial reflector (SS Block)
This case is the simplest since it contain only steel, the parameters are the following:

```
FUTEMP 1500.
CATEMP 900.
COTEMP 800.
VMVF   1.0E09
FIST   0.0
VMOD   0.0
VSTRUC 1.0
RF     0.4500
DC     0.0869
FUSD   0.95
COSD   1.0
```

Since there is no fuel, FUTEMP and FUSD are ignored, the same happens with COTEMP and COSD since there is not any coolant either, as well as RF and DC since there are no fuel pins. As mentioned earlier, VMVF = 1.0E09 indicates the code that the mixture does not contain fuel. Since VSTRUC = 1.0, all the mixture is filled with the structural material, in this case SS HT-9.

Axial reflector (SS pellets)
This case is a little more complex since it contains both structural material and coolant.

```
FUTEMP 1500.
CATEMP 900.
COTEMP 800.
VMVF   1.0E09
FIST   0.0
```

```
VMOD   0.2869
VSTRUC 0.7131
RF     0.4500
DC     0.0869
FUSD   0.95
COSD   1.0
```

Again, all fuel pin parameters are ignored, and this mixture is filled with 71.31% of steel and 28.69% Sodium, which are the proportions in a fuel assembly if a fuel pellet was replaced with a steel pellet.

Control Rods

In this case, we have structural material, coolant and B_4C.

```
FUTEMP 1500.
CATEMP 900.
COTEMP 800.
VMVF   1.0E09
FIST   0.0
VMOD   0.4785
VSTRUC 0.0710
RF     0.4500
DC     0.0869
FUSD   0.95
COSD   1.0
```

In a previous chapter the geometric characteristics of the control rods and the atomic density of the B_4C were presented. In this mixture, the volumetric fractions are 0.4785 for coolant, 0.0710 for the channel walls and 0.4505 for the control rods. The solution here consists in adding a card called `'ADDM'`, similar as `'ADDF'` but this one adds material to the coolant. In order to weight well the densities given in Table 3.4, it is needed to multiply it by the control rod volume and divide it by the sodium volume. The resulting vector is the following:

```
'ADDM' 4
'B 10 ' 300.  1.640028E-02
'B 11 ' 300.  1.822254E-03
'C 12 ' 300.  4.505524E-03
'C 13 ' 300.  5.011198E-05
```

6.4 Particularities of Each Case of Study

At this point all main input values that share all the models have been explained. Now it is time to describe their differences.

This work's intention was to keep the cases as identical as possible, in order to have a good benchmark between their results. The same geometry and fuel distribution at the beginning of cycle was kept for all cases. Also, the same time steps were used and the fuel reshufflings were done at the same time. What was different is the fuel reshuffling, fuel was reshuffled differently for every case.

The methodology is as follows: Tables 6.3 to 6.5 show all the time steps considered and the precise moment at which every reshuffling action was taken. Additionally to this, images (Figures 6.3 to 6.7) show the fuel assembly movements.

It is important to note that even when Figures 6.3 to 6.7 shows only fuel assemblies 21 to 55, which corresponds to the first axial layer, these movements are done in every axial layer of the active core. Additionally, it is important to explain that the fuel assemblies start at 21 because the user decided to leave the first 20 for mixture definition.

6.4.1 Case 1

Table 6.3: Description of the time steps and reshuffle times in Case 1

Steps	**Duration (Days)**	**Time After Step (Years)**	**Steps**	**Duration (Days)**	**Time After Step (Years)**
BEGINNING OF CYCLE			RESHUFFLING 1		
5	365	5.000	1	1	30.003
RESHUFFLING 1			1	364	31.000
1	1	5.003	4	365	35.000
1	364	6.000	RESHUFFLING 1		
4	365	10.000	1	1	35.003
RESHUFFLING 1			1	364	36.000
1	1	10.003	3	365	39.000
1	364	11.000	RESHUFFLING 1		

4	365	15.000	1	1	39.003
RESHUFFLING 1			1	364	40.000
1	1	15.003	3	365	43.000
1	364	16.000	RESHUFFLING 1		
4	365	20.000	1	1	43.003
RESHUFFLING 1			1	364	44.000
1	1	20.003	4	365	48.000
1	364	21.000			
4	365	25.000			
RESHUFFLING 1					
1	1	25.003			
1	364	26.000			
4	365	30.000			

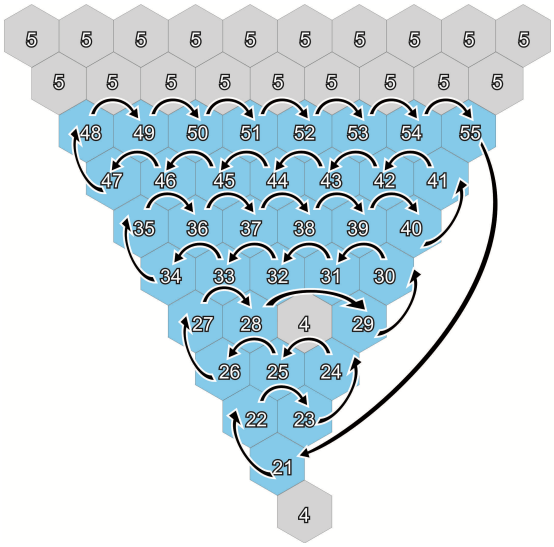

Figure 6.3: Description of Reshuffling 1.

6.4.2 Case 2

Table 6.4: Description of the time steps and reshuffle times in Case 1

Steps	Duration (Days)	Time After Step (Years)	Steps	Duration (Days)	Time After Step (Years)
BEGINNING OF CYCLE			RESHUFFLING 2		
5	365	5.000	1	1	30.003
RESHUFFLING 2			1	364	31.000
1	1	5.003	4	365	35.000
1	364	6.000	RESHUFFLING 2		
4	365	10.000	1	1	35.003
RESHUFFLING 2			1	364	36.000
1	1	10.003	3	365	39.000
1	364	11.000	RESHUFFLING 2		
4	365	15.000	1	1	39.003
RESHUFFLING 2			1	364	40.000
1	1	15.003	3	365	43.000
1	364	16.000	RESHUFFLING 2		
4	365	20.000	1	1	43.003
RESHUFFLING 2			1	364	44.000
1	1	20.003	4	365	48.000
1	364	21.000			
4	365	25.000			
RESHUFFLING 2					
1	1	25.003			
1	364	26.000			
4	365	30.000			

6.4.3 Case 3

Table 6.5: Description of the time steps and reshuffle times in Case 1

Steps	Duration (Days)	Time After Step (Years)	Steps	Duration (Days)	Time After Step (Years)
BEGINNING OF CYCLE			RESHUFFLING 3B		
5	365	5.000	1	1	30.003
RESHUFFLING 2			1	364	31.000

1	1	5.003	4	365	35.000
1	364	6.000	RESHUFFLING 2		
4	365	10.000	1	1	35.003
RESHUFFLING 2			1	364	36.000
1	1	10.003	3	365	39.000
1	364	11.000	RESHUFFLING 2		
4	365	15.000	1	1	39.003
RESHUFFLING 3A			1	364	40.000
1	1	15.003	3	365	43.000
1	364	16.000	RESHUFFLING 3C		
4	365	20.000	1	1	43.003
RESHUFFLING 2			1	364	44.000
1	1	20.003	4	365	48.000
1	364	21.000			
4	365	25.000			
RESHUFFLING 2					
1	1	25.003			
1	364	26.000			
4	365	30.000			

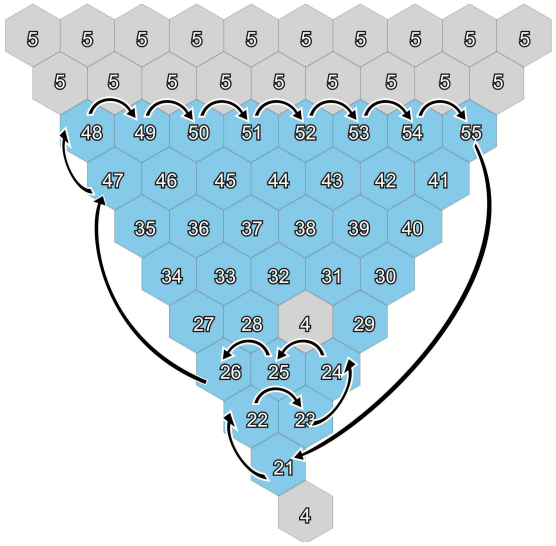

Figure 6.4: Description of Reshuffling 2.

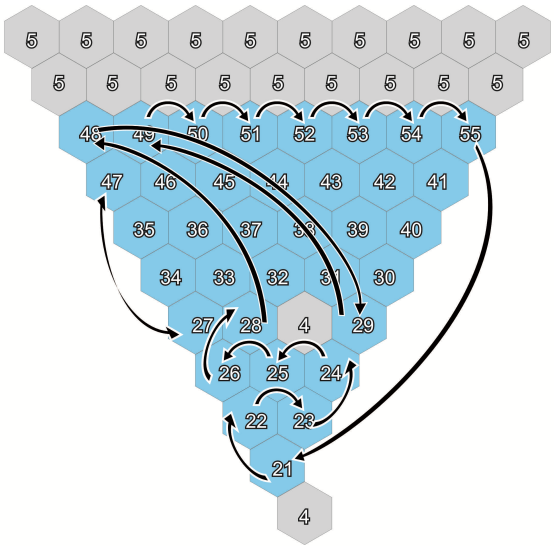

Figure 6.5: Description of Reshuffling 3A.

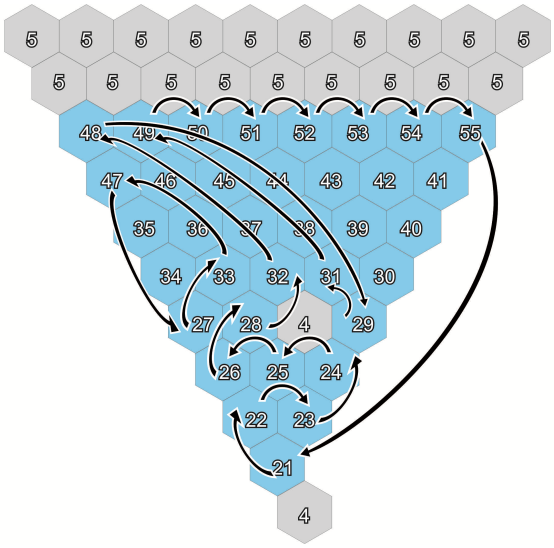

Figure 6.6: Description of Reshuffling 3B.

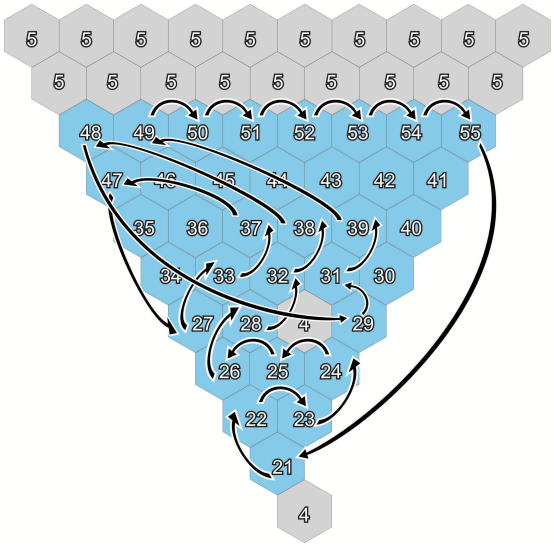

Figure 6.7: Description of Reshuffling 3C.

Chapter 7

RESULTS AND DISCUSSION

In the present chapter, the results of the simulations explained before are presented. The structure of this chapters is as follows: first the effective neutron multiplication factor is compared between all the cases treated, then a comparison of the main isotopes for various mixtures/positions is made, and finally a brief discussion of the phenomena is carried out.

7.1 Effective Neutron Multiplication Factor (k_{eff}) Results

In Figure 7.1 a plot of the four studied cases (cases 1 to 3 plus a non-reshuffling case) is presented.

As can be seen, a big improvement in the operation life capability is reached by the use of a fuel reshuffling scheme, compared with the same core configuration without reshuffling.

It can also be seen is that discharge burnup is about 430 GWd/T which corresponds to 44.8 % FIMA (fissions per initial heavy metals atoms), a previous work [Hejzlar et al., 2013] concluded that a minimum burnup of 30% is necessary for a Traveling Wave Reactor (TWR) operation, the results obtained in this research are consistent with this.

7.1.1 No Reshuffling

In the case where no reshuffling scheme was done, the results is very intuitive and meet with what is expected for a fuel that is being burned. At the beginning, k_{eff} grows slowly

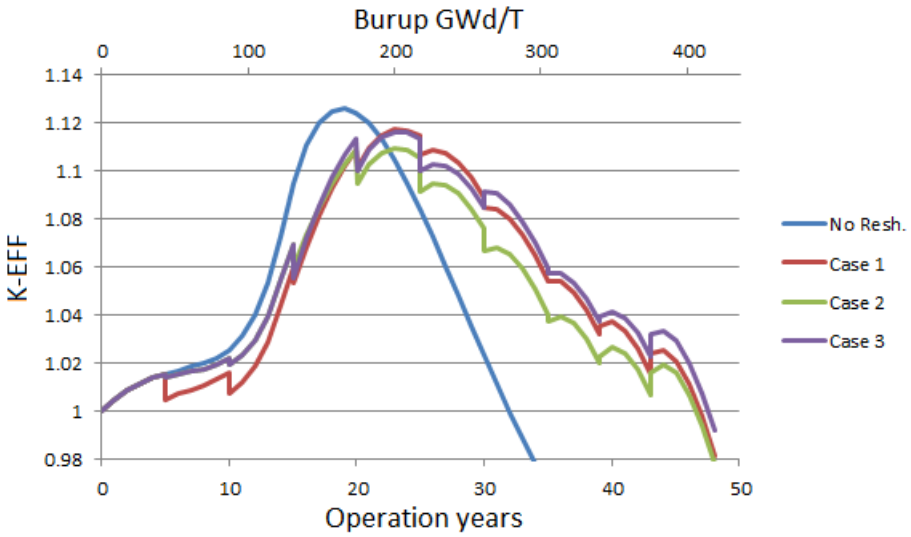

Figure 7.1: k_{eff} plot for the studied cases.

since some of the extra neutrons from the fissions are being captured by the fertile fuel, instead of being used for extra fissions. After a certain amount of Pu is breed (around the year 10) the k_{eff} grows faster until the fissile fuel gets exhausted, it goes down with a more or less constant rate until core gets subcritical beyonfd that point. This sudden growth in k_{eff} can be explained since enough Pu has been bred and the ^{235}U gets exhausted, because more fissions are taking place in the Pu, as the number of prompt neutrons per Pu fission becomes higher than in U, this creates a positive feedback as more Pu is being bred and burned.

As mentioned before, no surprises were found here and the behavior is consistent with what is expected.

7.1.2 Cases with Reshuffling

In the three cases where reshuffling was done, the results are consistent. The main differences on each case are the height of the reactivity jumps after each reshuffling and the final operation time that could be accomplished.

In order to analyze the whole operation, this should be divided into three stages: the first comprise the first 25 years, the second is from year 25 to approximately 38, and the third stage that covers the last 10 years of operation.

First stage: On the three cases the tendency of k_{eff} is to increase, and in fact after 10 years this tendency increases for the same reasons explained in the previous section. In this stage a reshuffling leads to a step-down in the k_{eff} plot, this can be explained for the fact that in the central area of the core the fuel breeding is higher than in the peripheral area then with each reshuffle a central assembly, that has already breed fissile fuel, is replaced by an assembly from the periphery with less breed fuel; this leads to a decrease in k_{eff} after this action. Despite this phenomena, the assembly that is recently inserted in the central zone starts breeding fuel faster, so the k_{eff} increases tendency is maintained.

Second stage: After 25 years of operations, the originally-fissile fuel has been exhausted for a while and the originally-fertile material has already breed and burned enough to have a global k_{eff} decreasing tendency in the whole core, this is due to the fact that fuel breeding is reduced considerably. In general fuel reshuffling here leads to a k_{eff} reduction for the same reason as described in the first stage, but this can be changed with a more complex and well thought strategy; as can be seen in the figure, for Case 3 one of the reshufflings in this stage led to a k_{eff} increase, this can be explained due to the fact that in the reshuffling scheme used for case 3, it was intended to remove the exhausted assemblies taking them to the periphery and replacing them by assemblies with breed fuel, one of this changes led to a configuration with higher reactivity. In this stage after each reshuffle, the curve tends to increase a little but eventually goes down keeping the decreasing tendency. This brief increasing tendency can be attributed to the fuel breeding in the assembly recently placed in the central zone.

Third stage: In this final part of the operation most of the fuel is depleted and most of the power is generated in the central area by the originally-fertile assemblies that now are in this zone. This causes an interesting effect on the k_{eff} plot, as there is still a big quantity of fertile material on those assemblies, fissile fuel is easily breed and then burned in a relatively short period of time, this causes the k_{eff} to increase until reaching a maximum and then to fall rapidly. It is important to note that around this point the fuel is so exhausted that the inclusion of a peripheral assembly to the central area leads to a k_{eff} step-up after the last reshuffle.

In order to justify the reasons of the asumptions made on the k_{eff} behavior, a more deep study on the fuel inventories will be carried out in the next section.

7.2 Cases Results Comparison

In this section the evolution of the main fissile/fertile isotopes (^{2}35U, ^{2}38U, ^{239}Pu and ^{241}Pu) inventories are presented; these results are expected to justify our assumptions on the k_{eff} curve behavior. As mentioned in the model description, the way the core is discretized lead to a set of 195 mixtures that are followed by the code, it is not practical to present results of every single mixture but only a representative part of it. The Figure 7.2 shows the assemblies selected to be tracked through core's life

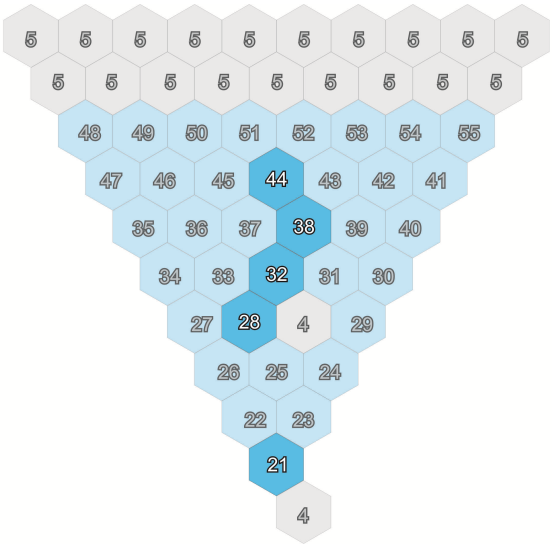

Figure 7.2: Selection of followed assemblies.

As mentioned in a previous chapter, the core is divided radially into fuel assemblies and axially into layers. As this thesis considers only neutronics and no thermalhydraulics effects, the core can be seen as axially symmetrical. Given this symmetry, only half of the nine axial layers will be considered. The tracked mixtures (related to axial and radial nodalization) are shown in Table 7.1.

Table 7.1: Followed mixtures

LAYER 1	21	28	32	38	44
LAYER 3	91	98	102	108	114
LAYER 3	161	168	172	178	184

An important thing to say is that KANEXT sends all the information of the fuel inventories

among other things, into a single output; this causes very heavy ASCII files (700 MB – 1.1 GB) which are hard to handle with a regular text processor. Additional to this, the output file does not follow a mixture though the reshuffling but gives the inventory of the mixture on a given fixed position, this leads to plots like Figure 7.3, which does not correspond to a unique mixture but all the mixtures that were placed in a fixed position.

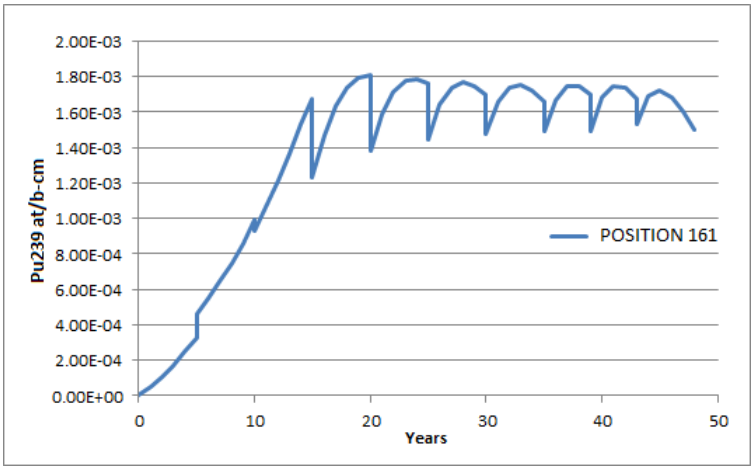

Figure 7.3: Example of the inventories displayed by the output.

In order to have the information about fuel inventories in the order that we required, it was decided to construct a post-process tool that read the fuel reshuffles as are set in the input and follow each mixture according to those moves, so it can be printed in a new output file dedicated to fuel evolution. In the Appendix A, B and C the tables describing the position of each mixture for each time step are given.

In addition, in order to see the effect of the axial position, more than one mixture are shown per plot.

The results will be presented as follows: fuel inventories for the selected mixtures in Table 7.1 are shown as well as power maps of those selected axial layers at the beginning and end of cycle. It is important to note that the numbers in the power maps correspond to the power (in MW) generated by the mixture in that position, for that reason the spaces for the control rods have no numbers at all. These images (Figures 7.4 to 7.42) are shown in the next section. After the plots, a discussion of the results will be given.

No results of case with no reshuffling are shown, since it was considered only to observe the operation time gain though fuel reshuffling, see Figure 7.1.

7.2.1 Case 1

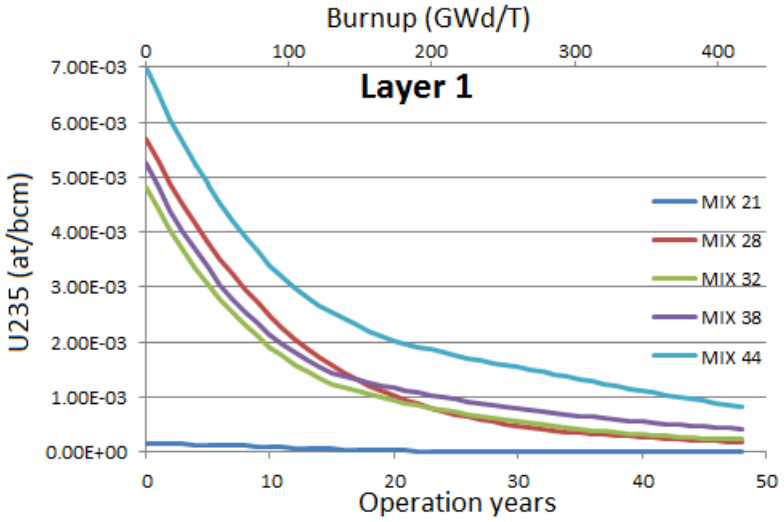

Figure 7.4: ^{235}U inventories for selected isotopes in Case 1, Layer 1.

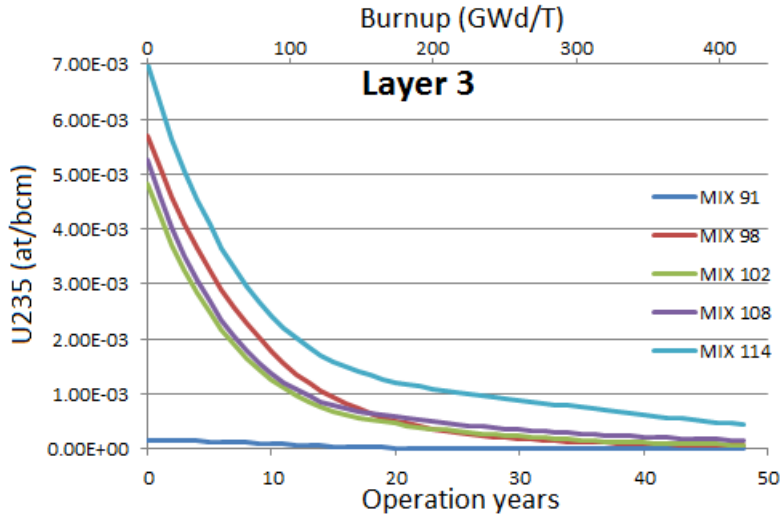

Figure 7.5: ^{235}U inventories for selected isotopes in Case 1, Layer 3.

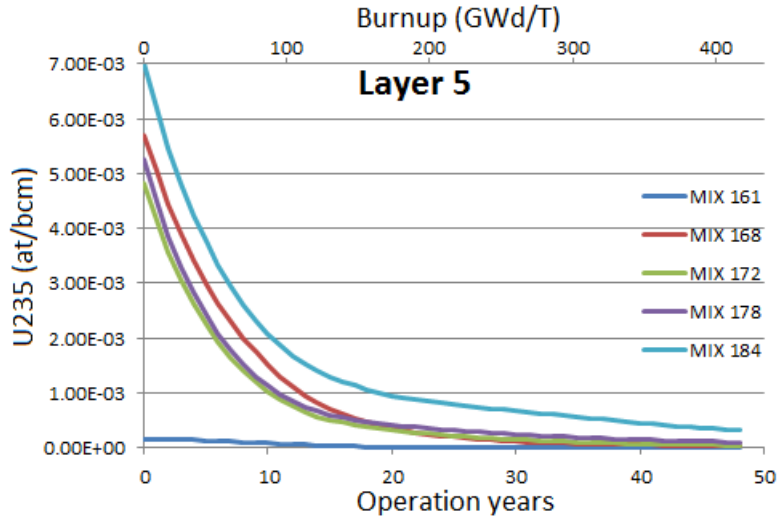

Figure 7.6: ^{235}U inventories for selected isotopes in Case 1, Layer 5.

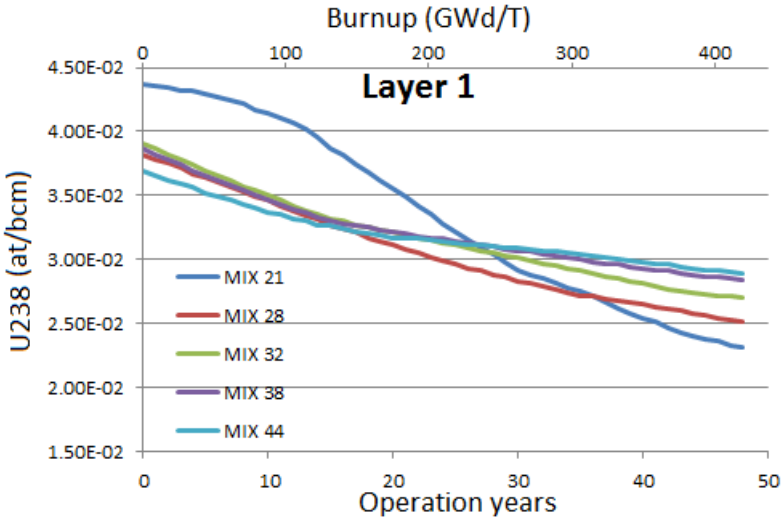

Figure 7.7: ^{238}U Inventories for selected isotopes in Case 1, Layer 1.

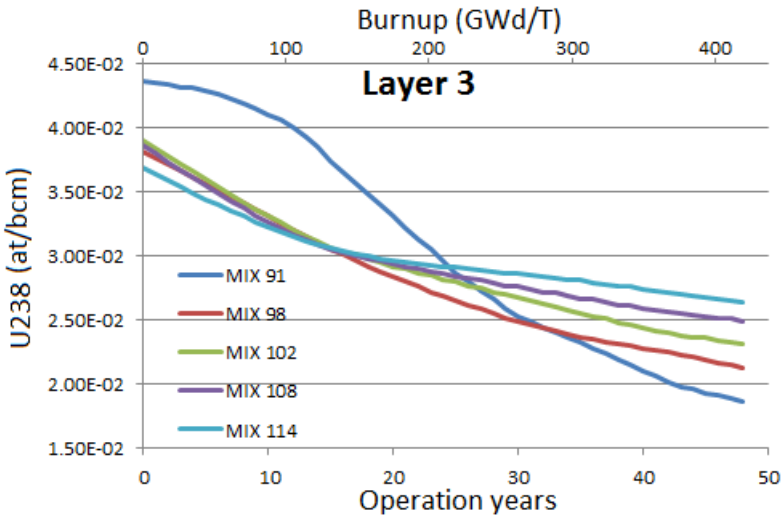

Figure 7.8: ^{238}U Inventories for selected isotopes in Case 1, Layer 3.

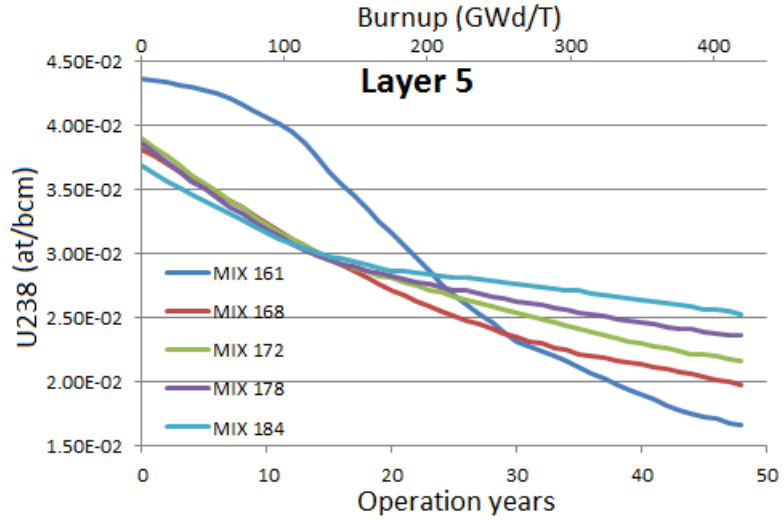

Figure 7.9: ^{238}U Inventories for selected isotopes in Case 1, Layer 5.

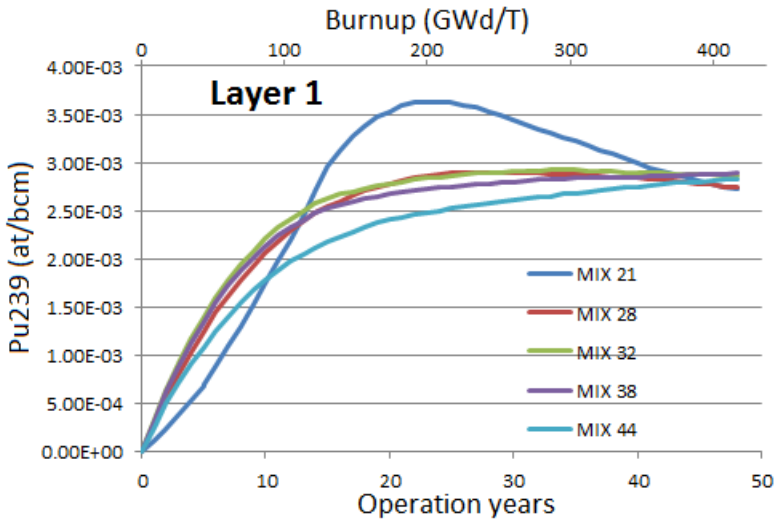

Figure 7.10: ^{239}Pu Inventories for selected isotopes in Case 1, Layer 1.

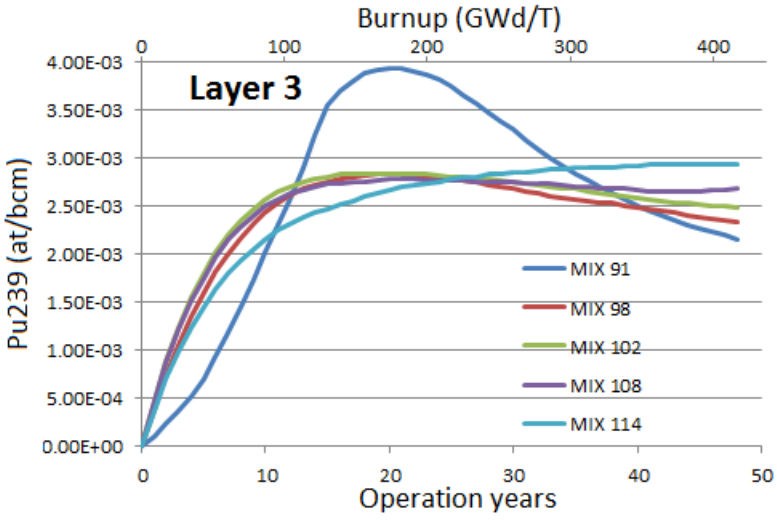

Figure 7.11: ^{239}Pu Inventories for selected isotopes in Case 1, Layer 3.

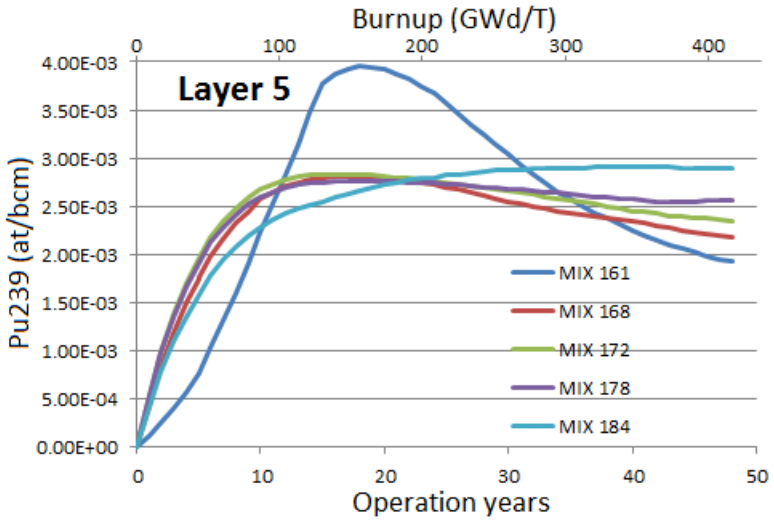

Figure 7.12: ^{239}Pu Inventories for selected isotopes in Case 1, Layer 5.

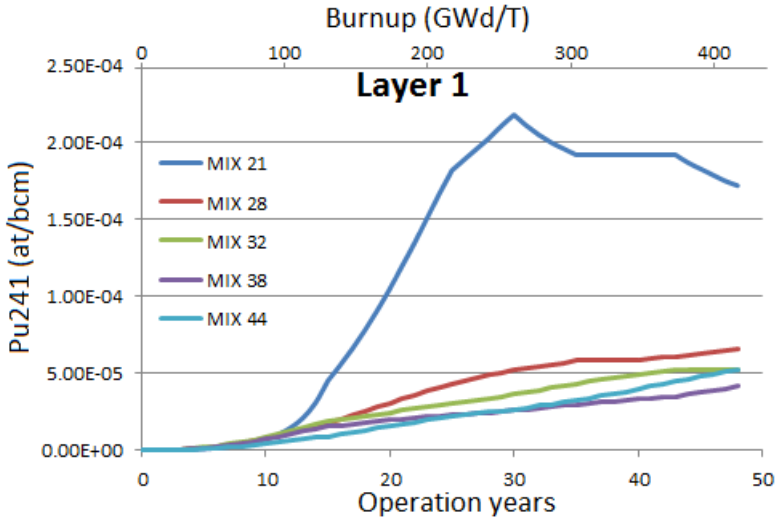

Figure 7.13: ^{241}Pu Inventories for selected isotopes in Case 1, Layer 1.

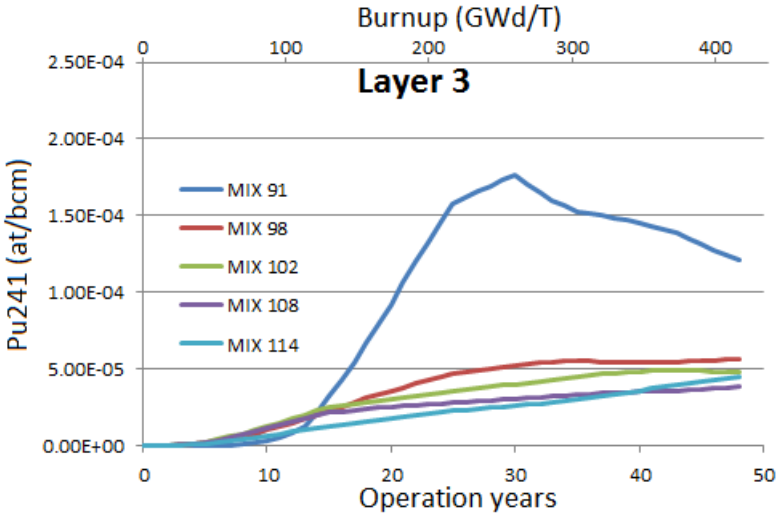

Figure 7.14: ^{241}Pu Inventories for selected isotopes in Case 1, Layer 3.

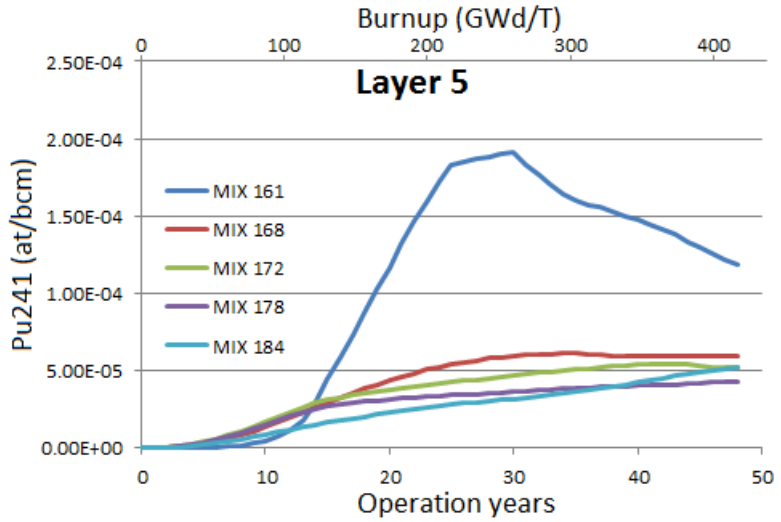

Figure 7.15: ^{241}Pu Inventories for selected isotopes in Case 1, Layer 5.

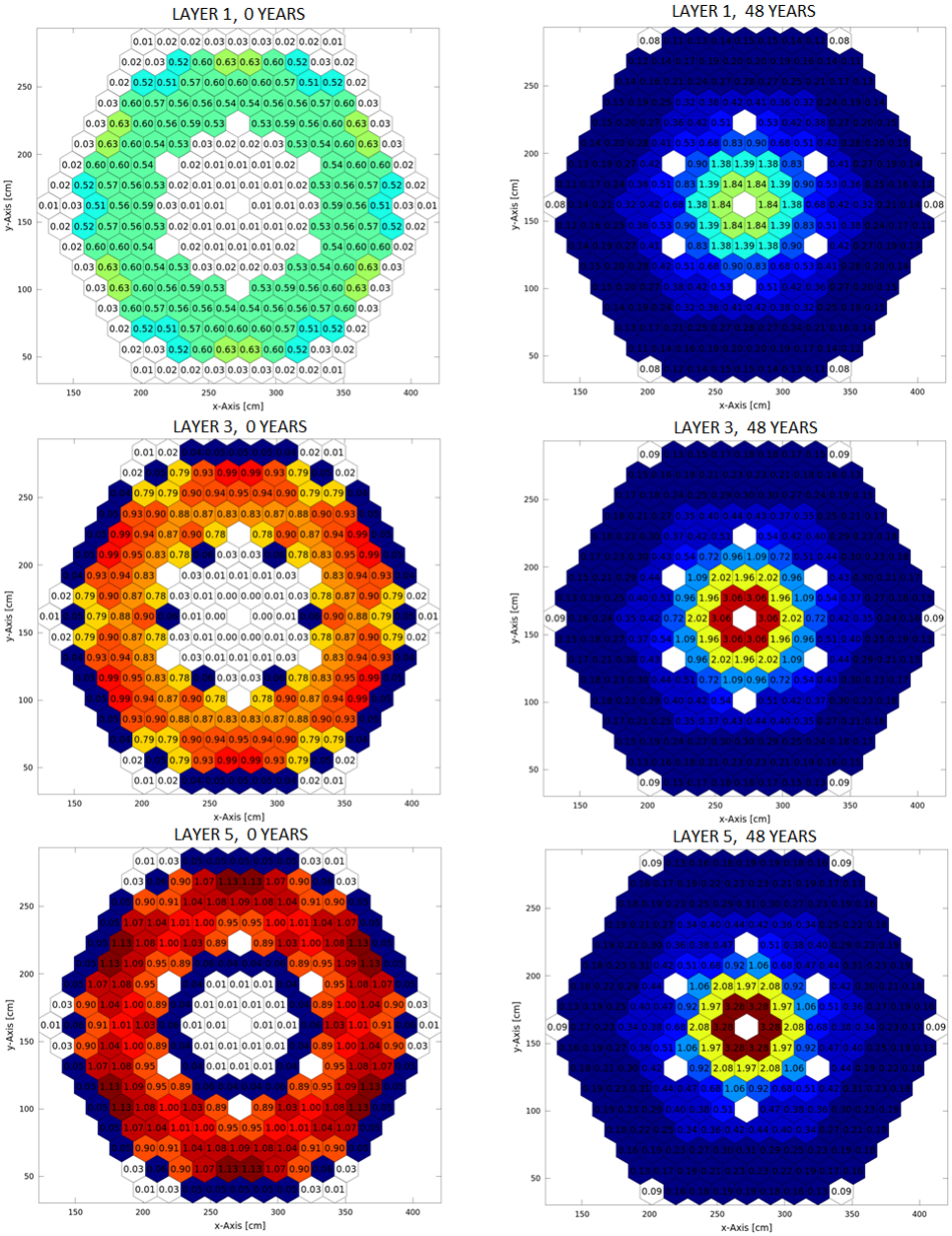

Figure 7.16: Power maps of the selected axial layers at the beginning of cycle (left) and end of cycle (right) for Case 1.

7.2.2 Case 2

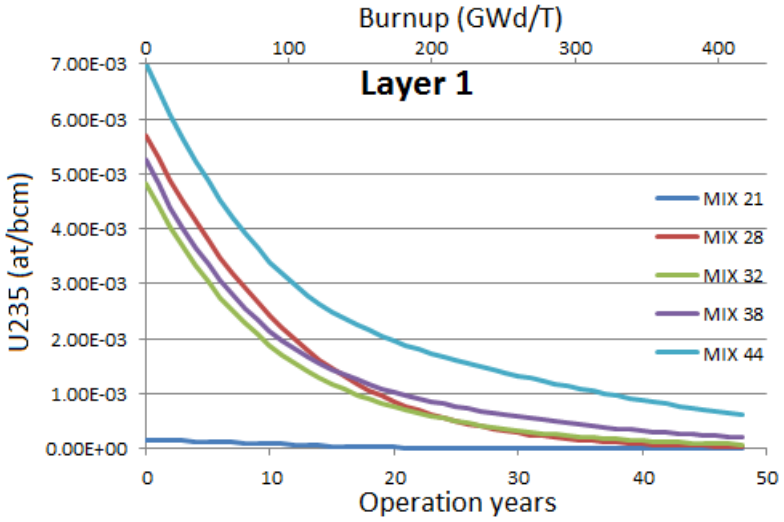

Figure 7.17: ^{235}U inventories for selected isotopes in Case 2, Layer 1.

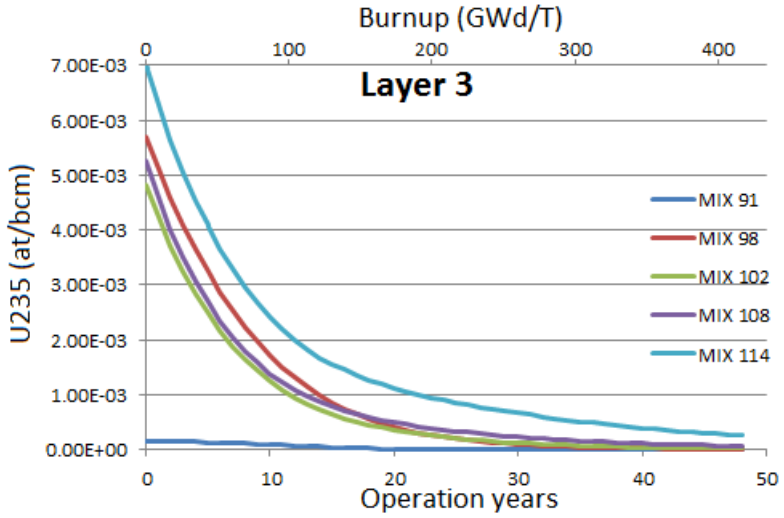

Figure 7.18: ^{235}U inventories for selected isotopes in Case 2, Layer 3.

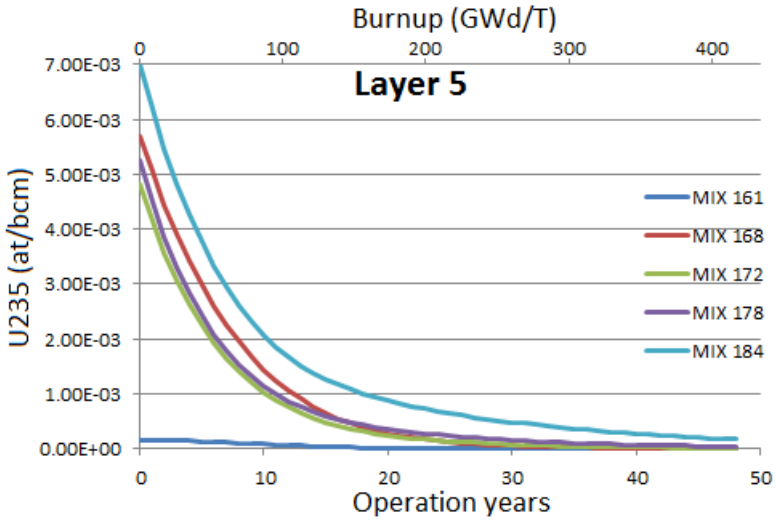

Figure 7.19: ^{235}U inventories for selected isotopes in Case 2, Layer 5.

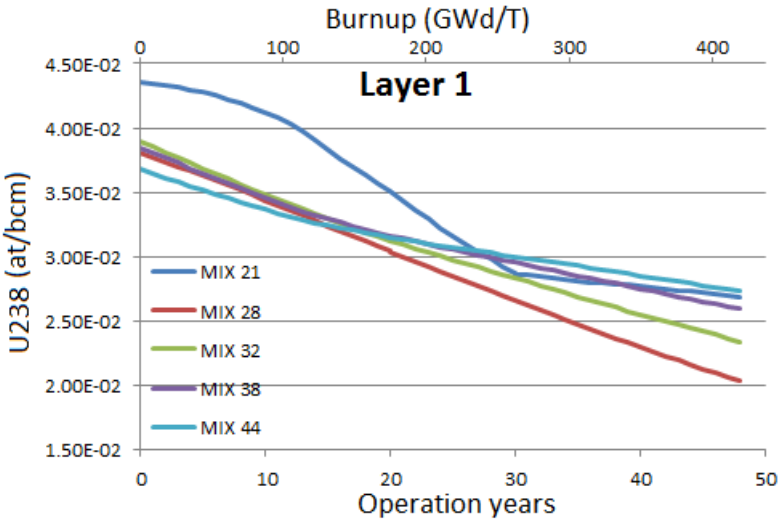

Figure 7.20: ^{238}U Inventories for selected isotopes in Case 2, Layer 1.

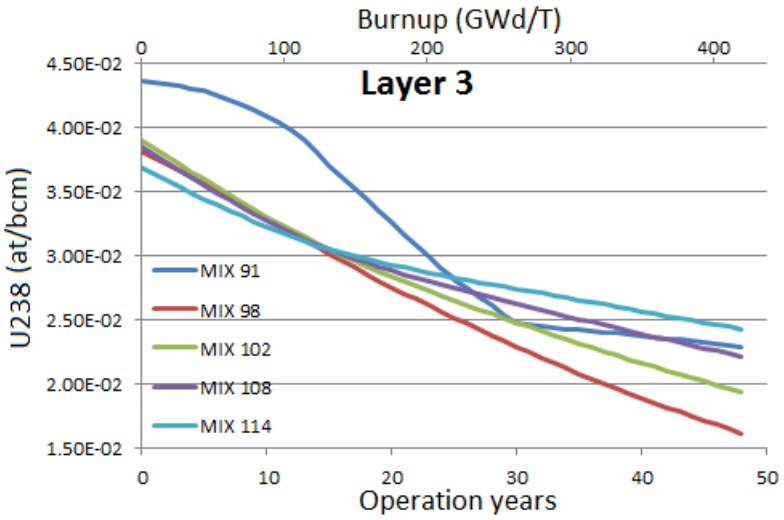

Figure 7.21: ^{238}U Inventories for selected isotopes in Case 2, Layer 3.

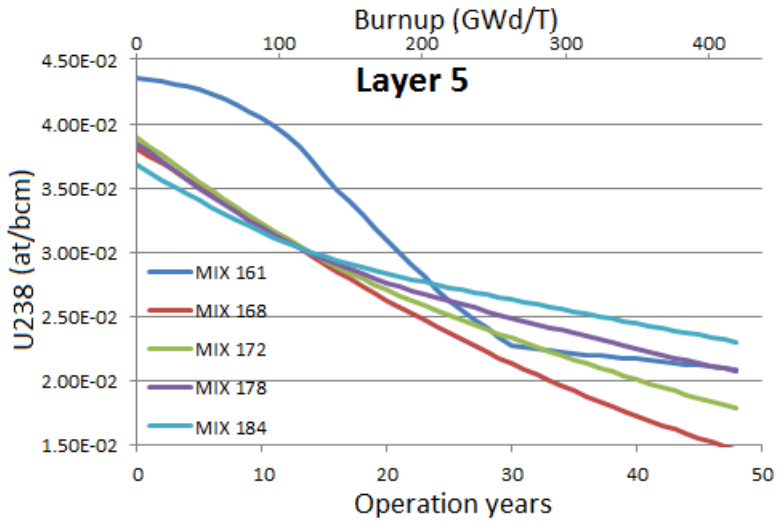

Figure 7.22: ^{238}U Inventories for selected isotopes in Case 2, Layer 5.

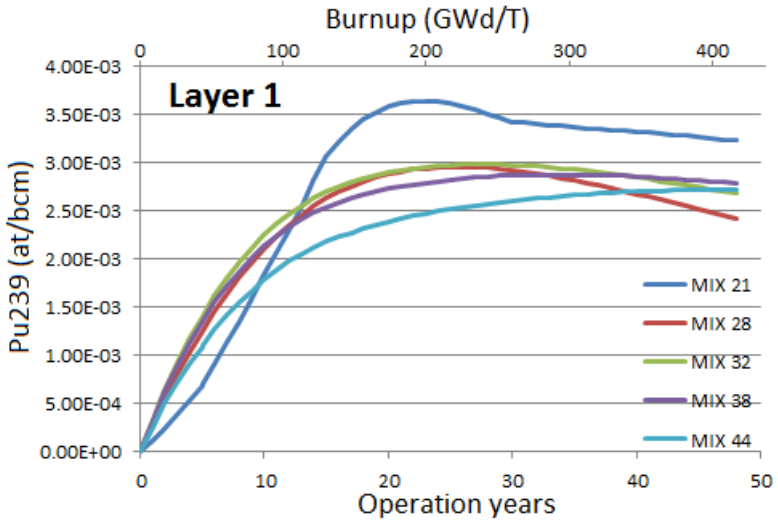

Figure 7.23: ^{239}Pu Inventories for selected isotopes in Case 2, Layer 1.

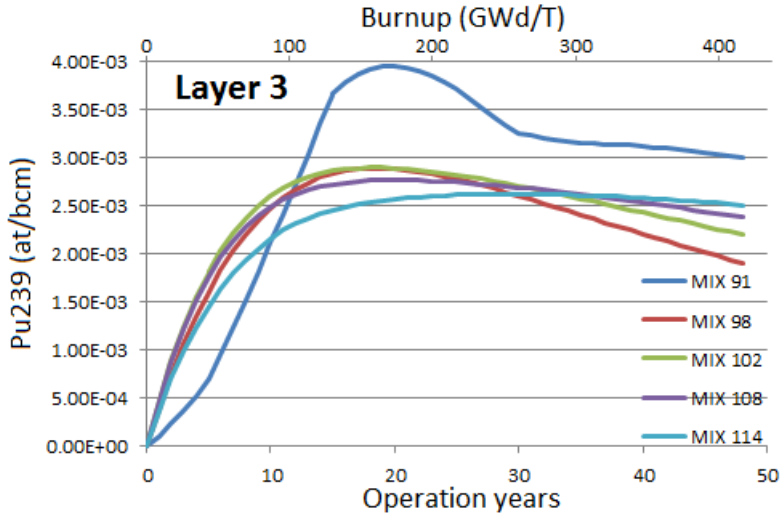

Figure 7.24: ^{239}Pu Inventories for selected isotopes in Case 2, Layer 3.

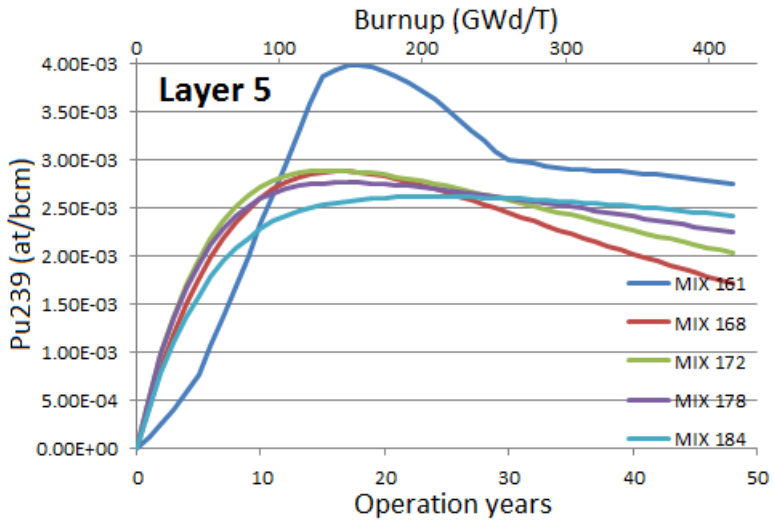

Figure 7.25: ^{239}Pu Inventories for selected isotopes in Case 2, Layer 5.

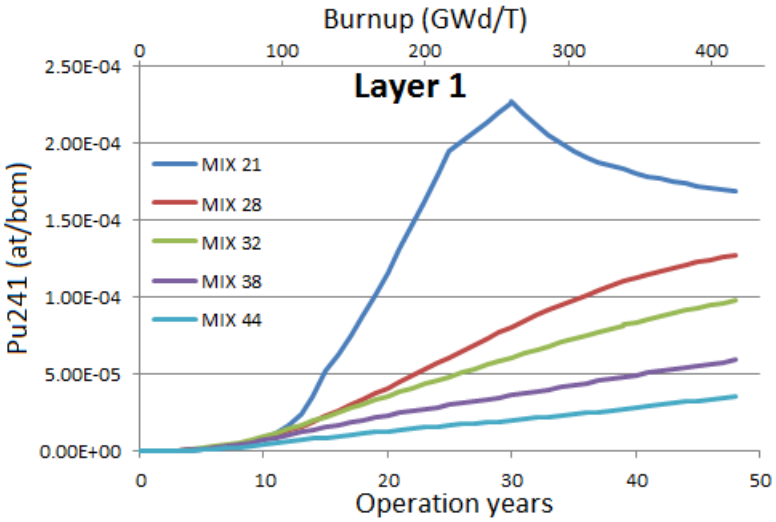

Figure 7.26: ^{241}Pu Inventories for selected isotopes in Case 2, Layer 1.

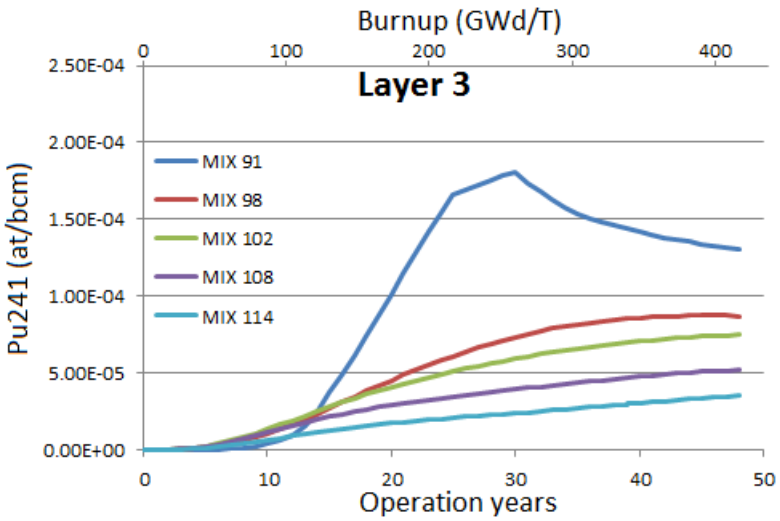

Figure 7.27: ^{241}Pu Inventories for selected isotopes in Case 2, Layer 3.

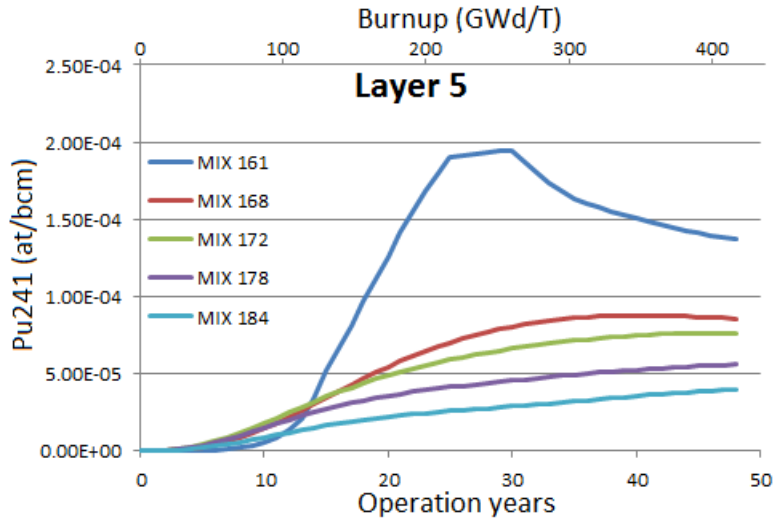

Figure 7.28: ^{241}Pu Inventories for selected isotopes in Case 2, Layer 5.

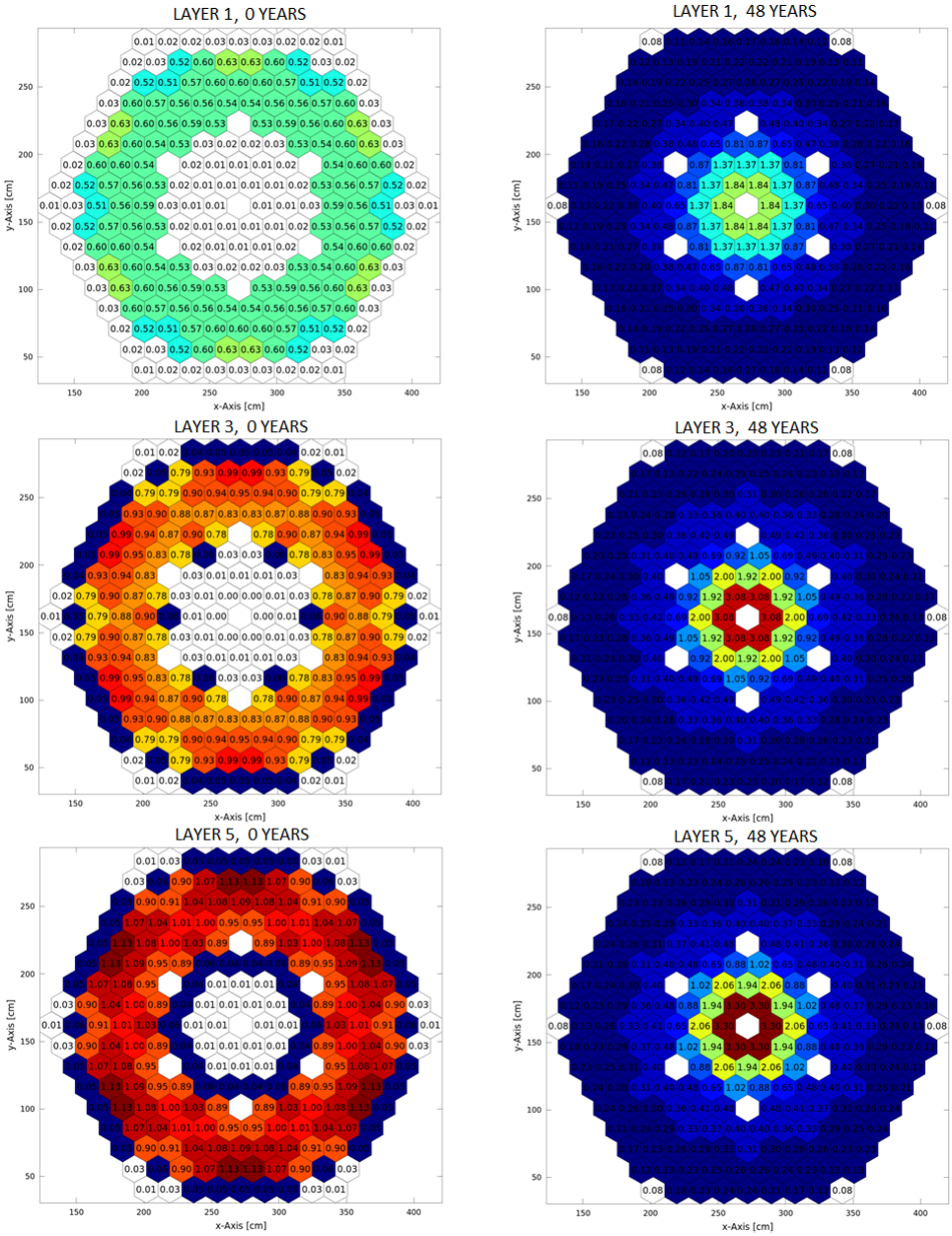

Figure 7.29: Power maps of the selected axial layers at the beginning of cycle (left) and end of cycle (right) for Case 2.

7.2.3 Case 3

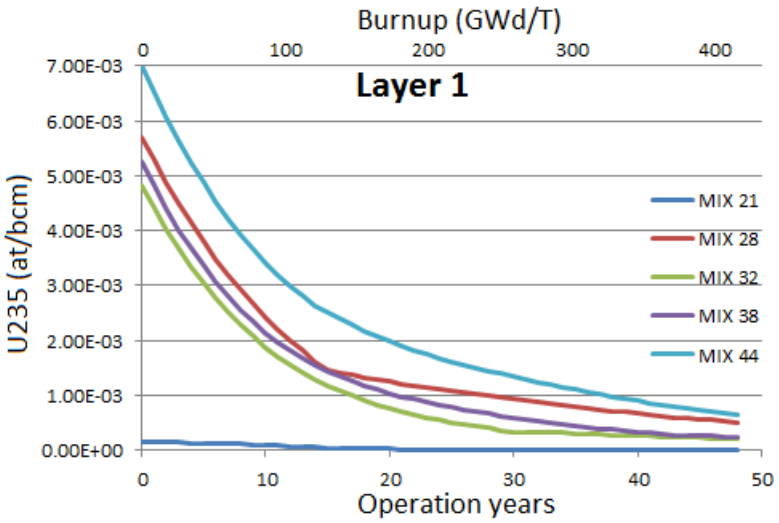

Figure 7.30: ^{235}U inventories for selected isotopes in Case 3, Layer 1.

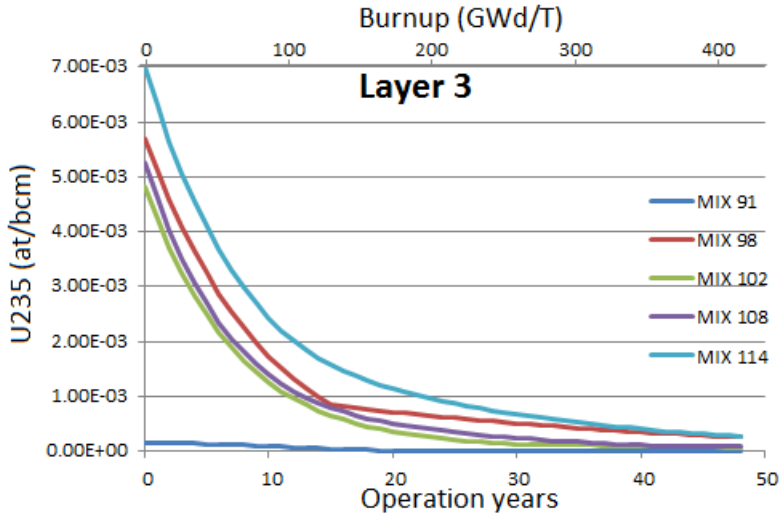

Figure 7.31: ^{235}U inventories for selected isotopes in Case 3, Layer 3.

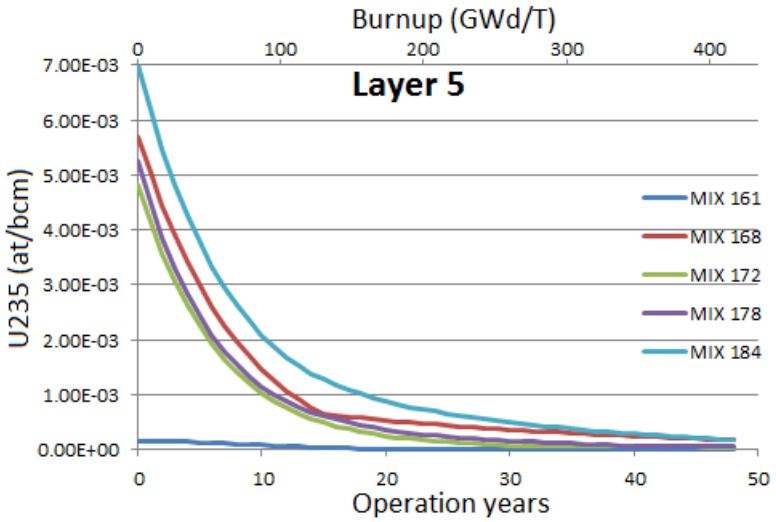

Figure 7.32: ^{235}U inventories for selected isotopes in Case 3, Layer 5.

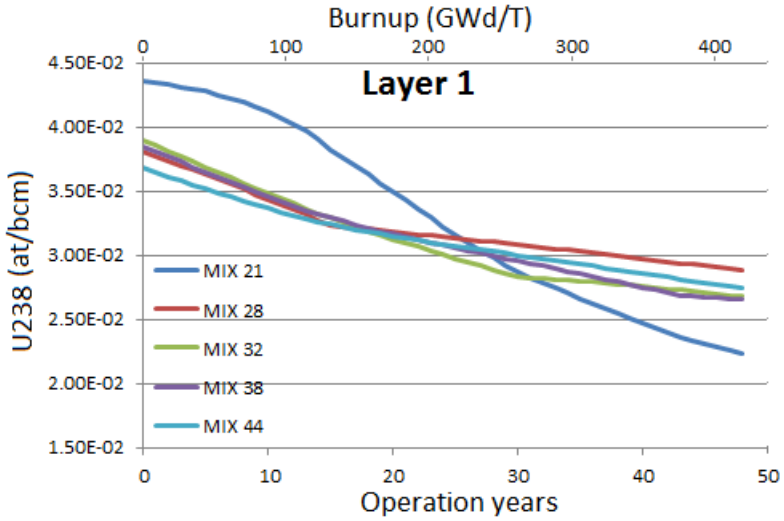

Figure 7.33: ^{238}U Inventories for selected isotopes in Case 3, Layer 1.

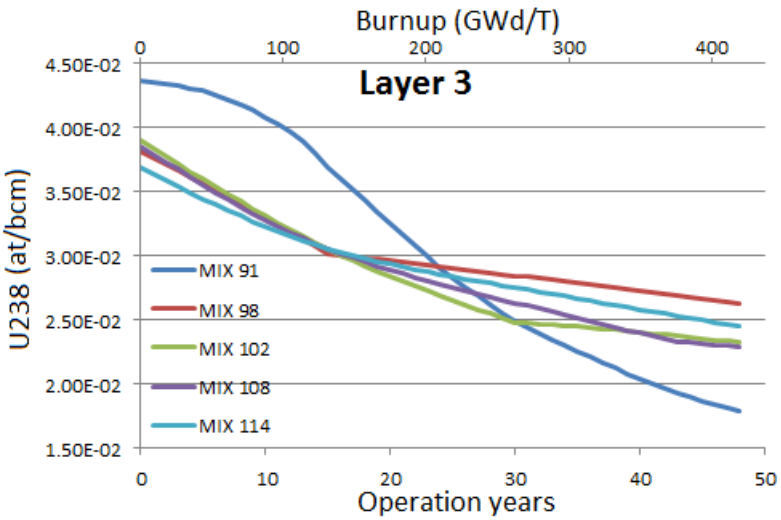

Figure 7.34: ^{238}U Inventories for selected isotopes in Case 3, Layer 3.

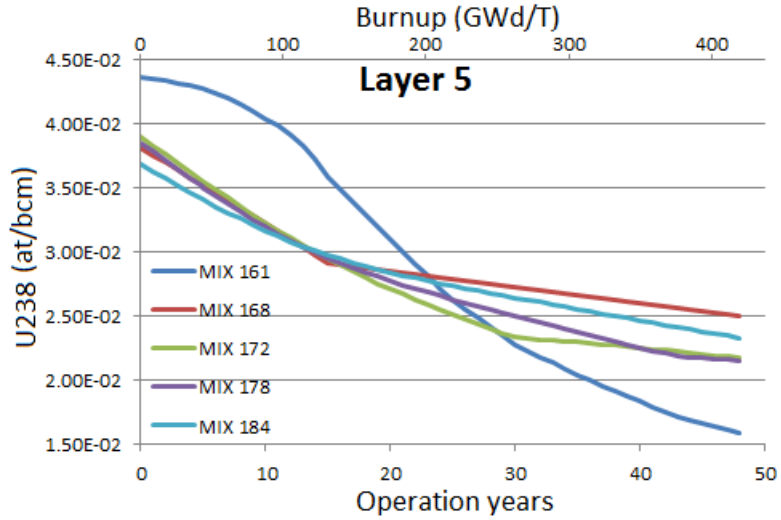

Figure 7.35: ^{238}U Inventories for selected isotopes in Case 3, Layer 5.

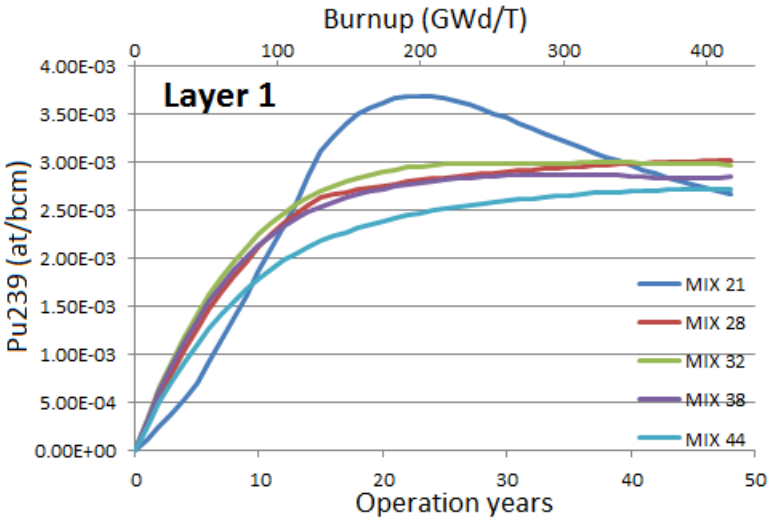

Figure 7.36: ^{239}Pu Inventories for selected isotopes in Case 3, Layer 1.

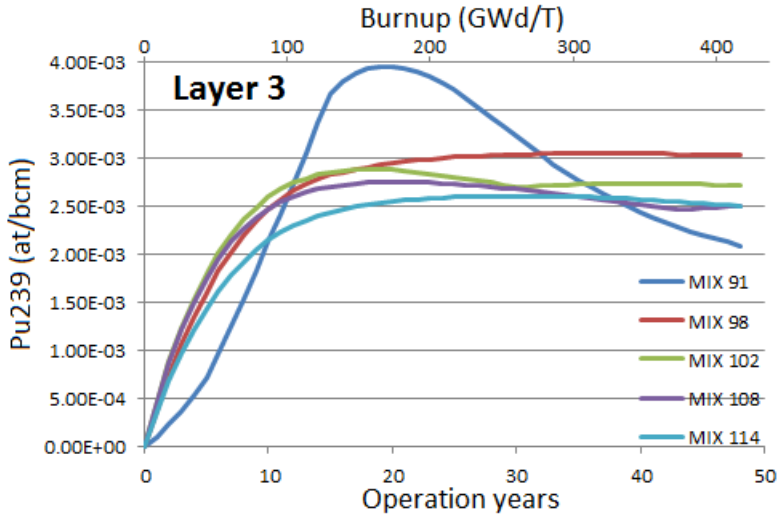

Figure 7.37: ^{239}Pu Inventories for selected isotopes in Case 3, Layer 3.

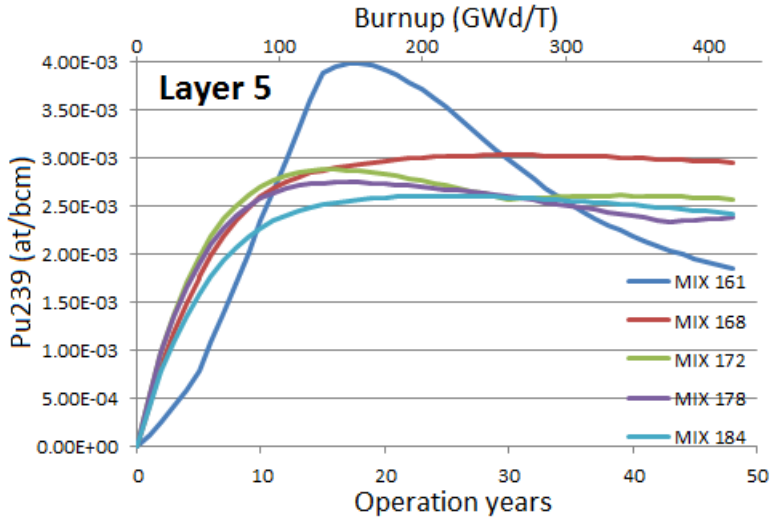

Figure 7.38: ^{239}Pu Inventories for selected isotopes in Case 3, Layer 5.

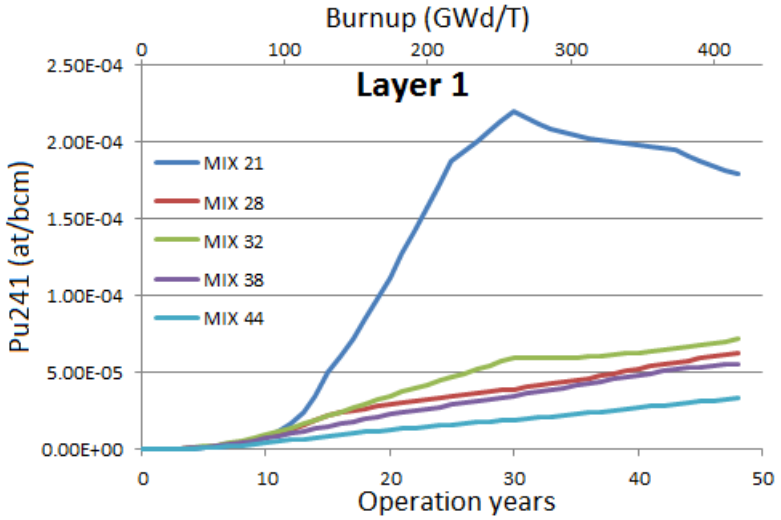

Figure 7.39: ^{241}Pu Inventories for selected isotopes in Case 3, Layer 1.

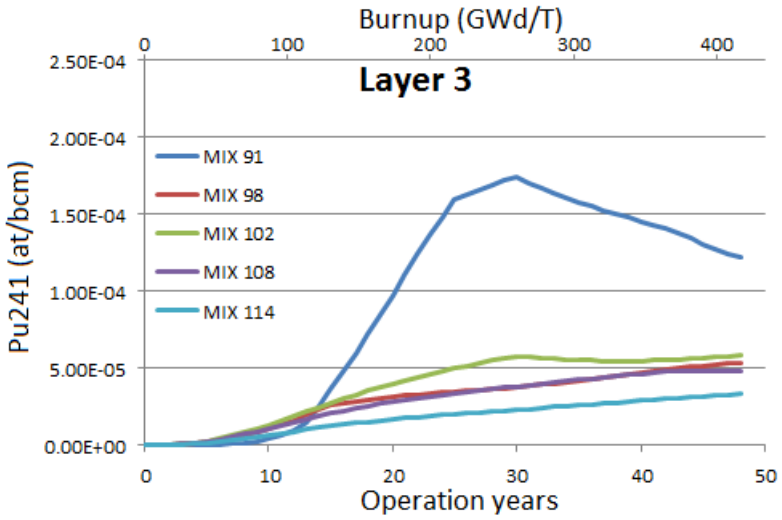

Figure 7.40: ^{241}Pu Inventories for selected isotopes in Case 3, Layer 3.

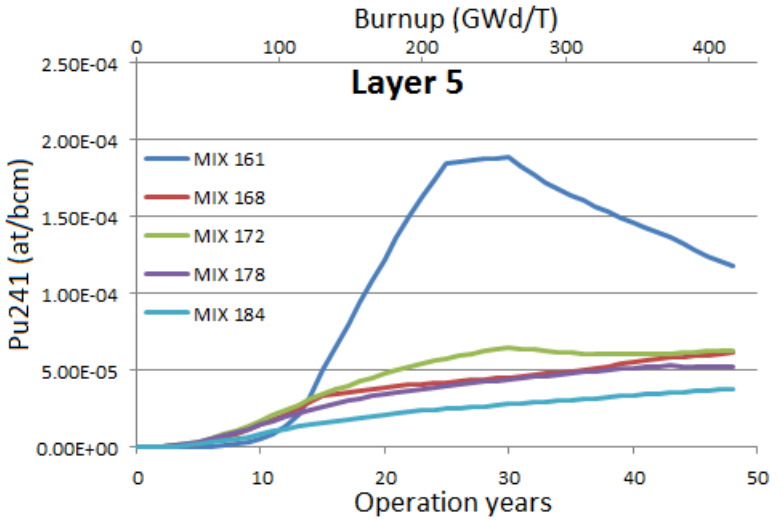

Figure 7.41: ^{241}Pu Inventories for selected isotopes in Case 3, Layer 5.

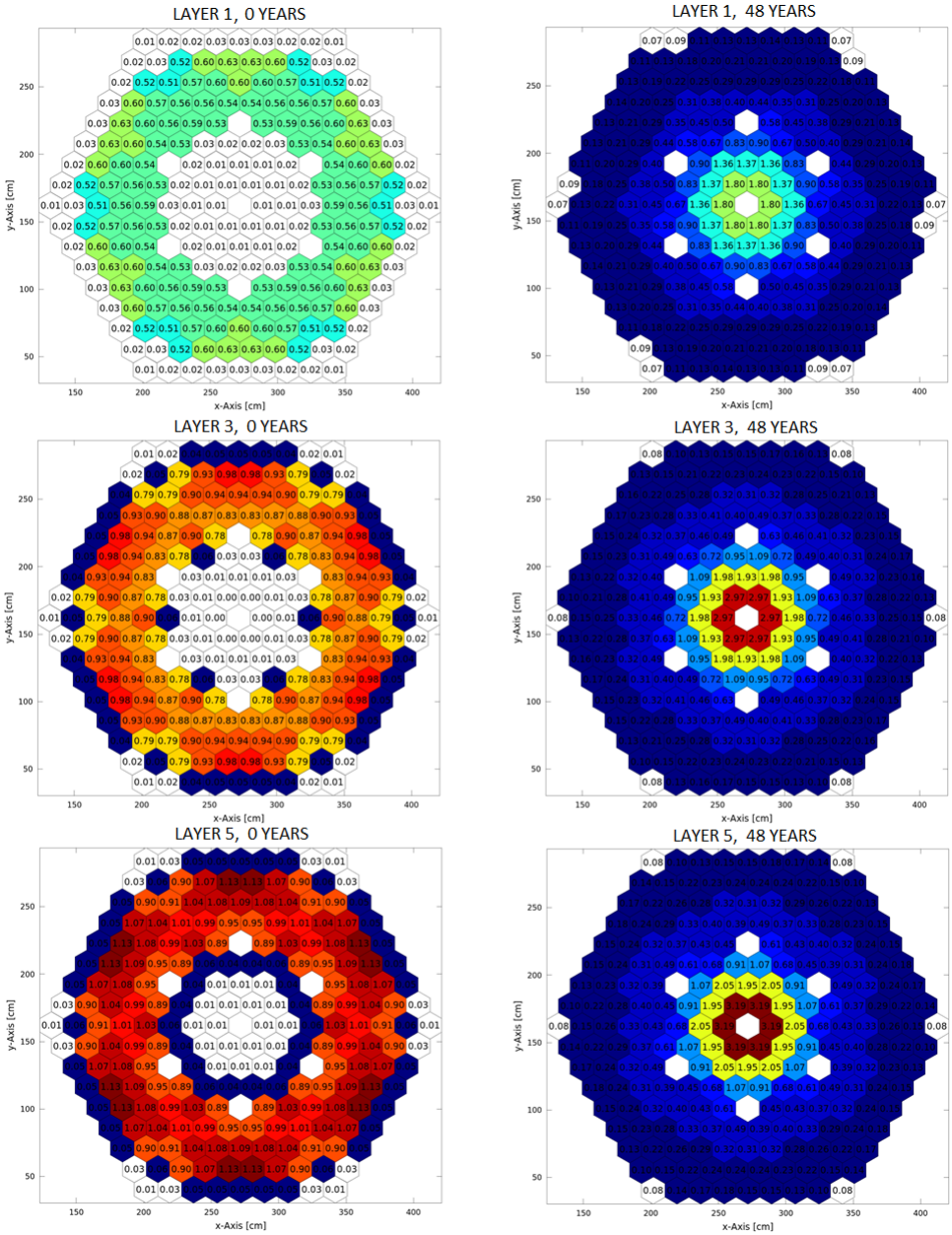

Figure 7.42: Power maps of the selected axial layers at the beginning of cycle (left) and end of cycle (right) for Case 3.

7.3 Discussion of Previous Results

The first plots to discuss in this sections are the power maps. As predicted in the beginning of this chapter, by the end of the cycle the power generation in the center is much bigger than in the rest of the core, explaining the behavior of the k_{eff} plot in the end of the cycle discussed earlier in this chapter.

Another highlight regarding the power maps is that by the end of cycle, in some regions there is alocal power of about 3.0 MW in only 11.1 cm height regions which would correspond to about 27 MW/m peak lineal power, which is three orders of magnitude higher than an usual value for SFR [Tucek et al., 2005] and two orders compared with the ones of Dounreay Fast Reactor [IAEA, 2007], it is evident that this design, as it is, cannot be used in reality and modifications should be made to aavoid this power gradient at the end of cycle.

On the fuel inventory plots, the first result to mark is that the developed tool worked properly since no discontinuities or jumps are found in the plots.

The other results are discussed in a per-case sequence.

7.3.1 Case 1

As in this case the fuel assemblies are moved one position a time, no sudden or strange variations in ^{235}U inventories are observed, what is indeed seen is that in the central layer the curves tend to decrease faster, this is expected due to the core geometry causes the fuel to be consumed faster in that region. The same behavior is also observed in the ^{238}U plot, where additionally, it is observed that the mixture 21, 91 and 181, which are the most central ones, present faster consumption.

^{238}U presents a growth in its consumption rate after about 10 years, this is caused for the same reasons previously explained in this chapter, in the section where k_{eff} curves are discussed. By the year 30 the U-238 consumption (which is mainly transmutation $^{238}\text{U}\rightarrow{}^{239}\text{U}\rightarrow{}^{239}\text{Np}\rightarrow{}^{239}\text{Pu}$) tends to decrease, explaining why by this time, k_{eff} has an evident decreasing tendency.

^{239}Pu present two different tendencies, depending on which mixture is being followed. The uranium depleted assemblies (mixtures 21, 91 and 181) present, as expected, a significant growth in ^{239}Pu inventories, until reaching a maximum a little after 20 years and after that the curve tends to decay; this means essentially that its consumption exceeds its

production, which is the reason why k_{eff} also reaches a maximum at approximately that time.

In the other assemblies, some considerations have to be made before discussion. For their locations, the neutron spectrum will not be as hard as if they were in the central region, at that energy region of the spectrum, there is presence of resonances on the fission cross section: $^{2}35$U as well as $^{2}38$U capture and $^{2}39$Pu capture, see figures 7.43, 7.44 and 7.45. As the $^{2}35$U is being fissioned, new Pu is also being bred, when the $^{2}35$U is mostly consumed (a little after 10 years) the fissions are being done more in the Pu, causing its net inventory not only to stop growing but start decreasing due to is being burned more than bred.

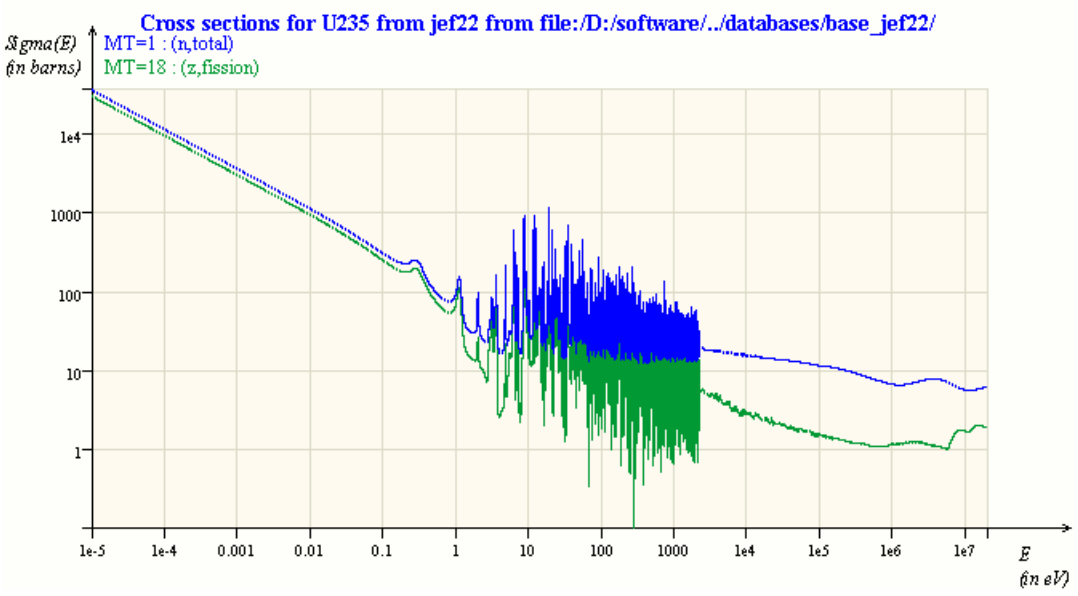

Figure 7.43: Total and fission cross sections of ^{235}U.

For ^{241}Pu, the two different tendencies are also present: in the case of mixtures with depleted uranium, the growth is higher than in the case of the mixtures with ^{235}U and more far away from the center where spectrum is harder. It is observable a peak in the mixture corresponding to the central layer is lower than in other layers. The explanation to this is first the presence of more ^{238}U, which allows more fuel breeding and secondly for the resonances in the fission cross section of ^{241}Pu in the fast spectrum, see Figure 7.46. The rest of the mixtures follows the same tendency as ^{239}Pu because of the same reasons, and because it depends on its density since formation of ^{241}Pu is due to neutron absorption of lighter Pu isotopes.

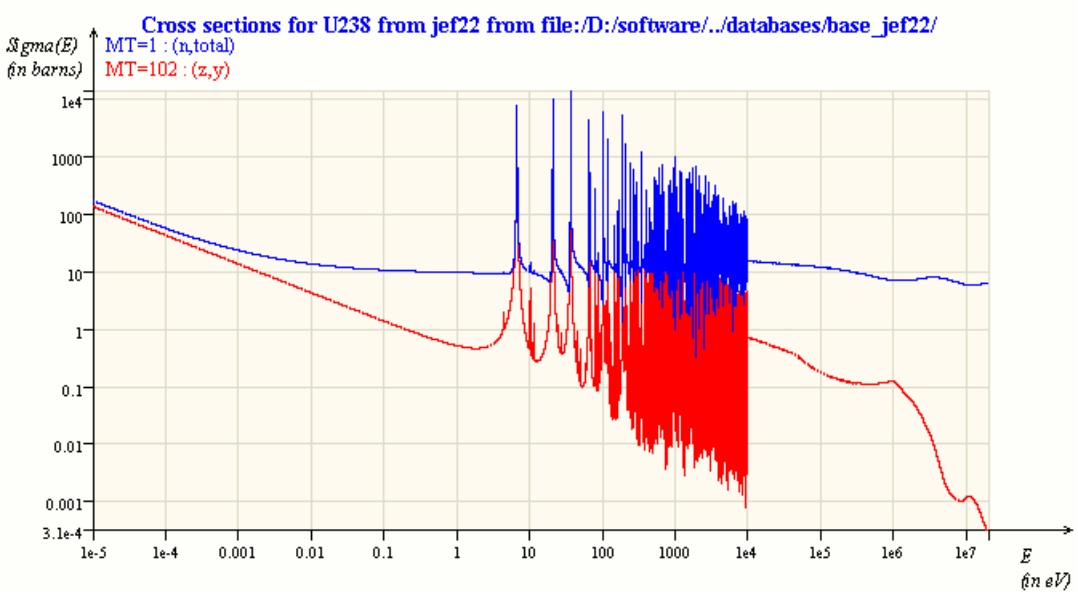

Figure 7.44: Total and capture cross sections of ^{238}U.

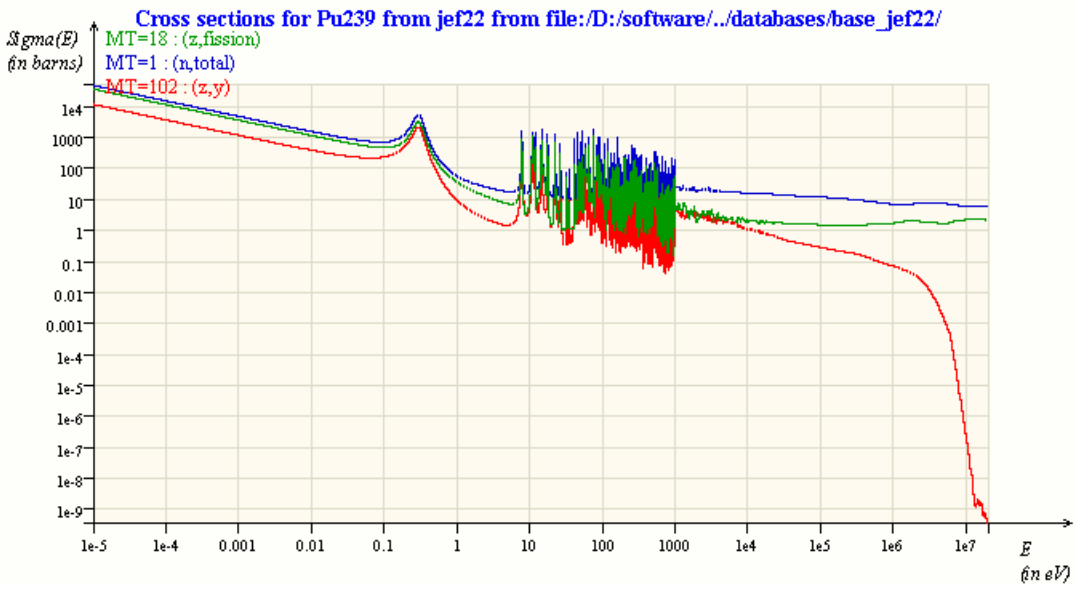

Figure 7.45: Total and capture cross sections of ^{239}Pu.

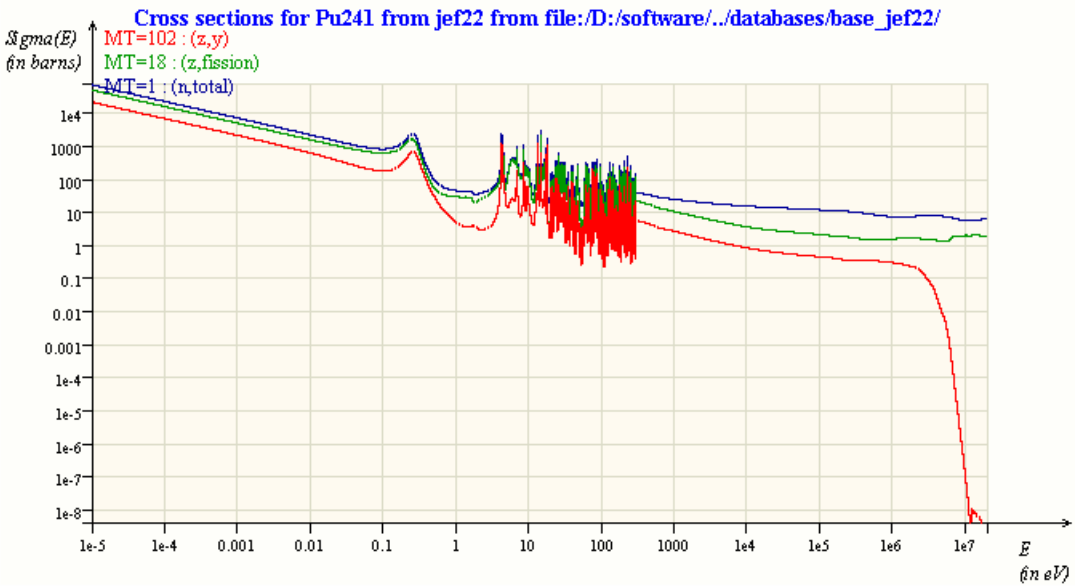

Figure 7.46: Total, capture and fission cross section of ^{241}Pu

7.3.2 Cases 2 and 3

In the cases 2 and 3, the tendencies of the curves are essentially the same as in case one, except for sudden changes in this tendencies; one good example of these changes is observed in the plot of ^{239}Pu in Case 2 around the year 30. The reasons of this changes is because in these cases, the fuel reshuffling scheme is more complex and imply the movement of fuel assemblies to different regions, contrary to Case 1 where is moved only one position at a time. Neutronically, the discussion given previously on the cross section resonances is still valid and explains the behavior of each curve, depending on the material and zone where is present. As explained previously, the Appendix A shows the position of all the 175 mixtures in every time steps for the three cases.

7.4 Reactivity Control Test

An important part of the core design is to assure if the number of control rods is enough to keep the core controlled, in order to verify this we simulated an SCRAM at the point where k_{eff} reaches its maximum value, the results are very satisfactory. A plot of k_{eff} before

and after the SCRAM is given in Figure 7.47. This plot clearly shows that the reactor is brought to a large subcritical state.

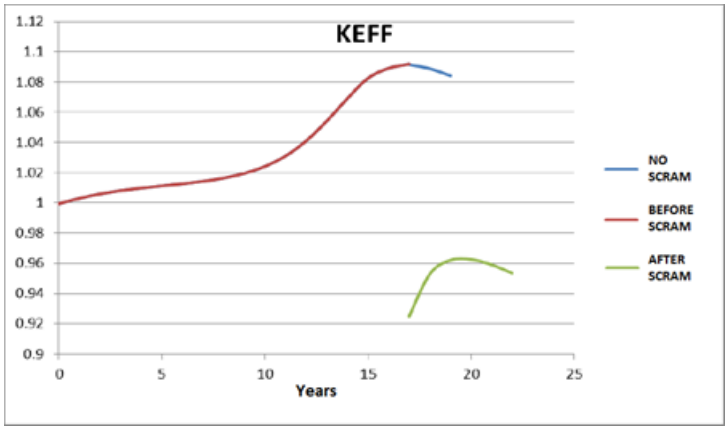

Figure 7.47: Total, capture and fission cross section of ^{241}Pu

Chapter 8

CONCLUSIONS

Before presenting conclusions some important considerations must be listed:

- This work considered only neutronics phenomena, and no thermal-hydraulical or mechanical effects were taken into account. If that were the case, the simplification of considering the core axial symmetry would not be valid.
- A not so ordinary 25 neutron energy groups approach was used instead of the conventional 33 groups.
- The code KANEXT, which was the main tool used, is still under constant improvement, and it is not 100% fault-free, despite our validation.
- The use of the fuel reshuffling for fuel management instead of a "traveling wave" choice was due to the tendency of the B&B core nuclear industry on this direction.

Keeping in mind these considerations, the conclusions of the realized work can be presented.

Given the results on k_{eff}, it can be assumed that the operation of a core for more than 40 years can be achieved without refueling, through fuel reshuffling management.

The treated long-life cycles imply very high discharge burnups, about 430 GWd/T or 44.8% FIMA, these high burnups are expected when dealing with very-long cycles and evidence the need of improved wrapping material and fuel fabrication technology. However these issues are beyond the slope of this thesis project as the goal was only the fuel management issues.

From the three reshuffling schemes tested, no big difference regarding total life cycle length was found, despite the simplicity or complexity of the reshuffling scheme. The

more complex and well thought scheme resulted in only a small life increase.

Based on the SCRAM test, the number of control rods considered are enough to keep the core subcritical once inserted.

Since all test were done with all control rods out of the core, a more flat k_{eff} curve can be obtained by the careful partial insertion of the rods during core operation, this can also improve the life cycle reducing the reactivity excess by a more controlled fuel burn.

It was found that at the end of the cycle the peak linear power exceeds the usual values, this was due to the fact that at the end of the cycle most of the power is generated in only a few assemblies in the center of the core. This does not mean that the reshuffling schemes do not work, but that modifications on the model as number of fuel elements, height, even power; should be done.

Regarding KANEXT code validation, it was compared with a more well-known MC code and obtained results were somewhat satisfactory, on this matter it is expected to have better results with a discretization of the energy spectrum that consider more energy groups, since this would model better the resonance area in the cross sections. Further steps should be aimed in this direction.

It was already mentioned that the choice of “standing wave” over “traveling wave” mode of operation was chosen following the industry tendency, nevertheless some tests with “traveling wave” mode were carried out (not shown in this work) with interesting results.

The use of deterministic codes is definitively a good decision when the computational power is limited. The validation section showed that results obtained by KANEXT, while improvable, are somewhat comparable with the results obtained with a more computational costly Monte Carlo code.

Appendix A

Table of mixture position for Case 1

Due to the size of table it will be divided into sections of 20 time steps. Another simplification on the table is that there will be show the mixtures 21-55 which corresponds to Layer 1, the other layer's mixtures can easily be tracked with the same table by adding multiples of 35, since the movements are exactly the same.

	0	1	2	3	4	5	6	7	8	9	10	11	12	13	14	15	16	17	18	19	Time Step
Position	0	1	2	3	4	5	5	6	7	8	9	10	10	11	12	13	14	15	15	16	Years
21	21	21	21	21	21	21	55	55	55	55	55	55	54	54	54	54	54	54	53	53	Mixture
22	22	22	22	22	22	22	21	21	21	21	21	21	55	55	55	55	55	55	54	54	
23	23	23	23	23	23	23	22	22	22	22	22	22	21	21	21	21	21	21	55	55	
24	24	24	24	24	24	24	23	23	23	23	23	23	22	22	22	22	22	22	21	21	
25	25	25	25	25	25	25	24	24	24	24	24	24	23	23	23	23	23	23	22	22	
26	26	26	26	26	26	26	25	25	25	25	25	25	24	24	24	24	24	24	23	23	
27	27	27	27	27	27	27	26	26	26	26	26	26	25	25	25	25	25	25	24	24	
28	28	28	28	28	28	28	27	27	27	27	27	27	26	26	26	26	26	26	25	25	
29	29	29	29	29	29	29	28	28	28	28	28	28	27	27	27	27	27	27	26	26	
30	30	30	30	30	30	30	29	29	29	29	29	29	28	28	28	28	28	28	27	27	

	31	31	31	31	31	30	30	30	30	30	29	29	29	29	29	29	29	29	28	28	28	29	29	30	30	31
	32	32	32	32	32	31	31	31	31	31	30	30	30	30	30	30	30	30	29	29	29	30	30	31	31	32
	33	33	33	33	33	32	32	32	32	32	31	31	31	31	31	31	31	31	30	30	30	31	31	32	32	33
	34	34	34	34	34	33	33	33	33	33	32	32	32	32	32	32	32	32	31	31	31	32	32	33	33	34
	35	35	35	35	35	34	34	34	34	34	33	33	33	33	33	33	33	33	32	32	32	33	33	34	34	35
	36	36	36	36	36	35	35	35	35	35	34	34	34	34	34	34	34	34	33	33	33	34	34	35	35	36
	37	37	37	37	37	36	36	36	36	36	35	35	35	35	35	35	35	35	34	34	34	35	35	36	36	37
	38	38	38	38	38	37	37	37	37	37	36	36	36	36	36	36	36	36	35	35	35	36	36	37	37	38
	39	39	39	39	39	38	38	38	38	38	37	37	37	37	37	37	37	37	36	36	36	37	37	38	38	39
	40	40	40	40	40	39	39	39	39	39	38	38	38	38	38	38	38	38	37	37	37	38	38	39	39	40
	41	41	41	41	41	40	40	40	40	40	39	39	39	39	39	39	39	39	38	38	38	39	39	40	40	41
	42	42	42	42	42	41	41	41	41	41	40	40	40	40	40	40	40	40	39	39	39	40	40	41	41	42
	43	43	43	43	43	42	42	42	42	42	41	41	41	41	41	41	41	41	40	40	40	41	41	42	42	43
	44	44	44	44	44	43	43	43	43	43	42	42	42	42	42	42	42	42	41	41	41	42	42	43	43	44
	45	45	45	45	45	44	44	44	44	44	43	43	43	43	43	43	43	43	42	42	42	43	43	44	44	45
	46	46	46	46	46	45	45	45	45	45	44	44	44	44	44	44	44	44	43	43	43	44	44	45	45	46
	47	47	47	47	47	46	46	46	46	46	45	45	45	45	45	45	45	45	44	44	44	45	45	46	46	47
	48	48	48	48	48	47	47	47	47	47	46	46	46	46	46	46	46	46	45	45	45	46	46	47	47	48
	49	49	49	49	49	48	48	48	48	48	47	47	47	47	47	47	47	47	46	46	46	47	47	48	48	49
	50	50	50	50	50	49	49	49	49	49	48	48	48	48	48	48	48	48	47	47	47	48	48	49	49	50
	51	51	51	51	51	50	50	50	50	50	49	49	49	49	49	49	49	49	48	48	48	49	49	50	50	51
	52	52	52	52	52	51	51	51	51	51	50	50	50	50	50	50	50	50	49	49	49	50	50	51	51	52
	53	53	53	53	53	52	52	52	52	52	51	51	51	51	51	51	51	51	50	50	50	51	51	52	52	53
	54	54	54	54	54	53	53	53	53	53	52	52	52	52	52	52	52	52	51	51	51	52	52	53	53	54
	55	55	55	55	55	54	54	54	54	54	53	53	53	53	53	53	53	53	52	52	52	53	53	54	54	55
31																										
32																										
33																										
34																										
35																										
36																										
37																										
38																										
39																										
40																										
41																										
42																										
43																										
44																										
45																										
46																										
47																										
48																										
49																										
50																										
51																										
52																										
53																										
54																										
55																										

	20	21	22	23	24	25	26	27	28	29	30	31	32	33	34	35	36	37	38	39	Time Step
Position	17	18	19	20	20	21	22	23	24	25	25	26	27	28	29	30	30	31	32	33	Years
21	53	53	53	53	52	52	52	52	52	52	51	51	51	51	51	51	50	50	50	50	Mixture
22	54	54	54	54	53	53	53	53	53	53	52	52	52	52	52	52	51	51	51	51	
23	55	55	55	55	54	54	54	54	54	54	53	53	53	53	53	53	52	52	52	52	
24	21	21	21	21	55	55	55	55	55	55	54	54	54	54	54	54	53	53	53	53	
25	22	22	22	22	21	21	21	21	21	21	55	55	55	55	55	55	54	54	54	54	
26	23	23	23	23	22	22	22	22	22	22	21	21	21	21	21	21	55	55	55	55	
27	24	24	24	24	23	23	23	23	23	23	22	22	22	22	22	22	21	21	21	21	
28	25	25	25	25	24	24	24	24	24	24	23	23	23	23	23	23	22	22	22	22	
29	26	26	26	26	25	25	25	25	25	25	24	24	24	24	24	24	23	23	23	23	
30	27	27	27	27	26	26	26	26	26	26	25	25	25	25	25	25	24	24	24	24	
31	28	28	28	28	27	27	27	27	27	27	26	26	26	26	26	26	25	25	25	25	
32	29	29	29	29	28	28	28	28	28	28	27	27	27	27	27	27	26	26	26	26	
33	30	30	30	30	29	29	29	29	29	29	28	28	28	28	28	28	27	27	27	27	
34	31	31	31	31	30	30	30	30	30	30	29	29	29	29	29	29	28	28	28	28	
35	32	32	32	32	31	31	31	31	31	31	30	30	30	30	30	30	29	29	29	29	
36	33	33	33	33	32	32	32	32	32	32	31	31	31	31	31	31	30	30	30	30	
37	34	34	34	34	33	33	33	33	33	33	32	32	32	32	32	32	31	31	31	31	
38	35	35	35	35	34	34	34	34	34	34	33	33	33	33	33	33	32	32	32	32	
39	36	36	36	36	35	35	35	35	35	35	34	34	34	34	34	34	33	33	33	33	
40	37	37	37	37	36	36	36	36	36	36	35	35	35	35	35	35	34	34	34	34	
41	38	38	38	38	37	37	37	37	37	37	36	36	36	36	36	36	35	35	35	35	
42	39	39	39	39	38	38	38	38	38	38	37	37	37	37	37	37	36	36	36	36	
43	40	40	40	40	39	39	39	39	39	39	38	38	38	38	38	38	37	37	37	37	
44	41	41	41	41	40	40	40	40	40	40	39	39	39	39	39	39	38	38	38	38	
45	42	42	42	42	41	41	41	41	41	41	40	40	40	40	40	40	39	39	39	39	
46	43	43	43	43	42	42	42	42	42	42	41	41	41	41	41	41	40	40	40	40	
47	44	44	44	44	43	43	43	43	43	43	42	42	42	42	42	42	41	41	41	41	
48	45	45	45	45	44	44	44	44	44	44	43	43	43	43	43	43	42	42	42	42	

49	46	46	46	46	45	45	45	45	45	45	44	44	44	44	44	44	43	43	43	43	
50	47	47	47	47	46	46	46	46	46	46	45	45	45	45	45	45	44	44	44	44	
51	48	48	48	48	47	47	47	47	47	47	46	46	46	46	46	46	45	45	45	45	
52	49	49	49	49	48	48	48	48	48	48	47	47	47	47	47	47	46	46	46	46	
53	50	50	50	50	49	49	49	49	49	49	48	48	48	48	48	48	47	47	47	47	
54	51	51	51	51	50	50	50	50	50	50	49	49	49	49	49	49	48	48	48	48	
55	52	52	52	52	51	51	51	51	51	51	50	50	50	50	50	50	49	49	49	49	

	40	41	42	43	44	45	46	47	48	49	50	51	52	53	54	55	56	57	Time Step
Position	34	35	35	36	37	38	39	39	40	41	42	43	43	44	45	46	47	48	Years
21	50	50	49	49	49	49	49	48	48	48	48	48	47	47	47	47	47	47	Mixture
22	51	51	50	50	50	50	50	49	49	49	49	49	48	48	48	48	48	48	
23	52	52	51	51	51	51	51	50	50	50	50	50	49	49	49	49	49	49	
24	53	53	52	52	52	52	52	51	51	51	51	51	50	50	50	50	50	50	
25	54	54	53	53	53	53	53	52	52	52	52	52	51	51	51	51	51	51	
26	55	55	54	54	54	54	54	53	53	53	53	53	52	52	52	52	52	52	
27	21	21	55	55	55	55	55	54	54	54	54	54	53	53	53	53	53	53	
28	22	22	21	21	21	21	21	55	55	55	55	55	54	54	54	54	54	54	
29	23	23	22	22	22	22	22	21	21	21	21	21	55	55	55	55	55	55	
30	24	24	23	23	23	23	23	22	22	22	22	22	21	21	21	21	21	21	
31	25	25	24	24	24	24	24	23	23	23	23	23	22	22	22	22	22	22	
32	26	26	25	25	25	25	25	24	24	24	24	24	23	23	23	23	23	23	
33	27	27	26	26	26	26	26	25	25	25	25	25	24	24	24	24	24	24	
34	28	28	27	27	27	27	27	26	26	26	26	26	25	25	25	25	25	25	
35	29	29	28	28	28	28	28	27	27	27	27	27	26	26	26	26	26	26	
36	30	30	29	29	29	29	29	28	28	28	28	28	27	27	27	27	27	27	
37	31	31	30	30	30	30	30	29	29	29	29	29	28	28	28	28	28	28	
38	32	32	31	31	31	31	31	30	30	30	30	30	29	29	29	29	29	29	
39	33	33	32	32	32	32	32	31	31	31	31	31	30	30	30	30	30	30	
40	34	34	33	33	33	33	33	32	32	32	32	32	31	31	31	31	31	31	
41	35	35	34	34	34	34	34	33	33	33	33	33	32	32	32	32	32	32	
42	36	36	35	35	35	35	35	34	34	34	34	34	33	33	33	33	33	33	
43	37	37	36	36	36	36	36	35	35	35	35	35	34	34	34	34	34	34	
44	38	38	37	37	37	37	37	36	36	36	36	36	35	35	35	35	35	35	
45	39	39	38	38	38	38	38	37	37	37	37	37	36	36	36	36	36	36	
46	40	40	39	39	39	39	39	38	38	38	38	38	37	37	37	37	37	37	
47	41	41	40	40	40	40	40	39	39	39	39	39	38	38	38	38	38	38	
48	42	42	41	41	41	41	41	40	40	40	40	40	39	39	39	39	39	39	

49	43	43	42	42	42	42	42	41	41	41	41	41	40	40	40	40	40	40	
50	44	44	43	43	43	43	43	42	42	42	42	42	41	41	41	41	41	41	
51	45	45	44	44	44	44	44	43	43	43	43	43	42	42	42	42	42	42	
52	46	46	45	45	45	45	45	44	44	44	44	44	43	43	43	43	43	43	
53	47	47	46	46	46	46	46	45	45	45	45	45	44	44	44	44	44	44	
54	48	48	47	47	47	47	47	46	46	46	46	46	45	45	45	45	45	45	
55	49	49	48	48	48	48	48	47	47	47	47	47	46	46	46	46	46	46	

Appendix B

Table of mixture position for Case 2

Due to the size of table it will be divided into sections of 20 time steps. Another simplification on the table is that there will be show the mixtures 21-55 which corresponds to Layer 1, the other layer's mixtures can easily be tracked with the same table by adding multiples of 35, since the movements are exactly the same.

	0	1	2	3	4	5	6	7	8	9	10	11	12	13	14	15	16	17	18	19	Time Step
Position	0	1	2	3	4	5	5	6	7	8	9	10	10	11	12	13	14	15	15	16	Years
21	21	21	21	21	21	21	55	55	55	55	55	55	54	54	54	54	54	54	53	53	Mixture
22	22	22	22	22	22	22	21	21	21	21	21	21	55	55	55	55	55	55	54	54	
23	23	23	23	23	23	23	22	22	22	22	22	22	21	21	21	21	21	21	55	55	
24	24	24	24	24	24	24	23	23	23	23	23	23	22	22	22	22	22	22	21	21	
25	25	25	25	25	25	25	24	24	24	24	24	24	23	23	23	23	23	23	22	22	
26	26	26	26	26	26	26	25	25	25	25	25	25	24	24	24	24	24	24	23	23	
27	27	27	27	27	27	27	27	27	27	27	27	27	27	27	27	27	27	27	27	27	
28	28	28	28	28	28	28	28	28	28	28	28	28	28	28	28	28	28	28	28	28	
29	29	29	29	29	29	29	29	29	29	29	29	29	29	29	29	29	29	29	29	29	
30	30	30	30	30	30	30	30	30	30	30	30	30	30	30	30	30	30	30	30	30	
31	31	31	31	31	31	31	31	31	31	31	31	31	31	31	31	31	31	31	31	31	

32	32	32	32	32	32	32	32	32	32	32	32	32	32	32	32	32	32	32	32	32
33	33	33	33	33	33	33	33	33	33	33	33	33	33	33	33	33	33	33	33	33
34	34	34	34	34	34	34	34	34	34	34	34	34	34	34	34	34	34	34	34	34
35	35	35	35	35	35	35	35	35	35	35	35	35	35	35	35	35	35	35	35	35
36	36	36	36	36	36	36	36	36	36	36	36	36	36	36	36	36	36	36	36	36
37	37	37	37	37	37	37	37	37	37	37	37	37	37	37	37	37	37	37	37	37
38	38	38	38	38	38	38	38	38	38	38	38	38	38	38	38	38	38	38	38	38
39	39	39	39	39	39	39	39	39	39	39	39	39	39	39	39	39	39	39	39	39
40	40	40	40	40	40	40	40	40	40	40	40	40	40	40	40	40	40	40	40	40
41	41	41	41	41	41	41	41	41	41	41	41	41	41	41	41	41	41	41	41	41
42	42	42	42	42	42	42	42	42	42	42	42	42	42	42	42	42	42	42	42	42
43	43	43	43	43	43	43	43	43	43	43	43	43	43	43	43	43	43	43	43	43
44	44	44	44	44	44	44	44	44	44	44	44	44	44	44	44	44	44	44	44	44
45	45	45	45	45	45	45	45	45	45	45	45	45	45	45	45	45	45	45	45	45
46	46	46	46	46	46	46	46	46	46	46	46	46	46	46	46	46	46	46	46	46
47	47	47	47	47	47	47	26	26	26	26	26	26	25	25	25	25	25	25	24	24
48	48	48	48	48	48	48	47	47	47	47	47	47	26	26	26	26	26	26	25	25
49	49	49	49	49	49	49	48	48	48	48	48	48	47	47	47	47	47	47	26	26
50	50	50	50	50	50	50	49	49	49	49	49	49	48	48	48	48	48	48	47	47
51	51	51	51	51	51	51	50	50	50	50	50	50	49	49	49	49	49	49	48	48
52	52	52	52	52	52	52	51	51	51	51	51	51	50	50	50	50	50	50	49	49
53	53	53	53	53	53	53	52	52	52	52	52	52	51	51	51	51	51	51	50	50
54	54	54	54	54	54	54	53	53	53	53	53	53	52	52	52	52	52	52	51	51
55	55	55	55	55	55	55	54	54	54	54	54	54	53	53	53	53	53	53	52	52

	20	21	22	23	24	25	26	27	28	29	30	31	32	33	34	35	36	37	38	39	Time Step
Position	17	18	19	20	20	21	22	23	24	25	25	26	27	28	29	30	30	31	32	33	Years
21	53	53	53	53	52	52	52	52	52	52	51	51	51	51	51	51	50	50	50	50	Mixture
22	54	54	54	54	53	53	53	53	53	53	52	52	52	52	52	52	51	51	51	51	
23	55	55	55	55	54	54	54	54	54	54	53	53	53	53	53	53	52	52	52	52	
24	21	21	21	21	55	55	55	55	55	55	54	54	54	54	54	54	53	53	53	53	
25	22	22	22	22	21	21	21	21	21	21	55	55	55	55	55	55	54	54	54	54	
26	23	23	23	23	22	22	22	22	22	22	21	21	21	21	21	21	55	55	55	55	
27	27	27	27	27	27	27	27	27	27	27	27	27	27	27	27	27	27	27	27	27	
28	28	28	28	28	28	28	28	28	28	28	28	28	28	28	28	28	28	28	28	28	
29	29	29	29	29	29	29	29	29	29	29	29	29	29	29	29	29	29	29	29	29	
30	30	30	30	30	30	30	30	30	30	30	30	30	30	30	30	30	30	30	30	30	
31	31	31	31	31	31	31	31	31	31	31	31	31	31	31	31	31	31	31	31	31	
32	32	32	32	32	32	32	32	32	32	32	32	32	32	32	32	32	32	32	32	32	
33	33	33	33	33	33	33	33	33	33	33	33	33	33	33	33	33	33	33	33	33	
34	34	34	34	34	34	34	34	34	34	34	34	34	34	34	34	34	34	34	34	34	
35	35	35	35	35	35	35	35	35	35	35	35	35	35	35	35	35	35	35	35	35	
36	36	36	36	36	36	36	36	36	36	36	36	36	36	36	36	36	36	36	36	36	
37	37	37	37	37	37	37	37	37	37	37	37	37	37	37	37	37	37	37	37	37	
38	38	38	38	38	38	38	38	38	38	38	38	38	38	38	38	38	38	38	38	38	
39	39	39	39	39	39	39	39	39	39	39	39	39	39	39	39	39	39	39	39	39	
40	40	40	40	40	40	40	40	40	40	40	40	40	40	40	40	40	40	40	40	40	
41	41	41	41	41	41	41	41	41	41	41	41	41	41	41	41	41	41	41	41	41	
42	42	42	42	42	42	42	42	42	42	42	42	42	42	42	42	42	42	42	42	42	
43	43	43	43	43	43	43	43	43	43	43	43	43	43	43	43	43	43	43	43	43	
44	44	44	44	44	44	44	44	44	44	44	44	44	44	44	44	44	44	44	44	44	
45	45	45	45	45	45	45	45	45	45	45	45	45	45	45	45	45	45	45	45	45	
46	46	46	46	46	46	46	46	46	46	46	46	46	46	46	46	46	46	46	46	46	
47	24	24	24	24	23	23	23	23	23	23	22	22	22	22	22	22	21	21	21	21	
48	25	25	25	25	24	24	24	24	24	24	23	23	23	23	23	23	22	22	22	22	

49	26	26	26	26	25	25	25	25	25	25	24	24	24	24	24	24	23	23	23	23	
50	47	47	47	47	26	26	26	26	26	26	25	25	25	25	25	25	24	24	24	24	
51	48	48	48	48	47	47	47	47	47	47	26	26	26	26	26	26	25	25	25	25	
52	49	49	49	49	48	48	48	48	48	48	47	47	47	47	47	47	26	26	26	26	
53	50	50	50	50	49	49	49	49	49	49	48	48	48	48	48	48	47	47	47	47	
54	51	51	51	51	50	50	50	50	50	50	49	49	49	49	49	49	48	48	48	48	
55	52	52	52	52	51	51	51	51	51	51	50	50	50	50	50	50	49	49	49	49	

	40	41	42	43	44	45	46	47	48	49	50	51	52	53	54	55	56	57	Time Step
Position	34	35	35	36	37	38	39	39	40	41	42	43	43	44	45	46	47	48	Years
21	50	50	49	49	49	49	49	48	48	48	48	48	47	47	47	47	47	47	Mixture
22	51	51	50	50	50	50	50	49	49	49	49	49	48	48	48	48	48	48	
23	52	52	51	51	51	51	51	50	50	50	50	50	49	49	49	49	49	49	
24	53	53	52	52	52	52	52	51	51	51	51	51	50	50	50	50	50	50	
25	54	54	53	53	53	53	53	52	52	52	52	52	51	51	51	51	51	51	
26	55	55	54	54	54	54	54	53	53	53	53	53	52	52	52	52	52	52	
27	27	27	27	27	27	27	27	27	27	27	27	27	27	27	27	27	27	27	
28	28	28	28	28	28	28	28	28	28	28	28	28	28	28	28	28	28	28	
29	29	29	29	29	29	29	29	29	29	29	29	29	29	29	29	29	29	29	
30	30	30	30	30	30	30	30	30	30	30	30	30	30	30	30	30	30	30	
31	31	31	31	31	31	31	31	31	31	31	31	31	31	31	31	31	31	31	
32	32	32	32	32	32	32	32	32	32	32	32	32	32	32	32	32	32	32	
33	33	33	33	33	33	33	33	33	33	33	33	33	33	33	33	33	33	33	
34	34	34	34	34	34	34	34	34	34	34	34	34	34	34	34	34	34	34	
35	35	35	35	35	35	35	35	35	35	35	35	35	35	35	35	35	35	35	
36	36	36	36	36	36	36	36	36	36	36	36	36	36	36	36	36	36	36	
37	37	37	37	37	37	37	37	37	37	37	37	37	37	37	37	37	37	37	
38	38	38	38	38	38	38	38	38	38	38	38	38	38	38	38	38	38	38	
39	39	39	39	39	39	39	39	39	39	39	39	39	39	39	39	39	39	39	
40	40	40	40	40	40	40	40	40	40	40	40	40	40	40	40	40	40	40	
41	41	41	41	41	41	41	41	41	41	41	41	41	41	41	41	41	41	41	
42	42	42	42	42	42	42	42	42	42	42	42	42	42	42	42	42	42	42	
43	43	43	43	43	43	43	43	43	43	43	43	43	43	43	43	43	43	43	
44	44	44	44	44	44	44	44	44	44	44	44	44	44	44	44	44	44	44	
45	45	45	45	45	45	45	45	45	45	45	45	45	45	45	45	45	45	45	
46	46	46	46	46	46	46	46	46	46	46	46	46	46	46	46	46	46	46	
47	21	21	55	55	55	55	55	54	54	54	54	54	53	53	53	53	53	53	
48	22	22	21	21	21	21	21	55	55	55	55	55	54	54	54	54	54	54	

49	23	23	22	22	22	22	22	21	21	21	21	21	55	55	55	55	55	55	
50	24	24	23	23	23	23	23	22	22	22	22	22	21	21	21	21	21	21	
51	25	25	24	24	24	24	24	23	23	23	23	23	22	22	22	22	22	22	
52	26	26	25	25	25	25	25	24	24	24	24	24	23	23	23	23	23	23	
53	47	47	26	26	26	26	26	25	25	25	25	25	24	24	24	24	24	24	
54	48	48	47	47	47	47	47	26	26	26	26	26	25	25	25	25	25	25	
55	49	49	48	48	48	48	48	47	47	47	47	47	26	26	26	26	26	26	

Appendix C

Table of mixture position for Case 3

Due to the size of table it will be divided into sections of 20 time steps. Another simplification on the table is that there will be show the mixtures 21-55 which corresponds to Layer 1, the other layer's mixtures can easily be tracked with the same table by adding multiples of 35, since the movements are exactly the same.

	0	1	2	3	4	5	6	7	8	9	10	11	12	13	14	15	16	17	18	19	Time Step
Position	0	1	2	3	4	5	5	6	7	8	9	10	10	11	12	13	14	15	15	16	Years
21	21	21	21	21	21	21	55	55	55	55	55	55	54	54	54	54	54	54	53	53	Mixture
22	22	22	22	22	22	22	21	21	21	21	21	21	55	55	55	55	55	55	54	54	
23	23	23	23	23	23	23	22	22	22	22	22	22	21	21	21	21	21	21	55	55	
24	24	24	24	24	24	24	23	23	23	23	23	23	22	22	22	22	22	22	21	21	
25	25	25	25	25	25	25	24	24	24	24	24	24	23	23	23	23	23	23	22	22	
26	26	26	26	26	26	26	25	25	25	25	25	25	24	24	24	24	24	24	23	23	
27	27	27	27	27	27	27	27	27	27	27	27	27	27	27	27	27	27	27	25	25	
28	28	28	28	28	28	28	28	28	28	28	28	28	28	28	28	28	28	28	24	24	
29	29	29	29	29	29	29	29	29	29	29	29	29	29	29	29	29	29	29	26	26	
30	30	30	30	30	30	30	30	30	30	30	30	30	30	30	30	30	30	30	30	30	
31	31	31	31	31	31	31	31	31	31	31	31	31	31	31	31	31	31	31	31	31	

32	32	32	32	32	32	32	32	32	32	32	32	32	32	32	32	32	32	32	32	32
33	33	33	33	33	33	33	33	33	33	33	33	33	33	33	33	33	33	33	33	33
34	34	34	34	34	34	34	34	34	34	34	34	34	34	34	34	34	34	34	34	34
35	35	35	35	35	35	35	35	35	35	35	35	35	35	35	35	35	35	35	35	35
36	36	36	36	36	36	36	36	36	36	36	36	36	36	36	36	36	36	36	36	36
37	37	37	37	37	37	37	37	37	37	37	37	37	37	37	37	37	37	37	37	37
38	38	38	38	38	38	38	38	38	38	38	38	38	38	38	38	38	38	38	38	38
39	39	39	39	39	39	39	39	39	39	39	39	39	39	39	39	39	39	39	39	39
40	40	40	40	40	40	40	40	40	40	40	40	40	40	40	40	40	40	40	40	40
41	41	41	41	41	41	41	41	41	41	41	41	41	41	41	41	41	41	41	41	41
42	42	42	42	42	42	42	42	42	42	42	42	42	42	42	42	42	42	42	42	42
43	43	43	43	43	43	43	43	43	43	43	43	43	43	43	43	43	43	43	43	43
44	44	44	44	44	44	44	44	44	44	44	44	44	44	44	44	44	44	44	44	44
45	45	45	45	45	45	45	45	45	45	45	45	45	45	45	45	45	45	45	45	45
46	46	46	46	46	46	46	46	46	46	46	46	46	46	46	46	46	46	46	46	46
47	47	47	47	47	47	47	26	26	26	26	26	26	25	25	25	25	25	25	27	27
48	48	48	48	48	48	48	47	47	47	47	47	47	26	26	26	26	26	26	28	28
49	49	49	49	49	49	49	48	48	48	48	48	48	47	47	47	47	47	47	29	29
50	50	50	50	50	50	50	49	49	49	49	49	49	48	48	48	48	48	48	47	47
51	51	51	51	51	51	51	50	50	50	50	50	50	49	49	49	49	49	49	48	48
52	52	52	52	52	52	52	51	51	51	51	51	51	50	50	50	50	50	50	49	49
53	53	53	53	53	53	53	52	52	52	52	52	52	51	51	51	51	51	51	50	50
54	54	54	54	54	54	54	53	53	53	53	53	53	52	52	52	52	52	52	51	51
55	55	55	55	55	55	55	54	54	54	54	54	54	53	53	53	53	53	53	52	52

	20	21	22	23	24	25	26	27	28	29	30	31	32	33	34	35	36	37	38	39	Time Step
Position	17	18	19	20	20	21	22	23	24	25	25	26	27	28	29	30	30	31	32	33	Years
21	53	53	53	53	52	52	52	52	52	52	51	51	51	51	51	51	50	50	50	50	Mixture
22	54	54	54	54	53	53	53	53	53	53	52	52	52	52	52	52	51	51	51	51	
23	55	55	55	55	54	54	54	54	54	54	53	53	53	53	53	53	52	52	52	52	
24	21	21	21	21	55	55	55	55	55	55	54	54	54	54	54	54	53	53	53	53	
25	22	22	22	22	21	21	21	21	21	21	55	55	55	55	55	55	54	54	54	54	
26	23	23	23	23	22	22	22	22	22	22	21	21	21	21	21	21	55	55	55	55	
27	25	25	25	25	25	25	25	25	25	25	25	25	25	25	25	25	22	22	22	22	
28	24	24	24	24	24	24	24	24	24	24	24	24	24	24	24	24	21	21	21	21	
29	26	26	26	26	26	26	26	26	26	26	26	26	26	26	26	26	23	23	23	23	
30	30	30	30	30	30	30	30	30	30	30	30	30	30	30	30	30	30	30	30	30	
31	31	31	31	31	31	31	31	31	31	31	31	31	31	31	31	31	26	26	26	26	
32	32	32	32	32	32	32	32	32	32	32	32	32	32	32	32	32	24	24	24	24	
33	33	33	33	33	33	33	33	33	33	33	33	33	33	33	33	33	25	25	25	25	
34	34	34	34	34	34	34	34	34	34	34	34	34	34	34	34	34	34	34	34	34	
35	35	35	35	35	35	35	35	35	35	35	35	35	35	35	35	35	35	35	35	35	
36	36	36	36	36	36	36	36	36	36	36	36	36	36	36	36	36	36	36	36	36	
37	37	37	37	37	37	37	37	37	37	37	37	37	37	37	37	37	37	37	37	37	
38	38	38	38	38	38	38	38	38	38	38	38	38	38	38	38	38	38	38	38	38	
39	39	39	39	39	39	39	39	39	39	39	39	39	39	39	39	39	39	39	39	39	
40	40	40	40	40	40	40	40	40	40	40	40	40	40	40	40	40	40	40	40	40	
41	41	41	41	41	41	41	41	41	41	41	41	41	41	41	41	41	41	41	41	41	
42	42	42	42	42	42	42	42	42	42	42	42	42	42	42	42	42	42	42	42	42	
43	43	43	43	43	43	43	43	43	43	43	43	43	43	43	43	43	43	43	43	43	
44	44	44	44	44	44	44	44	44	44	44	44	44	44	44	44	44	44	44	44	44	
45	45	45	45	45	45	45	45	45	45	45	45	45	45	45	45	45	45	45	45	45	
46	46	46	46	46	46	46	46	46	46	46	46	46	46	46	46	46	46	46	46	46	
47	27	27	27	27	23	23	23	23	23	23	22	22	22	22	22	22	33	33	33	33	
48	28	28	28	28	27	27	27	27	27	27	23	23	23	23	23	23	32	32	32	32	

49	29	29	29	29	28	28	28	28	28	28	27	27	27	27	27	27	31	31	31	31
50	47	47	47	47	29	29	29	29	29	29	28	28	28	28	28	28	27	27	27	27
51	48	48	48	48	47	47	47	47	47	47	29	29	29	29	29	29	28	28	28	28
52	49	49	49	49	48	48	48	48	48	48	47	47	47	47	47	47	29	29	29	29
53	50	50	50	50	49	49	49	49	49	49	48	48	48	48	48	48	47	47	47	47
54	51	51	51	51	50	50	50	50	50	50	49	49	49	49	49	49	48	48	48	48
55	52	52	52	52	51	51	51	51	51	51	50	50	50	50	50	50	49	49	49	49

	40	41	42	43	44	45	46	47	48	49	50	51	52	53	54	55	56	57	Time Step
Position	34	35	35	36	37	38	39	39	40	41	42	43	43	44	45	46	47	48	Years
21	50	50	49	49	49	49	49	48	48	48	48	48	47	47	47	47	47	47	Mixture
22	51	51	50	50	50	50	50	49	49	49	49	49	48	48	48	48	48	48	
23	52	52	51	51	51	51	51	50	50	50	50	50	49	49	49	49	49	49	
24	53	53	52	52	52	52	52	51	51	51	51	51	50	50	50	50	50	50	
25	54	54	53	53	53	53	53	52	52	52	52	52	51	51	51	51	51	51	
26	55	55	54	54	54	54	54	53	53	53	53	53	52	52	52	52	52	52	
27	22	22	22	22	22	22	22	22	22	22	22	22	54	54	54	54	54	54	
28	21	21	21	21	21	21	21	21	21	21	21	21	53	53	53	53	53	53	
29	23	23	23	23	23	23	23	23	23	23	23	23	55	55	55	55	55	55	
30	30	30	30	30	30	30	30	30	30	30	30	30	30	30	30	30	30	30	
31	26	26	26	26	26	26	26	26	26	26	26	26	23	23	23	23	23	23	
32	24	24	24	24	24	24	24	24	24	24	24	24	21	21	21	21	21	21	
33	25	25	25	25	25	25	25	25	25	25	25	25	22	22	22	22	22	22	
34	34	34	34	34	34	34	34	34	34	34	34	34	34	34	34	34	34	34	
35	35	35	35	35	35	35	35	35	35	35	35	35	35	35	35	35	35	35	
36	36	36	36	36	36	36	36	36	36	36	36	36	36	36	36	36	36	36	
37	37	37	37	37	37	37	37	37	37	37	37	37	25	25	25	25	25	25	
38	38	38	38	38	38	38	38	38	38	38	38	38	24	24	24	24	24	24	
39	39	39	39	39	39	39	39	39	39	39	39	39	26	26	26	26	26	26	
40	40	40	40	40	40	40	40	40	40	40	40	40	40	40	40	40	40	40	
41	41	41	41	41	41	41	41	41	41	41	41	41	41	41	41	41	41	41	
42	42	42	42	42	42	42	42	42	42	42	42	42	42	42	42	42	42	42	
43	43	43	43	43	43	43	43	43	43	43	43	43	43	43	43	43	43	43	
44	44	44	44	44	44	44	44	44	44	44	44	44	44	44	44	44	44	44	
45	45	45	45	45	45	45	45	45	45	45	45	45	45	45	45	45	45	45	
46	46	46	46	46	46	46	46	46	46	46	46	46	46	46	46	46	46	46	
47	33	33	55	55	55	55	55	54	54	54	54	54	37	37	37	37	37	37	
48	32	32	33	33	33	33	33	55	55	55	55	55	38	38	38	38	38	38	

49	31	31	32	32	32	32	32	33	33	33	33	33	39	39	39	39	39	39	
50	27	27	31	31	31	31	31	32	32	32	32	32	33	33	33	33	33	33	
51	28	28	27	27	27	27	27	31	31	31	31	31	32	32	32	32	32	32	
52	29	29	28	28	28	28	28	27	27	27	27	27	31	31	31	31	31	31	
53	47	47	29	29	29	29	29	28	28	28	28	28	27	27	27	27	27	27	
54	48	48	47	47	47	47	47	29	29	29	29	29	28	28	28	28	28	28	
55	49	49	48	48	48	48	48	47	47	47	47	47	29	29	29	29	29	29	

Bibliography

[Ahlfeld et al., 2011] Ahlfeld, C., Burke, T., Ellis, T., Hejzlar, P., Weaver, K., Whitmer, C., Gilleland, J., Cohen, M., Johnson, B., Stephen, M., McWhriter, J., Odedra, A., Touran, N., Davidson, C., Walter, J., Petroski, R., Zimmerman, G., Weaver, T., Schweiger, P., and Russick, R. (2011). Conceptual Design of a 500 MWe Traveling Wave Demonstration Reactor Plant. In *Proceedings of ICAPP 2011*, number 11199, Nice, France.

[Akhiezer et al., 1999] Akhiezer, A., Belozorov, D. P., Rofe-Beketov, F. S., Davydov, L. N., and Spolnik, Z. A. (1999). Propagation of a Nuclear Chain Reaction in the Diffusion Approximation. *Physics of Atomic Nuclei*, 62:1474–1481.

[Akhiezer et al., 2001] Akhiezer, A., Khizhnyak, N., Shulga, N., Pilipenko, V., and Davydov, L. (2001). Slow Nuclear Burning. *Problems in Atomic Science & Technology*, 6:272–275.

[ANL, 2015] ANL (2015). Pyroprocessing Technologies: Recycling Used Nuclear Fuel for a Sustainable Energy Future. Brochure, Argone National Laboratory. Brochure available at http://www.cse.anl.gov/pdfs/pyroprocessing_brochure.pdf.

[ARC, 2015] ARC (2015). A Sustainable, Cost-Effective Energy Solution for the 21st Century. Brochure, Advanded Reactor Concepts, LLC. Brochure available at http://www.arcnuclear.com/uploads/File/arc-100-product-brochure.pdf.

[Becker et al., 2011] Becker, M., Van Criekingen, S., and Broeders, C. H. M. (2011). KANEXT, a tool for nuclear reactor calculations: Description of the export version. Technical report, Karlsruhe Institute of Technology, Institute for Neutron Physics and Reactor Technology, Karlsruhe, Germany.

[Cetnar, 2006] Cetnar, J. (2006). General Solution of Bateman Equations for Nuclear Transmutations. *Annals of Nuclear Energy*, 33:640–645.

[Chen and Maschek, 2005] Chen, X.-N. and Maschek, W. (2005). Transverse Buckling Effects on Solitary Burn-up Waves. *Annals of Nuclear Energy*, 32:377–1390.

[Chersola et al., 2014] Chersola, D., Lomonaco, G., Marotta, R., and Mazzini, G. (2014). Comparison Between SERPENT and MONTEBURNS Codes Applied to Burnup Calculations of a GFR-like Configuration. *Nuclear Engineering and Design*, 273:542–554.

[Feinberg and Kunegin, 1958] Feinberg, S. M. and Kunegin, E. (1958). Nuclear power plants, part 2, discussion. In *Proceedings of the 2nd U.N. International Conference on Peaceful Uses of Atomic Energy*, volume 9, page 447.

[Feoktistov, 1989a] Feoktistov, L. P. (1989a). An analysis of a Concept of a Physically Safe Reactor. In *Proceedings of the USSR Academy of Science*, number 309, pages 864–867, Moscow, Russia. (in russian), Preprint IAE-4605/4.

[Feoktistov, 1989b] Feoktistov, L. P. (1989b). Neutron Fission Wave. *Proceedings of the USSR Academy of Science*, v.34:1071. (in russian).

[Feoktistov, 1989c] Feoktistov, L. P. (1989c). Variant of Safe Reactor. *Nature*, 1. (in Russian).

[Fischer et al., 1979a] Fischer, G. J., Cerbone, R. J., Ludewig, H., Majumdar, D., Shenoy, S., Durston, C., Segev, M., and Sillis, T. (1979a). The Fast-Mixed Spectrum Reactor - Initial Feasibility Study. Technical Report BNL-50976, Brookhaven National Laboratory, Upton, New York, US.

[Fischer et al., 1979b] Fischer, G. J., Kouts, H. J. C., Cerbone, R. J., Shenoy, S., Durston, C., Ludewig, H., Majumdar, D., Segev, M., Kittel, J. H., Neimark, L., Walter, L., Moran, T. J., and Fulford, P. J. (1979b). Physics and Feasibility Study of the Fast-Mixed-Spectrum Reactor Concept. Technical Report BNL-25598, Brookhaven National Laboratory, Upton, New York, US.

[Fischer and Wiese, 1983] Fischer, U. and Wiese, H. (1983). Improved and Consistent Determination of the Nuclear Inventory of Spent PWR Fuel on the Basis of Cell Burnup Methods Using KORIGEN. Technical Report KFK3014, Kernforschungszentrum Karlsruhe, Karlsruhe, Germany. Translated from German.

[Fomin et al., 2005] Fomin, S. P., Mel'nik, Y. P., Pilipenko, V. V., and Shul'ga, N. F. (2005). Investigation of Self-Organization of the Non-Linear Nuclear Burning Regime in Fast Neutron Reactors. *Annals of Nuclear Energy*, 32(1435).

[Fuchs and Hessel, 1961] Fuchs, K. and Hessel, H. (1961). Uber die Moglichkeiten des Betriebs eines Natururanbrutreaktors ohne Brensttoffaufbereitung. *Kernenergie*, 4:619–326. (in german).

[Gaveau et al., 2005] Gaveau, B., Maillard, J., Maurel, G., and Silva, J. (2005). Hybrid Soliton Nuclear Reactors: A Model and Simulation. *Nuclear Engineering and Design*, 235(1665).

[Gen4 Energy, 2015] Gen4 Energy (2015). Hyperion power, new clear energy. Brochure. Available at http://www.uxc.com/smr/Library%5CDesign%20Specific/G4M%20%28HPM%29-/Other%20Documents/Brochure%20Hyperion%20Module.pdf.

[GIF, 2009] GIF (2009). GIF R&D Outlook for Generation IV Nuclear Energy Systems. Technical report, Generation IV International Forum. Available at https://www.gen-4.org/gif/jcms/c_40482/gen-iv-rd-outlook.

[GIF, 2015] GIF (2015). Generation IV International Forum. Organization's web page. http://www.gen-4.org.

[Halper, 2013] Halper, M. (2013). Bill Gates stops chasing nuclear 'wave', pursues variety of reactors. *ZDNet Magazine*. Available at http://www.zdnet.com/article/bill-gates-stops-chasing-nuclear-wave-pursues-variety-of-reactors/.

[Hejzlar et al., 2013] Hejzlar, P., Petroski, R., Cheatham, J., Touran, N., Michael, C., Troung, B., Latta, R., Werner, M., Burke, T., Tandy, J., Garrett, M., Johnson, B., Ellis, T., McWhirter, J., Odedra, A., Schweiger, P., Adiksson, D., and Gilleland, J. (2013). TerraPower, LLC Traveling Wave Reactor Development Program Overview. *Nuclear Engineering and Technology*, 45:731–744.

[IAEA, 2007] IAEA (2007). Fast Reactor Database 2006 Update. Technical Report IAEA-TECDOC-1531, Vienna, Austria.

[Isotalo and Aarnio, 2011] Isotalo, A. and Aarnio, P. (2011). Comparison of Depletion Algorithms for Large Systems of Nuclides. *Annals of Nuclear Energy*, 38:261–268.

[Kasten, 1998] Kasten, P. (1998). Review of the Radkowsky Thorium Reactor Concept. *Science & Global Security*, 7:237–269.

[Kim and Taiwo, 2010a] Kim, T. K. and Taiwo, T. A. (2010a). Feasibility Study of Ultra-Long Life Fast Reactor Core Concept. In *Proceedings of PHYSOR 2010 - Advances in Reactor Physics to Power the Nuclear Renaissance*, Pittsburgh, Pennsylvania, USA. American Nuclear Society.

[Kim and Taiwo, 2010b] Kim, T. K. and Taiwo, T. A. (2010b). Fuel Cycle Analysis of Once-Through Nuclear Systems: Fuel Cycle Research & Development. Technical Report ANL-FCRD-308, Lemont, Illinois, US.

[Lamarsh and Baratta, 2001] Lamarsh, J. and Baratta, A. (2001). *Introduction to Nuclear Engineering*. Prentice-Hall, Inc., Upper Saddle River, New Jersey, US.

[Leppänen, 2013] Leppänen, J. (2013). Serpent - a Continuous-energy Monte Carlo Reactor Physics Burnup Calculation Code. User's Manual NEA-1840, VTT Technical Research Centre of Finland, Espoo, Finland. Abstract available at: http://www.oecd-nea.org/tools/abstract/detail/nea-1840.

[Leppänen and Pusa, 2009] Leppänen, J. and Pusa, M. (2009). Burnup calculation capability in the PSG2 / Serpent Monte Carlo reactor physics code. In *International Conference on Mathematics, Computational Methods & Reactor Physics 2009*, Saratoga Springs, New York, US.

[Loh et al., 1980] Loh, W. T., Driscoll, M. J., and Lanning, D. D. (1980). An Evaluation of the Fast Mixed Spectrum Reactor. Technical Report MITNE-232, Massachusetts Institute of Technology, Dept. of Nuclear Engineering, Cambridge, Massachusetts, US.

[Lopez and Francois, 2015] Lopez, R. C. and Francois, J. L. (2015). Design of a Fast Breed/Burn Reactor Core Using the Deterministic Code KANEXT. In *Advances in Nuclear Fuel Management V (ANFM 2015)*, Hilton Head Island, South Carolina, USA.

[Palmiotti et al., 1995] Palmiotti, M., Lewis, E. E., and Carrico, C. B. (1995). VARIANT: VARIational Anisotropic Nodal Transport for Multidimensional Cartesian and Hexagonal Geometry Calculation. Technical Report ANL-95/40, Argonne National Laboratory.

[Pilipenko et al., 2003] Pilipenko, V., Belozorov, D., Davydov, L., and Shul'ga, N. (2003). Some Aspects of Slow Nuclear Burning. In *Proceedings of ICAPP'03*, Cordoba, Spain.

[Ponomarev et al., 2010] Ponomarev, A., Broeders, C. H. M., Dagan, R., and Becker, M. (2010). Evaluation of Neutron Physics Parameters and Reactivity Coefficients for Sodium Cooled Fast Reactors. In *Proceedings of ICAPP'10*, San Diego, California, USA.

[Pusa and Leppänen, 2010] Pusa, M. and Leppänen, J. (2010). Computing the matrix exponential in burnup calculations. *Nuclear Science and Engineering*, 164:140–150.

[Pusa and Leppänen, 2013] Pusa, M. and Leppänen, J. (2013). Solving Linear Systems with Sparse Gaussian Elimination in the Chebyshev Rational Approximation Method (CRAM). *Nuclear Science and Engineering*, 175:250–258.

[Ren et al., 2006] Ren, X., Sridharan, K., and Allen, T. R. (2006). Corrosion of Ferritic–Martensitic Steel HT9 in Supercritical Water. *Journal of Nuclear Materials*, 358:227–234.

[Rosenthal et al., 1965] Rosenthal, M. W., Adams, R. E., Bennett, L. L., Carter, W. L., A., D. D., Haskins, R. E., Lawson, C. G., Lotts, A. L., Olson, R. C., Perry, A. M., Roberts, J. T., Salmon, R., and Vondy, D. R. (1965). A Comparative Evaluation of Advanced Converters. Technical Report ORNL-3686, Oak Ridge National Laboratory, Oak Ridge, Tennessee, US.

[Schleicher et al., 2009] Schleicher, Choi, H., Baxter, A., and Bertch, T. C. (2009). Improved Utilization of U.S. Nuclear Energy Resources without Reprocessing. In *Transactions of the American Nuclear Society*. Winter 2009 Meeting.

[Seifritz, 1995] Seifritz, W. (1995). Non-Linear Burn-up Waves in Opaque Neutron Absorbers. *Kerntechnik*, 60:185–188.

[Sekimoto and Nagata, 2010] Sekimoto, H. and Nagata, A. (2010). Introduction of "MOTO" Cycle to CANDLE Fast Reactor. In *Advances in Reactor Physics to Power the Nuclear Renaissance- PHYSOR 2010*, Pittsburgh, Pennsylvania, USA.

[Sekimoto et al., 2001] Sekimoto, H., Ryu, K., and Yoshimura, Y. (2001). CANDLE: The New Burnup Strategy. *Nuclear Science and Engineering*, 139:306–317.

[SERPENT, 2015] SERPENT (2015). Serpent: a Continuous Energy Monte Carlo Reactor Physics Burnup Calculation Code. Serpent Code web page. Available at http://montecarlo.vtt.fi/.

[Simpson, 2012] Simpson, M. F. (2012). Developments of Spent Nuclear Fuel Pyroprocessing Technology at Idaho National Laboratory. Technical Report INL/EXT-12-25124.

[Slesarev et al., 1984] Slesarev, J. S., Stukalov, V. A., and Subbotin, S. (1984). Problems of Development of Fast Reactors Self-Provision without Fuel Reprocessing. *Atomkernenenergie, Kerntechnik*, 45:58–64.

[Smith et al., 2008] Smith, C. F., Halsey, W. G., Brown, N. W., Sienicki, J. J., Moisseytsev, A., and Wade, D. C. (2008). SSTAR: The US lead-cooled fast reactor (LFR). *Journal of Nuclear Materials*, pages 255–259.

[Suikkanen and Kyrki-Rajamäki, 2010] Suikkanen, H., R. V. and Kyrki-Rajamäki, R. (2010). An Approach for Detailed Reactor Physics Modelling of Randomly Packed Pebble Beds. In *Proceedings of the 5th International Conference on High Temperature Reactor Technology*, Prague, Czech Republic.

[Teller et al., 1996] Teller, E., Ishikawa, M., and Wood, L. (1996). Completely Automated Nuclear Power Reactors for Long-Term Operation. In *Proceedings of the Frontiers in Physics Symposium*, Lubbock, Texas, US.

[Todreas and Kazimi, 1990] Todreas, N. and Kazimi, M. (1990). *Nuclear Systems I: Thermal Hydraulic Fundamentals*. Hemisphere Publishing Corporation, Panama City, Panama.

[Tucek et al., 2005] Tucek, K., Carlsson, J., and Wider, H. (2005). Comparison of Sodium and Lead-Cooled Fast Reactors Regarding Severe Safety and Economical Issues. In *Proceedings of the 13th International Conference on Nuclear Engineering*, Beijing, China.

[Ueda et al., 2005] Ueda, N., Kinoshita, I., Minato, A., Kasai, S., Yokoyama, T., and Maruyama, S. (2005). Sodium Cooled Small Fast Long-Life Reactor 4S. *Progress in Nuclear Energy*, 47:222–230.

[Van Criekingen et al., 2009] Van Criekingen, S., Dagan, R., Becker, M., and Broeders, C. H. M. (2009). The KANEXT modular program for reactor physics calculation. Presentation of a Seminar, Karlsruhe Institute of Technology. Available at http://inrwww.webarchiv.kit.edu/pdfs/KANEXTseminar_INR_2009.pdf.

[Van Dam, 1998] Van Dam, H. (1998). Burnup Waves. *Annals of Nuclear Energy*, 25:1409–417.

[Waltar et al., 2012] Waltar, A. E., Todd, D. R., and Tsvetkov, P. V. (2012). *Fast Spectrum Reactors*. Springer Science+Business Media, LLC, New York, US.

[Weaver et al., 2010] Weaver, K., Gilleland, J., Ahlfeld, C., Whitmer, C., and Zimmerman, G. (2010). A Once-Through Fuel Cycle for Fast Reactors. *Journal of Engineering for Gas Turbines and Power*, 132. 102917-1.

[Wikipedia, 2015] Wikipedia (2015). Boron carbide. Article from Wikipedia, the free encyclopedia. Available at https://en.wikipedia.org/?title=Boron_carbide.

[WNA, 2015] WNA (2015). Processing of Used Nuclear Fuel. Article, World Nuclear Association. Available at http://www.world-nuclear.org/info/Nuclear-Fuel-Cycle/Fuel-Recycling/Processing-of-Used-Nuclear-Fuel/.

[Woll, 2005] Woll, D. (2005). Introduction to the use of the UNIX-version of the KArlsruhe PROgram System KAPROS. Technical Report FZKA-6280, Forschungszentrum Karlsruhe, Karlsruhe, Germany. Available at inr-www.webarchiv.kit.edu/pdfs/fzka6280m.pdf.

Index